Phosphate Diester Cleavage Mediated by Transition Metal Complexes

Mary Jane Young

A thesis submitted to the Faculty of Graduate Studies and Research of McGill University in partial fulfillment of the requirements for the degree of Doctor of Philosophy

June 1996
Department of Chemistry
McGill University
Montreal, Quebec
Canada

ISBN 0-612-19788-3

For My Family
Mom, Dad, William, Laurie, and Dave

Abstract

Two independent studies have been developed in this thesis. In the first study, the reactivities of metal-alkoxide and metal-hydroxide nucleophiles are compared for cleaving phosphate diesters. In the second study, the reactivity of a dinuclear metal complex is compared to a mononuclear metal complex for hydrolyzing RNA.

Copper(II) complexes of bis(2-pyridylmethyl)amine (Cu(II)bpa), N-(2-hydroxyethyl)bis(2-pyridylmethyl)amine (Cu(II)hebpa) and N-(3-hydroxypropyl)bis(2-pyridylmethyl)amine (Cu(II)hpbpa) have been synthesized and their reactivities and mechanisms for cleaving bis(2,4-dinitrophenyl) phosphate (BDNPP) have been investigated. Cu(II)hpbpa is observed to be the most reactive ($k = 7.2 \times 10^{-1}$ M^{-1} s^{-1} at 25 °C, pH 8.8) for cleaving BDNPP followed by Cu(II)bpa ($k = 2.0 \times 10^{-2}$ M^{-1} s^{-1}) and Cu(II)hebpa ($k = 2.0 \times 10^{-2}$ M^{-1} s^{-1}). HPLC product analyses indicated that Cu(II)hpbpa cleaves BDNPP mostly through transesterification while the complexes Cu(II)bpa and Cu(II)hebpa cleave BDNPP predominantly by hydrolysis. The differences in the mechanisms and the reactivities are explained in terms of the differences in the structures of the three copper(II) complexes.

Copper(II) complexes of 1,8-bis(1,4,7-triazacyclononyl-N-methyl)naphthalene (tntn), 1,4,7-triazacyclononane (tacn), and N-benzyl-1,4,7-triazacyclononane (btacn) have been prepared and their reactivities compared for cleaving RNA. The novel dinuclear copper(II) complex, $Cu(II)_2$tntn, is observed to be 200-500 fold faster per metal center than the mononuclear copper(II)complexes, Cu(II)tacn and Cu(II)btacn, for cleaving a diribonucleotide, ApA, and its cyclic phosphate intermediate, 2'3'-cAMP. $Cu(II)_2$tntn (2.0 mM) reduces the half life of ApA (0.05 mM) to 50 minutes (pH 6, 50 °C); this represents a rate acceleration of approximately 10^5 fold over the background hydroxide rate. The half life of 2'3'-cAMP (0.05 mM) is decreased to 4 minutes in the presence of $Cu(II)_2$tntn (2.0 mM, pH 6, 25 °C); this represents a rate acceleration of about 10^8 fold over the background hydroxide rate.

Résumé

Deux études indépendantes ont été développées dans cette thèse. Dans la première étude, les réactivités de complexes métal-hydroxyde et métal-alkoxyde nucléophiliques sont comparées pour cliver les diesters de phosphate. Dans la deuxième étude, la réactivité d'un complexe dinucléaire de métal est comparée a un complexe mononucléaire de métal pour hydrolyser l'ARN.

Les complexes de cuivre(II) de bis(2-pyridylmethyl)amine (Cu(II)bpa), N-(2-hydroxyethyl)bis(2-pyridylmethyl)amine (Cu(II)hebpa) et N-(3-hydroxypropyl)bis(2-pyridylmethyl)amine (Cu(II)hpbpa) ont été synthétisés et leurs réactivités et mécanismes pour cliver le bis-(2,4-dinitrophenyl) phosphate (BDNPP) ont été étudiés. Cu(II)hpbpa est observé être le plus réactif ($k = 7.2 \times 10^{-1}$ M^{-1} s^{-1} at 25 °C, pH 8.8) pour cliver BDNPP suivi par Cu(II)bpa ($k = 2.0 \times 10^{-2}$ M^{-1} s^{-1}) et Cu(II)hebpa ($k = 2.0 \times 10^{-2}$ M^{-1} s^{-1}). Les analyses de produit par HPLC ont indiquées que Cu(II)hpbpa clive BDNPP principalement par transestérification alors que les complexes Cu(II)bpa et Cu(II)hebpa clivent BDNPP principalement par hydrolyse. Les différences entre les mécanismes et les réactivités sont expliquées en termes des différences de stucture des trois complexes de cuivre(II).

Les complexes de cuivre(II) de 1,8-bis(1,4,7-triazacyclonoyl-N-methyl)naphthalene (tntn), 1,4,7-triazacyclononane (tacn), et N-benzyl-1,4,7-triazacyclononane (btacn) ont été préparés et leurs réactivités pour cliver l'ARN sont comparées. Le nouveau complexe dinucléaire de cuivre(II), $Cu(II)_2$tntn, est observé être 200 à 500 fois plus rapide par centre métallique que les complexes de cuivre(II) mononucléaires, Cu(II)tacn et Cu(II)btacn, pour cliver un dinucléotide d'ARN (ApA), et son intermediare phosphate cyclique, 2'3'-cAMP. $Cu(II)_2$tntn (2.0 mM) réduit la demie-vie d'ApA (0.05 mM) à 50 minutes (pH 6, 50 °C); ceci représente une accélération de la vitesse d'environ 10^5 fois par rapport à celle sans catalyseur. La demie-vie de 2'3'-cAMP (0.05 mM) est réduite à 4 minutes en présence de $Cu(II)_2$tntn (2.0 mM, pH 6, 25 °C); ceci représente une accélération de la vitesse d'environ 10^8 fois par rapport à celle sans catalyseur.

Acknowledgments

I would like to thank my research supervisor, Dr. Jik Chin, for his advice, guidance, and numerous ideas throughout my post-graduate studies at McGill.

I would like to acknowledge Dr. Anne-Marie Lebuis for the X-ray structure determinations, for translating the abstract into french, and for being a friendly neighbor.

I am thankful for the use of the C-18 reverse phase column and help from Dr. Gour and Stephanie Michaud in Room 25.

I am thankful to all my friends in Room 230: James Connolly, William Cheung, Dr. Andrea Erxleben, Philip Hurst, Dr. Barry Linkletter, Erik Rubin, Jin Seog Seo, Dr. Bryan Takasaki, Dr. Daphne Wahnon, Mark Wall, Dan Williams, and Dr. Nick Williams.

Thank you to everyone that proofread my thesis.

Cheers to all my broomball, softball, and soccer friends in the city.

Finally I would like to thank Dave for his love and support during the past five years.

Glossary of Symbols and Abbreviations

δ	chemical shift
ε	extinction coefficient
λ	wavelength
2'-AMP	adenosine 2'-monophosphate
2'3'-cAMP	adenosine 2',3'-cyclic monophosphate
3'-AMP	adenosine 3'-monophosphate
A	adenosine
Å	Angstrom
anal.	analysis
ApA	adenylyl(3'-5')adenosine
ATP	adenosine triphosphate
bamp	2,6-bis(aminomethyl)pyridine
bba	bis(2-benzimidazolylmethyl)amine
BDNPP	bis(2,4-dinitrophenyl) phosphate
BNPP	bis(4-nitrophenyl) phosphate
b.p.	boiling point
bpa	bis(2-pyridylmethyl)amine
btacn	N-benzyl-1,4,7-triazacyclononane
calcd.	calculated
CHES	2-(cyclohexylamino)ethanesulfonic acid
conc.	concentrated
cyclen	1,4,7,10-tetraazacyclododecane
DMP	dimethyl phosphate
DNA	deoxyribonucleic acid
DNase	deoxyribonuclease

DENPP	diethyl 4-nitrophenyl phosphate
DNPP	2,4-dinitrophenyl phosphate
DSS	3-(trimethylsilyl)-1-propanesulfonic acid
EDTA	ethylenediaminetetracetic acid disodium salt
ether	anhydrous diethyl ether
FAB	fast atomic bombardment
hebba	N-(2-hydroxyethyl)bis(2-benzimidazolylmethyl)amine
hebpa	N-(2-hydroxyethyl)bis(2-pyridylmethyl)amine
HEPES	4-(2-hydroxyethyl)-1-piperazineethanesulfonic acid
His	histidine
HP	Hewlett Packard
hpbpa	N-(3-hydroxypropyl)bis(2-pyridylmethyl)amine
HPLC	high pressure liquid chromatography
HPNPP	2-hydroxypropyl 4-nitrophenyl phosphate
HPPP	2-hydroxypropyl phenyl phosphate
h	hour(s)
ida	iminodiacetic acid
Hz	Hertz
K	equilibrium constant
k	rate constant
K_a	acid dissociation constant
k_{obs}	observed rate constant
L	Litres
Lys	lysine
M	Molarity (moles/litre)
MeCN	acetonitrile
MeOH	methanol

MES	4-morpholineethanesulfonic acid
min	minute(s)
mL	millilitre(s)
mm	millimeter
mM	millimolar
mol	mole(s)
MPNPP	methyl 4-nitrophenyl phosphate
mRNA	messenger RNA
MW	molecular weight
neo	neocuproine
NEM	N-ethylmorpholine
NMR	nuclear magnetic resonance
NPP	4-nitrophenyl phosphate
pD	-log[deuterium concentration]
phen	1,10-phenanthroline
ppm	parts per million
R	correlation coefficient
RNA	ribonucleic acid
RNase	ribonuclease
s	second(s)
T	temperature
t	time
tacn	1,4,7-triazacyclononane
TBP	trigonal bipyramidal
THF	tetrahydrofuran
TMP	trimethyl phosphate
TMS	tetramethylsilane

tntn	1,8-bis(1,4,7-triazacyclononyl-N-methyl)naphthalene
tren	tris(2-ethylamino)amine
tRNA	transfer RNA
trien	triethylenetetramine
TRIS	tris(hydroxymethyl)aminomethane
trpn	tris(3-aminopropyl)amine
UV-vis	ultraviolet-visible
µL	microlitre(s)
UpU	uridyl(3'-5')uridine

Structures of Ligands

bamp

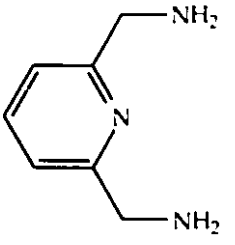

bba

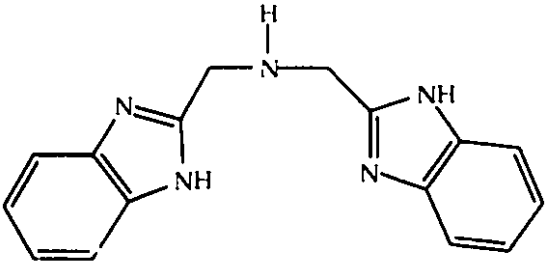

bpa

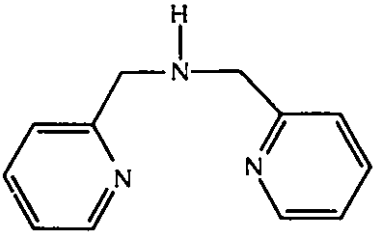

btacn

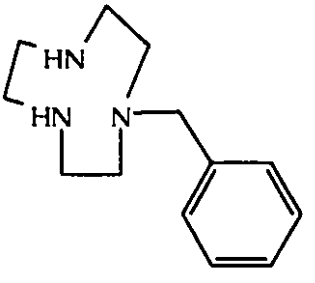

cyclen

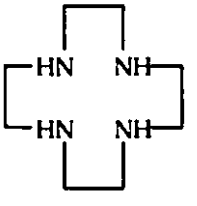

hebamp

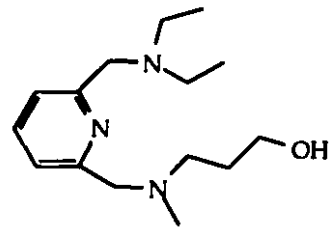

hebba

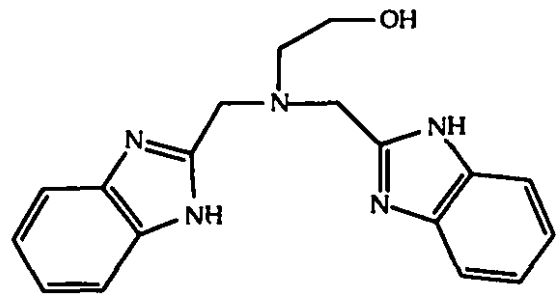

hebpa

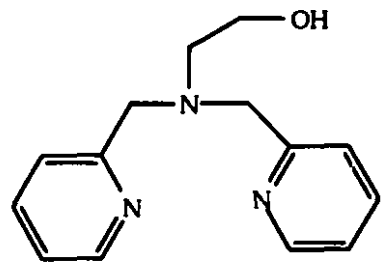

hpbpa

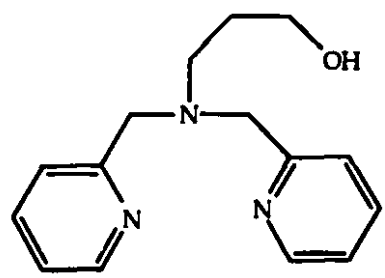

ida

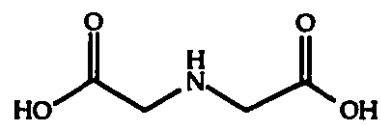

neo

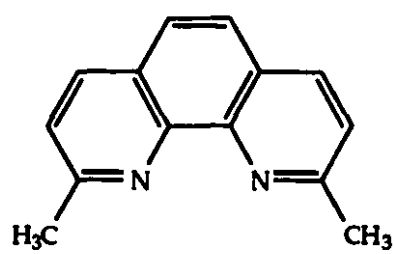

phen

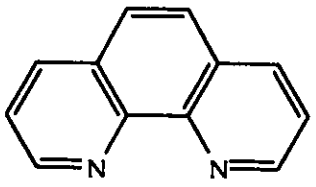

tacn

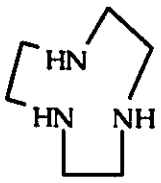

ter

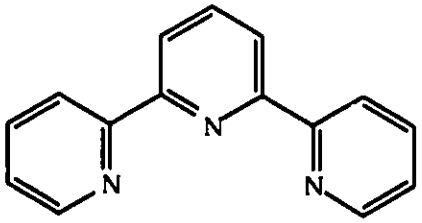

tntn

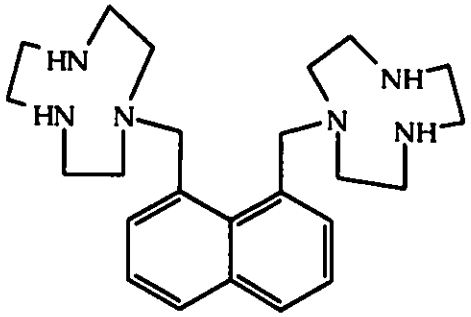

tren

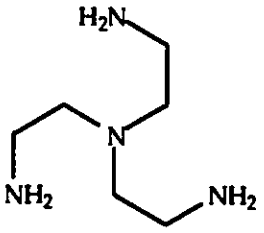

trpn

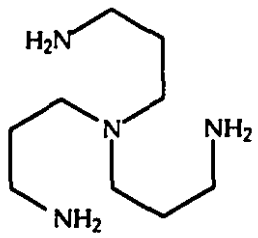

Structures of Substrates

2'AMP

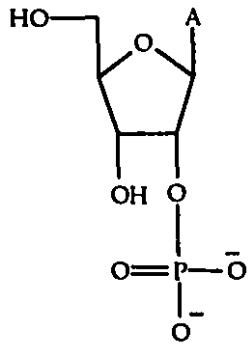

2'3'cAMP

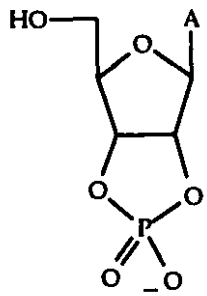

3'AMP

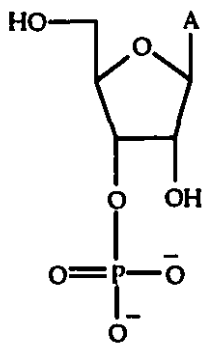

ApA

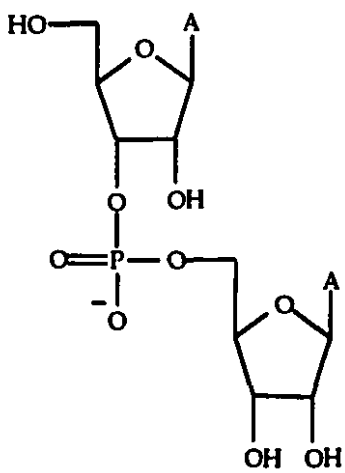

BDNPP

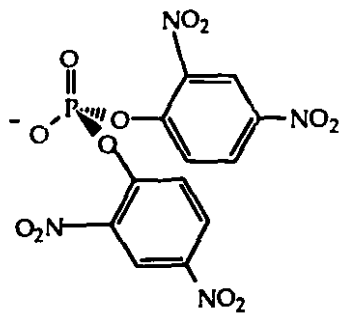

BNPP

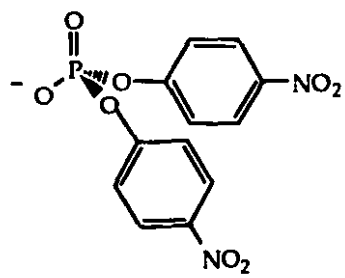

DENPP

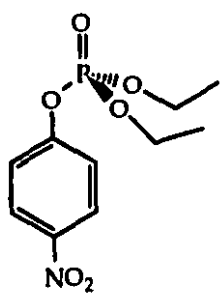

DNPP

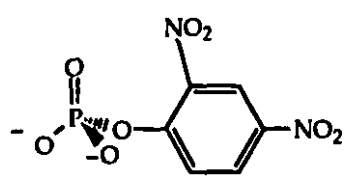

HPNPP

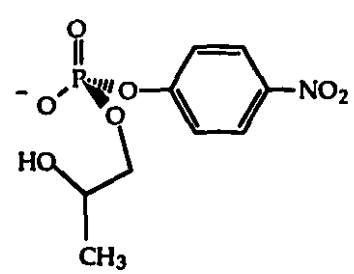

NPP

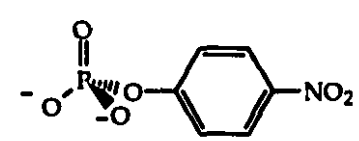

Table of Contents

Chapter 1. Introduction.

1.1. Phosphate Esters in Nature.

1.1.1. Structures and Functions of Biological Phosphate Esters.

Phosphate esters play a number of essential roles in biological processes. The phosphate diester linkage is a key component of the genetic material deoxyribonucleic acid (DNA). A main source of energy within cells is contained in adenosine triphosphate (ATP). Nicotinamide adenine dinucleotide (NAD^+) is an important oxidizing agent that is required as a cofactor for many biological enzymes (Figure 1.1).

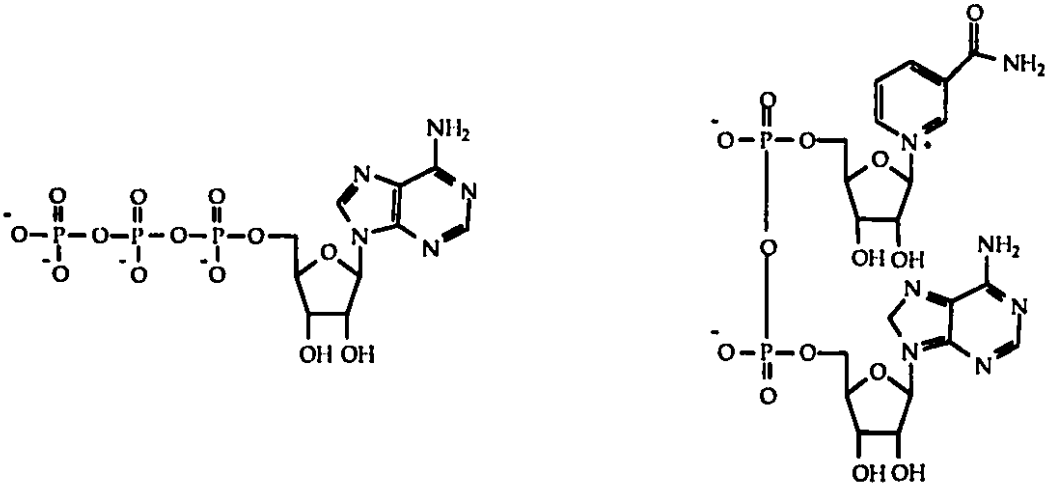

ATP NAD$^+$

Figure 1.1. Chemical Structure of ATP and NAD^+.

The phosphate binds at the 3′ and 5′ positions of the sugar and any one of four different bases binds at the 1′ position of the sugar (Figure 1.2). The bases are

derivatives of two nitrogen heterocyclic ring systems: the purines, which include the bases adenine and guanine, and the pyrimidines, which include the bases cytosine, thymine (DNA), and uracil (RNA). The order of the bases on the backbone of DNA constitutes the genetic code. The information within the sequence of deoxyribonucleotides is transcribed into a shorter lived sequence of ribonucleotides, mRNA. The mRNA subsequently moves to the ribosome in the cell where the four base code of nucleic acids is translated into amino acids, the building blocks of proteins.

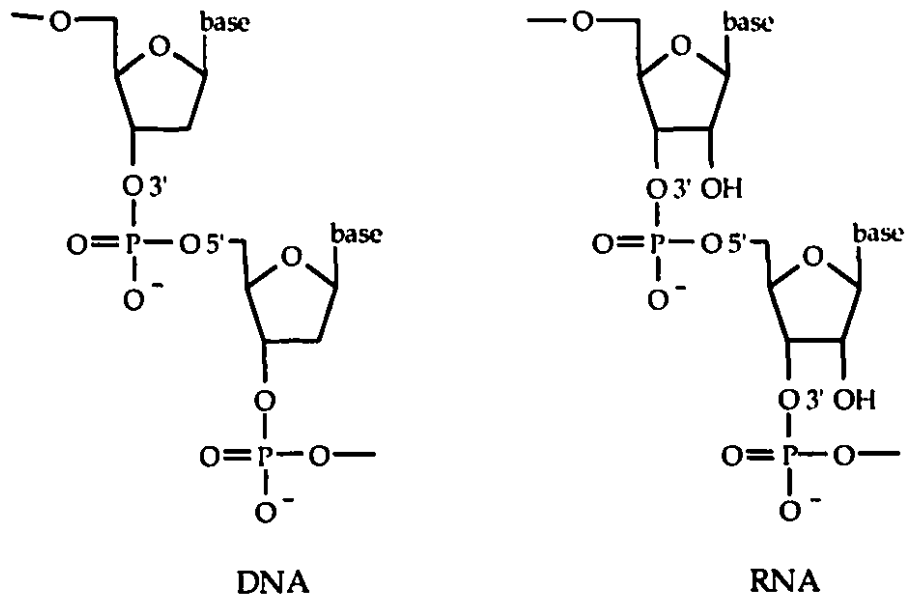

Figure 1.2. Primary Structure of DNA and RNA.

1.1.2. DNA Double Helix.

The secondary structure of DNA was proposed by Watson and Crick in 1953.[1,2] The Watson-Crick structure of DNA is a double helix of oligodeoxyribonucleotides such that the more hydrophobic nitrogen bases are inside the helix and the more hydrophilic sugar and phosphate groups are on the outside. The two strands of the double helix are held together by

hydrogen bonding between the base pairs adenine and thymine and the base pairs guanine and cytosine (Figure 1.3).

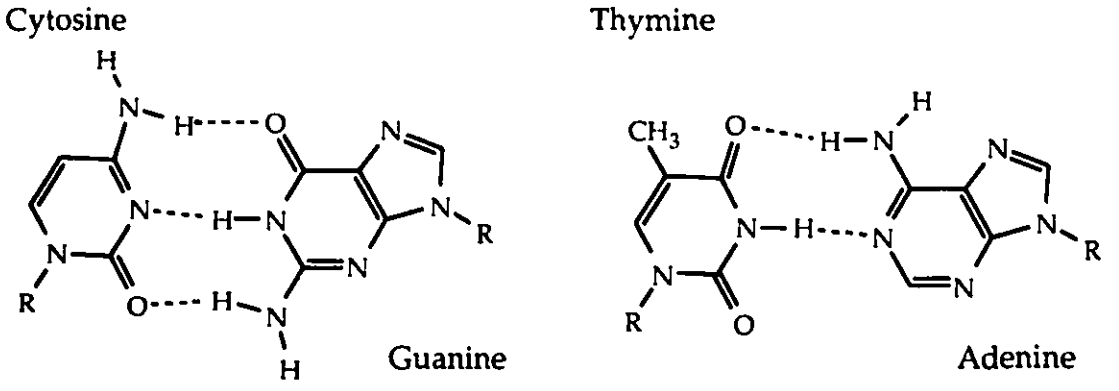

Figure 1.3. Hydrogen Bonding Responsible for Base Pairing in DNA.

1.1.3. DNA Stability Versus RNA Stability.

DNA is a highly effective medium for storing the genetic code in living organisms due to its remarkable stability under physiological conditions. The negatively charged phosphate diester backbone of DNA impedes the rate of hydrolytic nucleophilic attack, the mechanism of cleavage used by biological systems. The half-life of DNA has been estimated to exceed 200 million years at pH 7 and 25 °C.[3] In order to hydrolyze a phosphate diester bond of DNA with a half life of one hour at pH 7 and 25 °C a catalyst must provide at least 10^{12} fold acceleration over the background hydroxide rate. RNA is less stable than DNA due to the presence of an internal nucleophile and is considered to be approximately 10^{7} fold more activated than DNA towards hydrolysis (Figure 1.4).[4,5]

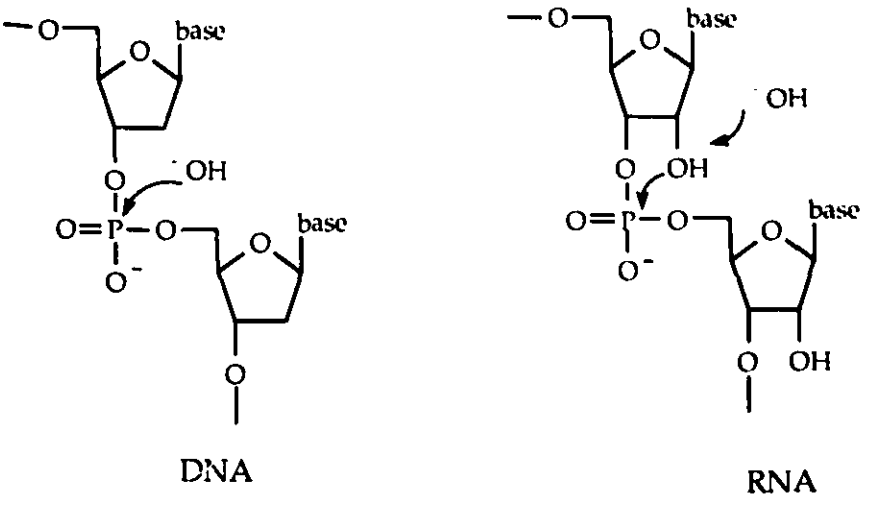

Figure 1.4. Comparison of the mechanism for the base catalyzed hydrolysis of DNA and RNA.

1.2. Non-Enzymatic Phosphate Diester Hydrolysis.

1.2.1. Mechanism of Base-Catalyzed Hydrolysis of Phosphate Diesters.

The mechanism of phosphate diester hydrolysis has been extensively studied.[6-10] The More O'Ferrall plot (Figure 1.5) is useful for envisioning the various pathways available for base-catalyzed hydrolysis of phosphate diesters. If all possible pathways are considered, then the reaction could proceed anywhere from a dissociative S_N1 (P) pathway through to an associative S_N2 (P) pathway. It has been established that the base-catalyzed hydrolysis of phosphate diesters occurs by an associative nucleophilic attack at the phosphorus atom.[6-10]

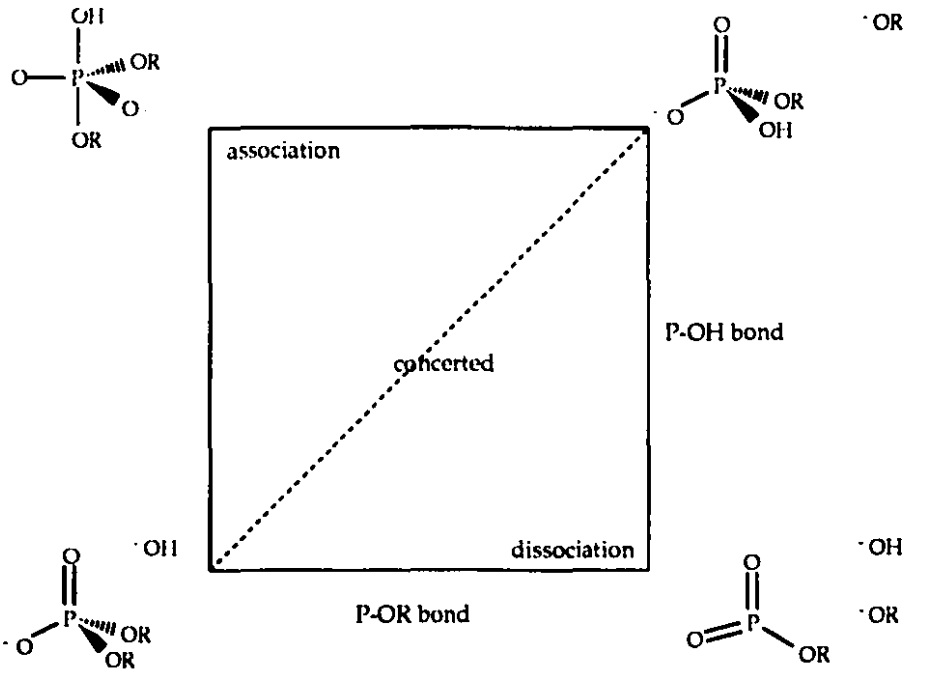

Figure 1.5. More O'Ferrall diagram depicting various pathways available for base-catalyzed phosphate diester hydrolysis.

1.2.2. Guidelines for Base-Catalyzed Hydrolysis of Phosphate Diesters.

Thatcher and Kluger have condensed the extensive research on the mechanism of base-catalyzed phosphate diester hydrolysis into the following guidelines.[11]

(a) Attack of the nucleophile on tetrahedral phosphorus will lead to a trigonal bipyramidal (TBP) species, which may be an intermediate.

(b) The nucleophiles may occupy apical or equatorial positions about the TBP phosphorus, but if the TBP is an intermediate then ligand reorganization may occur by geometrically defined pseudorotational processes (Figure 1.6).[6]

Figure 1.6. Pseudorotation of TBP intermediate.

(c) Nucleophiles will enter at and leaving groups depart from apical positions.

(d) A set of rules govern the dynamics of the TBP intermediate:

(i) when phosphorus is contained in a four- or five-membered ring, this ring prefers to be attached apical/equatorial to the TBP intermediate;

(ii) more-electronegative ligands prefer apical positions;

(iii) π-electron donor ligands prefer equatorial positions;

(iv) steric effects are minimized by placement of bulky substituents in equatorial positions.

1.3. Enzymatic Hydrolysis of DNA and RNA.

1.3.1. Nucleases.

Despite the stability of DNA and RNA towards spontaneous hydrolysis they can be readily hydrolyzed by enzymes called nucleases. Nucleases are essential to nature and are involved in a wide variety of regulatory processes within the cell; including the removal of incorrectly incorporated nucleotides during replication by the 3′,5′-exonuclease site of DNA polymerase I,[12] the

degradation of RNA during digestion by pancreatic ribonuclease A,[13] and the cleavage of precursor tRNA to produce mature tRNA by ribonuclease P.[14,15]

1.3.2. Mechanisms of DNA and RNA Cleavage.

There are three general pathways of RNA and DNA hydrolysis that are activated by natural nucleases.[16] The first pathway involves the hydrolysis of RNA which proceeds through a 2',3'-cyclic phosphoryl intermediate and results in 3'PO_4 and 5'OH products. This pathway has been established for pancreatic ribonuclease A (RNase A).[17] The reaction effected by RNase A is facilitated by two histidine residues and one lysine residue (Figure 1.7). Histidine 12 acts as a general base by accepting the proton from the 2'OH, thus activating the 2'-oxygen for attack on the phosphorus. Histidine 119 acts as a general acid to protonate the leaving group, a 5'alkoxide ion, in the phosphorane transition state. The positively charged side chain of lysine 41 has been suggested to form an electrostatic interaction with the negatively charged pentacoordinate transition state.[18] Hydrolysis of the 2'3'-cyclic phosphate intermediate proceeds essentially in reverse to that of the RNA substrate; histidine 119 acts as a general base to activate an attacking water molecule and histidine 12 acts as a general acid for the transition state.

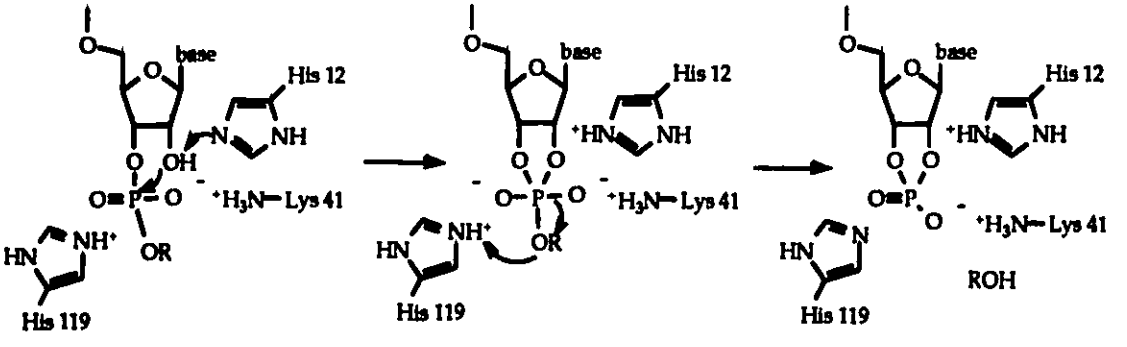

Figure 1.7. Mechanism of Action of RNase A.[17]

An alternative mechanism for RNA cleavage by RNase A has been proposed by Breslow *et al.* based on their investigations of the imidazole catalyzed cleavage of diribonucleotides.[19-21] They observed a bell shaped pH rate profile for the hydrolysis of uridyl(3'-5')uridine (UpU) and adenylyl(3'-5')adenosine (ApA) as the ratio of imidazolium ion to imidazole was varied from 1:0 to 0:1. From their studies they concluded that the substrates were hydrolyzed through a common intermediate by sequential buffer catalysis. In contrast to the previously accepted mechanism for RNase A (Figure 1.7) they proposed that the imidazolium ion was catalyzing the formation of the phosphorane intermediate and that imidazole catalyzed its breakdown. The data analysis and experimental technique have been criticized and as a result have prompted further studies upon the system.[22-25] Kirby *et al.* convincingly explain the bell shape pH-rate profile observed by Breslow *et al.* as a result of medium effects.[25] They determined that the hydroxide catalyzed rate of cleavage, which becomes significant at 80-90% free base, of a similar substrate was being inhibited by the increasing concentrations of imidazole. Upon correction for these effects the pH rate profile was no longer bell shaped as the ratio of imidazolium ion to imidazole was varied from 1:0 to 0:1, but instead it was linear.

The second pathway of nucleic acid hydrolysis that is effected by nucleases involves DNA cleavage such that 5'PO_4 and 3'OH products are formed. The nuclease, bovine pancreatic DNase I, uses a calcium(II) ion as a Lewis acid to interact with the phosphate and a histidine residue as a general base to activate an attacking water molecule (Figure 1.8).[12]

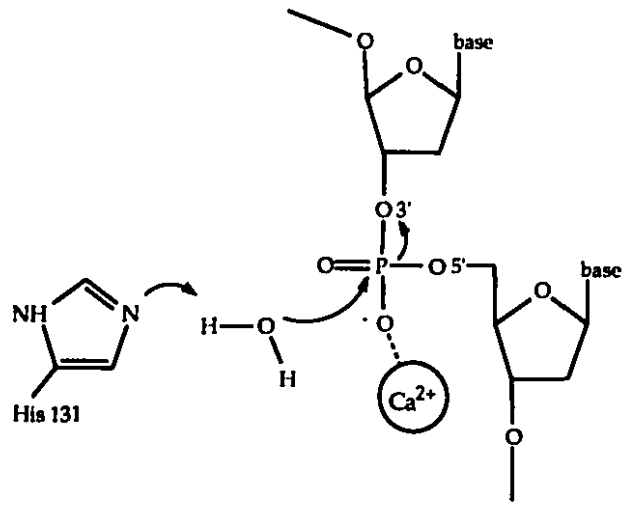

Figure 1.8. Proposed mechanism of Action of DNase I.[12]

The third pathway of DNA or RNA cleavage promoted by nucleases, which yields 3'OH and 5'PO_4 products, can be represented by the 3',5'-exonuclease domain of DNA polymerase I.[26] The proposed mechanism of catalysis of the 3'5'-exonuclease activity of DNA polymerase I requires two metals and does not depend on the chemical properties of the protein side chains (Figure 1.9). The first metal (Metal A) interacts with a water molecule as a Lewis acid to produce a metal hydroxide nucleophile that carries out an in-line attack on the phosphorus, and also acts as a Lewis acid with the phosphate ester oxygen. The second metal (Metal B) acts as a Lewis acid through interactions with the phosphate ester oxygen and also by facilitating the departure of the 3'-OH group. A similar mechanism has been proposed for alkaline phosphatase,[27] and is possible for RNase H,[28] P1 nuclease,[29] and phospolipase C.[30] In each of the five enzymes discussed above there are two divalent metal ions 3.8-4.0 Å apart in the active site.

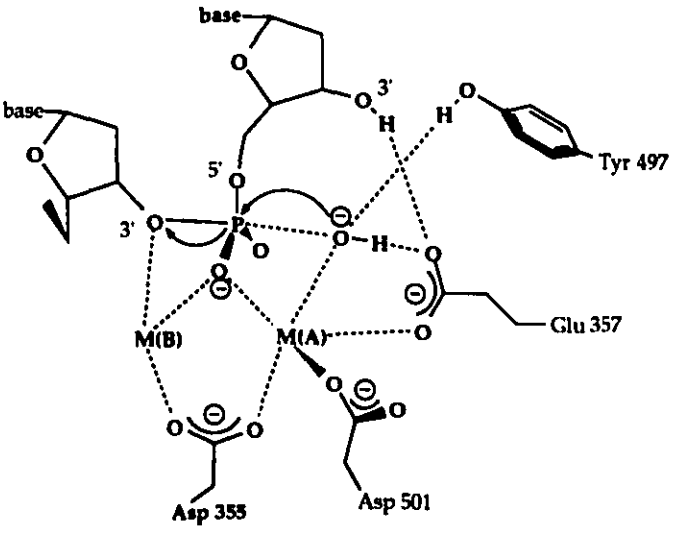

Figure 1.9. Proposed mechanism of Action of 3'5'-exonuclease Activity of DNA Polymerase I.[26]

An alternative mechanism for RNase H has been proposed by Cowan *et al.* based upon site-directed mutagenesis studies and inert transition-metal complexes as probes of the reaction mechanism.[31-33] From their studies they have suggested that the divalent metal cofactor serves to stabilize the phosphorane transition state by formation of an outer-sphere complex with the posititively charged metal center. The generality of the two metal ion mechanism proposed for 3'5'-exonuclease activity has yet to be established.

1.3.3. Ribozymes.

Ribozymes are an important class of metalloenzymes composed entirely of RNA that have only recently been discovered. The discovery of catalytic RNA has sparked debate about the existence of an RNA world from which life evolved. In the RNA world, RNA would have necessarily served a dual role of carrying genetic information and catalyzing key processes for its own replication and maintenance.

All currently known ribozymes are metalloenzymes requiring divalent cations for structural stability of the folded RNA and also for catalysis.[34] The group I intron ribozyme self-cleaves through two consecutive transesterification reactions, resulting in intron removal and ligation of flanking exons as depicted in Figure 1.10. Reactions by this class of ribozyme do not involve the intramolecular attack of an adjacent 2'OH group on phosphorus, but rather an external nucleophile provided typically by guanosine.

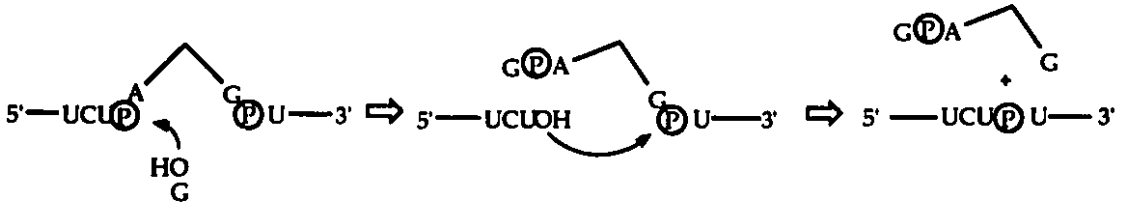

Figure 1.10. Self-splicing of the group I intron ribozyme by consecutive transesterification reactions.

The proposed mechanism[16] of self-cleavage for the group I intron (Figure 1.11) parallels the proposed mechanism of cleavage of DNA by the 3'-5'-exonuclease activity of DNA polymerase I (Figure 1.9).

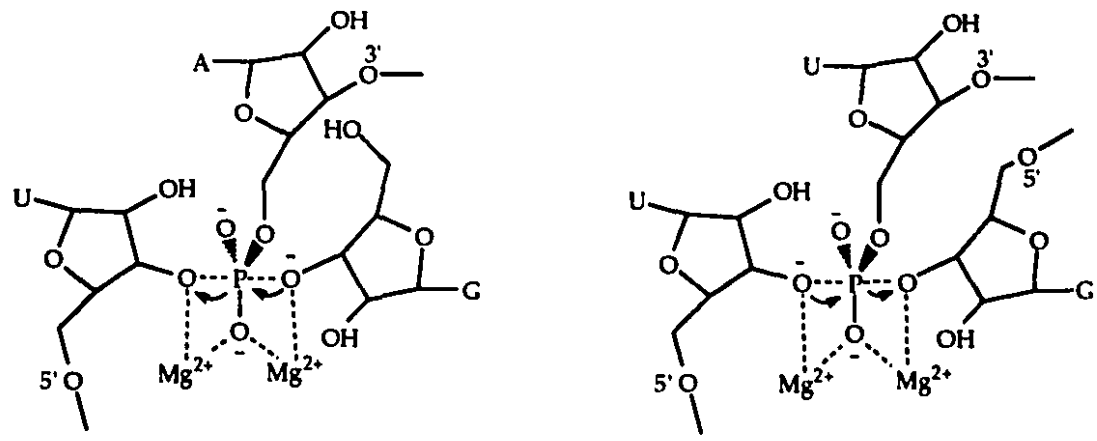

Figure 1.11. Proposed mechanism of cleavage of the group I intron ribozyme.[16]

1.4. Synthetic Nucleases.

1.4.1. Applications of Synthetic Nucleases.

Currently there is considerable interest in developing agents that can cleave nucleic acids under physiological conditions. The sequence specific cleavage of double helical DNA by restriction endonucleases is essential for many techniques in molecular biology including gene isolation, DNA sequence determination and recombinant DNA manipulations.[35-37] Naturally occurring restriction enzymes recognize specific sequences 4 to 8 base pairs in length and typically hydrolyze a symmetrical phosphodiester bond on each strand of double stranded DNA. Synthetic nucleases that can sequence specifically cleave RNA or DNA, with greater specificity than natural enzymes, are important goals for molecular biology and the antisense and antigene fields. A synthetic nuclease is herein defined as a compound that can mediate the cleavage of phosphate diester bonds. An antisense agent is a compound that prevents translation of a specific mRNA strand to the

target protein; whereas an antigene agent is a compound that interrupts the transcription of DNA to mRNA and thereby results in the suppression of the expression of a specific gene (Figure 1.12). Sequence specific cleavage of RNA or DNA, respectively possible antisense and antigene strategies, represents a versatile approach towards developing potential therapeutics for a wide variety of diseases and viruses.[38,39]

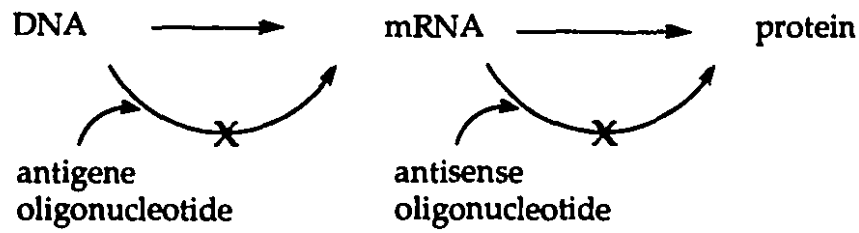

Figure 1.12. Schematic Representation of the Antigene and Antisense Strategies.

1.4.2. Synthetic Oxidative Nucleases.

Redox active coordination complexes, in particular ferrous-ethylenediaminetetraacetic acid (Fe(II)EDTA)[37,40,41] and copper(I)(1,10-phenanthroline) ($Cu(I)phen_2$),[42,43] are capable of efficiently cleaving phosphate diester bonds at neutral pH and ambient temperature (Figure 1.13). Highly selective scission reagents have been generated by binding the redox active complex to a ligand with high affinity for a specific nucleic acid sequence.

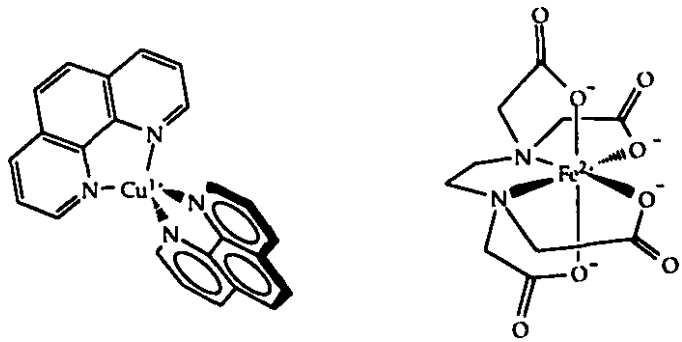

Figure 1.13. Oxidative cleavage agents Cu(I)phen$_2$ and Fe(II)EDTA.

Moser *et al.* have combined a sequence-specific binding moiety for double helical DNA and the Fe(II)EDTA moiety to achieve sequence specific cleavage of double helical DNA.[37] Triple helix formation, or Hoogsteen binding, results from hydrogen bonding interactions in the major groove of DNA between pyrimidine oligonucleotides of the third strand to purines already engaged in Watson-Crick hydrogen bonding to pyrimidines (Figure 1.14).

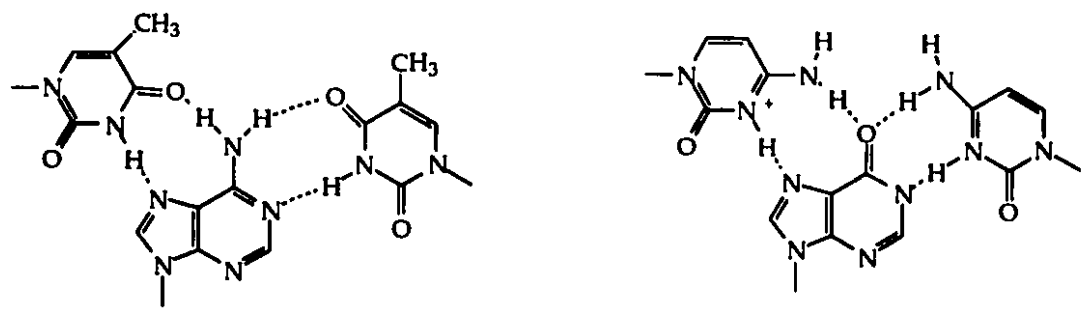

TAT base triplet C$^+$GC base triplet

Figure 1.14. Base Triplets formed by Hoogsteen bonding between pyrimidines and the Watson-Crick AT and GC base pairs.

In the study by Moser *et al.* a homopyrimidine strand was tethered to the Fe(II)EDTA cleaving agent to achieve sequence-specific cleavage of a large

double-stranded DNA fragment in the presence of molecular oxygen and dithiothreitol (DTT) at pH 7.4 and 25 °C (Figure 1.15). Although the chemical mechanism for the scission of DNA by Fe(II)EDTA is not completely understood it has been established that the deoxyribose moiety is oxidized by a short-lived diffusable hydroxyl radical. The Fe(II)EDTA complex is an effective cleaving reagent, however due to the diffusable hydroxyl radical generated multiple products are detected. The affinity cleaving of DNA by homopyrimidine-Fe(II)EDTA firmly established the orientation of the third strand to DNA and the binding specificities of triple helix formation.

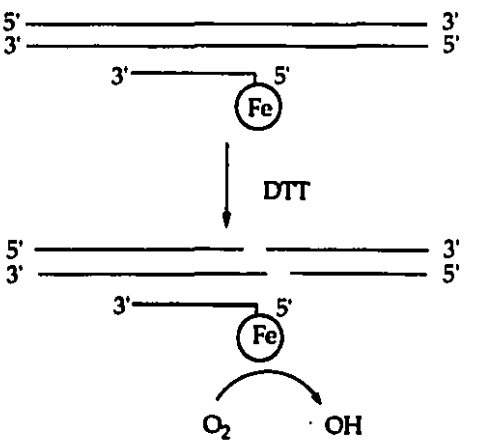

Figure 1.15. Triple Helix directed cleavage of double stranded DNA.[37]

Sigman *et al.* used RNA modified with Cu(I)phen$_2$ to achieve sequence specific cleavage of single- and double-stranded DNA in the presence of hydrogen peroxide.[42,43] R-loops are formed between RNA and double-stranded DNA under specific reaction conditions and involve the displacement of one strand of DNA by the RNA of identical sequence.[44-46] The R-loop directed sequence is the first method for DNA recognition applicable to any sequence. The Cu(I)phen$_2$ cleaving moiety cleaves the phosphodiester backbone by oxidative attack at the C-1 hydrogen of the

deoxyribose moiety by a non-diffusable copper-oxo intermediate as shown in Figure 1.16.

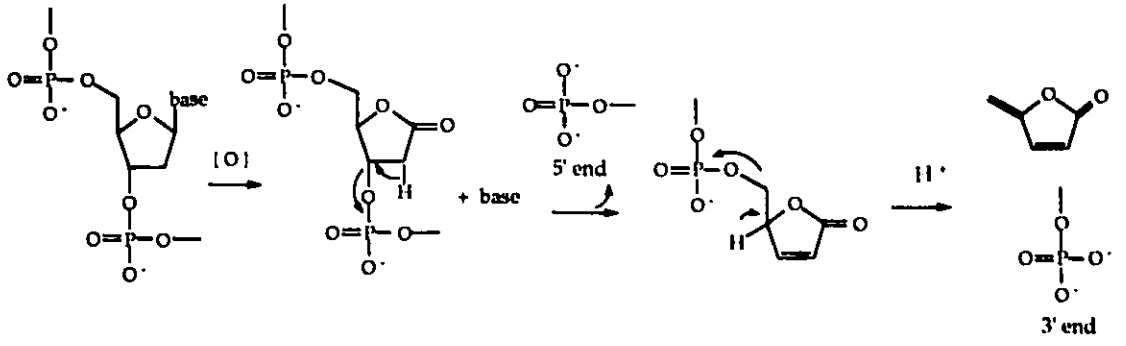

Figure 1.16. Major pathway for oxidative cleavage of DNA by Cu(I)phen$_2$.[43]

The redox-active complexes Cu(I)phen$_2$ and Fe(II)EDTA are efficient agents for cleaving phosphate diesters at neutral pH, however the oxidative nature of the cleavage suffers from the disadvantage that at each nick site a sugar is destroyed, thereby preventing religation of the products.

1.4.3. Synthetic Hydrolytic Nucleases.

Nature has developed many hydrolytic enzymes that can efficiently cleave vital biological substrates including proteins, RNA, and DNA. In nature the products of hydrolytic cleavage are reused in their entirety during biological processes such as protein synthesis and DNA replication. Synthetic nucleases that cleave substrates hydrolytically do not suffer from the disadvantages that pertain to those that cleave oxidatively, however until recently they were considerably less reactive for cleaving phosphoester bonds. Recently there have been several studies reported of highly reactive synthetic nucleases that cleave phosphate diesters hydrolytically.[47-50]

Many of nature's hydrolytic enzymes require metal ions as cofactors. Examples of hydrolytic metalloenzymes that exist in nature include: the zinc(II) containing proteases carboxypeptidase A[51] and thermolysin,[52] zinc(II) and magnesium(II) containing phosphomonoesterase alkaline phosphatase,[27] *Pseudomonas diminuta* phosphotriesterase which contains two metal ions in the active site,[53] *Escherichia coli* methionine aminopeptidase which contains two metal ions in the active site,[54] and kidney bean purple acid phosphatase which contains a dinuclear iron(III)-zinc(II) active site.[55] The prevalence of metal ions as cofactors in many different naturally occurring hydrolytic enzymes has prompted numerous model studies upon the various roles available for the metal ion to effect hydrolysis.

1.4.3.1. Mechanistic Roles of Metal Ions.

1.4.3.1a. Lewis Acid Activation/Metal-Hydroxide Nucleophile. Lewis acid activation refers to the affect upon the rate of hydrolysis when the substrate binds to the metal. Buckingham *et al.* have studied the influence of Lewis acid activation upon the rate of hydrolysis of an amide bond bound to Co(III)pentaammine ($Co(III)(NH_3)_5$) (Figure 1.17).[56] The researchers observed a rate enhancement of 10^4 times over the base-catalyzed background rate when the amide was bound to $Co(III)(NH_3)_5$.

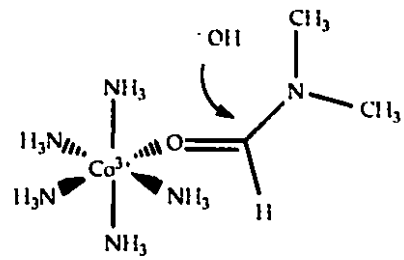

Figure 1.17. Activation of an amide towards hydrolysis by the Lewis acid, $Co(III)(NH_3)_5$.[56]

Many studies require strong Lewis acids in order to achieve any rate acceleration. Palladium(II) and lead(II) have been shown to be effective for promoting the hydrolysis of amides[57] and RNA molecules.[58] A difficult challenge in developing synthetic hydrolytic metalloenzymes is the incorporation of the weaker biological Lewis acids such as magnesium(II) and calcium(II) into highly reactive systems for promoting hydrolysis.

Metal ions can facilitate the hydrolysis of substrates by providing a metal-hydroxide nucleophile at physiological pH. The metal-hydroxide efficacy for promoting amide hydrolysis has been demonstrated in a novel system designed by Groves and Baron.[59] The amide substrate was anchored to the ligand of the cobalt(III) complex as shown in Figure 1.18. The intramolecular metal-hydroxide accelerated the cleavage of the bound amide by 10^8 fold at pH 7.0 and 25 °C.

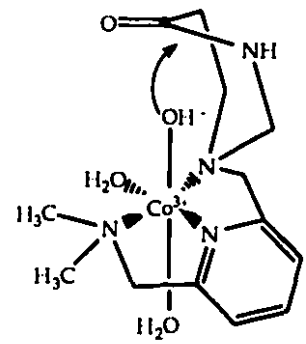

Figure 1.18. Amide hydrolysis activated by a metal-hydroxide nucleophile.[59]

Studies have shown that an intermolecular metal-hydroxide is a poor nucleophile unless the substrates are very electrophilic such as SO_2 or CO_2, or when a very good leaving group is involved, such as acid chlorides and anhydrides.[60] With less electrophilic substrates and poorer leaving groups the intermolecular metal-hydroxide has difficulty competing with the aqueous hydroxide nucleophile at neutral pH.

Chin *et al.* have compared the reactivity of two complexes, cobalt(III)tris(3-aminopropyl)amine (Co(III)trpn) and cobalt(III)tris(2-aminoethyl)amine (Co(III)tren), for promoting the hydrolysis of an activated phosphate diester, bis(4-nitrophenyl) phosphate (BNPP).[3,61] Co(III)trpn (0.01M) and Co(III)tren (0.01 M) provided ~10^{10} and ~10^{8} fold rate acceleration, respectively, at pH 7 and 25 °C for the hydrolysis of BNPP. The proposed mechanism of cleavage of BNPP by the aquo-hydroxo form of the cobalt(III) complexes involved a combination of Lewis acid activation and intramolecular metal-hydroxide attack (Figure 1.19). The difference in rate accelerations between the two complexes was determined to result from the ability of Co(III)trpn to better stabilize the four-membered transition state that formed during the course of the reaction, due to the greater flexibility of the angle opposite the four-membered ring. Sargeson *et al.* have shown that

Co(III)$(NH_3)_5$ accelerated the hydrolysis of an activated phosphate diester by 10^2-10^3 fold through Lewis acid activation.[62] Therefore in the Chin *et al.* studies the intramolecular metal-hydroxide accounted for up to 10^8 fold rate acceleration for the hydrolysis of a phosphate diester.

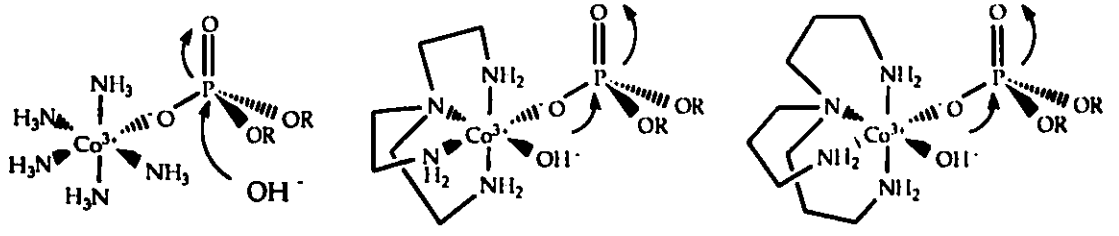

Co(III)$(NH_3)_5$ Co(III)tren Co(III)trpn

Figure 1.19. Lewis Acid /Metal Hydroxide Activation of Phosphate Diesters.[3,62]

1.4.3.1b. Lewis Acid Activation/Metal-Hydroxide General Base. The substrate RNA contains an internal nucleophile rendering the metal-hydroxide nucleophile redundant. The metal-hydroxide can however act as a general base thereby activating the internal nucleophile through deprotonation. Matsumoto and Komiyama have reported the cleavage of a diribonucleotide, adenylyl(3'-5')adenosine (ApA), by Co(III)triethylenetetramine (Co(III)trien).[63] Co(III)trien (0.2M) provided 10^4 fold rate-acceleration for the hydrolysis of ApA at pD 6.0 and 50 °C through the proposed mechanisms of joint Lewis acid/metal-hydroxide general base (Figure 1.20). If the rate acceleration due to Lewis acid activation is subtracted then the metal-hydroxide general base provided at the most 10^2 fold rate acceleration. Typically intramolecular general base catalysis does not greatly affect the rate of hydrolysis. Kirby has reported that the highest observed effective molarity for intramolecular general base catalysis is 80 M and that

usually for intramolecular general base catalysis the effective molarity is less than 10 M.[64]

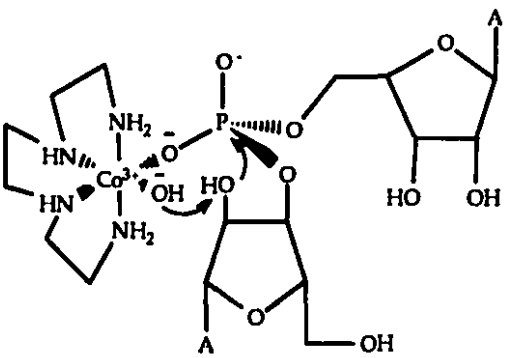

Figure 1.20. Co(III)trien promoted cleavage of ApA through joint Lewis acid activation/metal-hydroxide general base mechanism.[63]

1.4.3.1c. Leaving Group Activation. Leaving group activation, a stabilizing interaction between the positively charged metal and the oxyanion leaving group of the hydrolysis reaction, is difficult to achieve in model systems. Studies have been completed with phosphate substrates that incorporate alkoxide leaving groups capable of coordinating metal ions.[65-68] Browne and Bruice have synthesized two novel phosphate esters; sodium bis(8-hydroxyquinoline) phosphate (B8HQP) and sodium bis(6-hydroxyquinoline) phosphate (B6HQP).[68] The rate of hydrolysis of B8HQP (0.2 mM) was considerably enhanced in the presence of (1 M) Ni^{2+}, Co^{2+}, and Zn^{2+} whereas the rate of hydrolysis of B6HQP (0.2 mM) was not affected by the presence of 1 M metal ions (Ni^{2+}, Co^{2+}, Zn^{2+}, Mn^{2+}). The rate enhancement of B8HQP hydrolysis, due to a combination of intramolecular nucleophilic catalysis and metal leaving group activation, was estimated to be 10^7 fold (Figure 1.21). The combination of nucleophilic and specific acid catalysis provided 10^3 rate enhancement for B8HQP in the absence of metals, therefore

in the presence of metals the metal leaving group activation accounted for a rate enhancement of at least 10^4 fold.

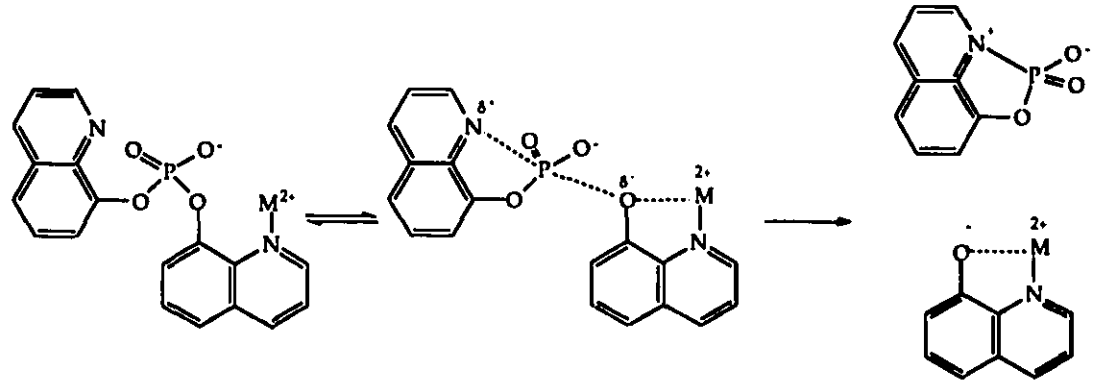

B8HQP-M^{2+}

Figure 1.21. Nucleophilic catalysis and leaving group activation by divalent metal ions upon a phosphate diester.[68]

1.4.3.1d. Dinuclear Activation. The cooperation between two metals for the transesterification of HPNPP, an RNA analog, has been demonstrated by Wall and Chin.[69] The dinuclear copper(II) complex $Cu(II)_2$bbima (0.5 mM) demonstrated ~50 fold greater reactivity per metal center than the corresponding mononuclear copper(II) complex, Cu(II)bima (1 mM), at pH 7.0 and 25 °C (Figure 1.22). The difference in reactivity was proposed to result from the ability of $Cu(II)_2$bbima to bridge the substrate, thus providing double Lewis acid activation, whereas Cu(II)bima provided only single Lewis acid activation.

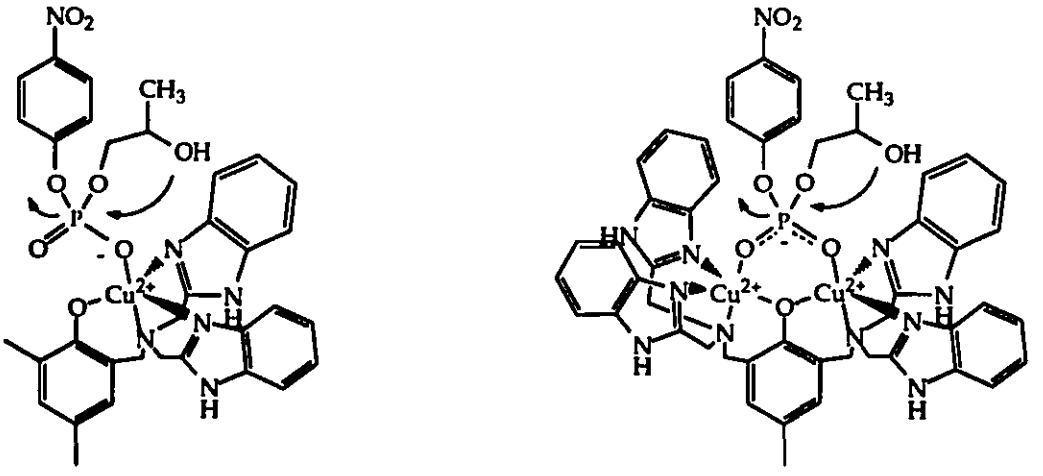

Cu(II)bima

Cu(II)$_2$bbima

Figure 1.22. Single Lewis acid activation versus double Lewis acid activation for promoting the transesterification of an RNA analog.[69]

Murthy *et al.* have designed a dinuclear copper(II) complex that has demonstrated remarkable reactivity for amide hydrolysis.[70] The hydrolysis of N,N-dimethylformamide (DMF) was achieved by two different routes; the dinuclear copper(I) complex (Cu(I)$_2$PD) reacted with molecular oxygen to generate the reactive species and effect hydrolysis in the presence of DMF and also by reacting the dinuclear copper(II) complex (Cu(II)$_2$PDO) in the presence of DMF under mildly acidic conditions (Figure 1.23). The authors proposed that the reactivity of the complex for amide hydrolysis resulted from metal-hydroxide activation on one copper(II) ion and Lewis acid activation of the bound substrate by the second copper(II), or alternatively attack by a strong nucleophile, a copper(II)-peroxo species generated *in situ*, upon DMF.

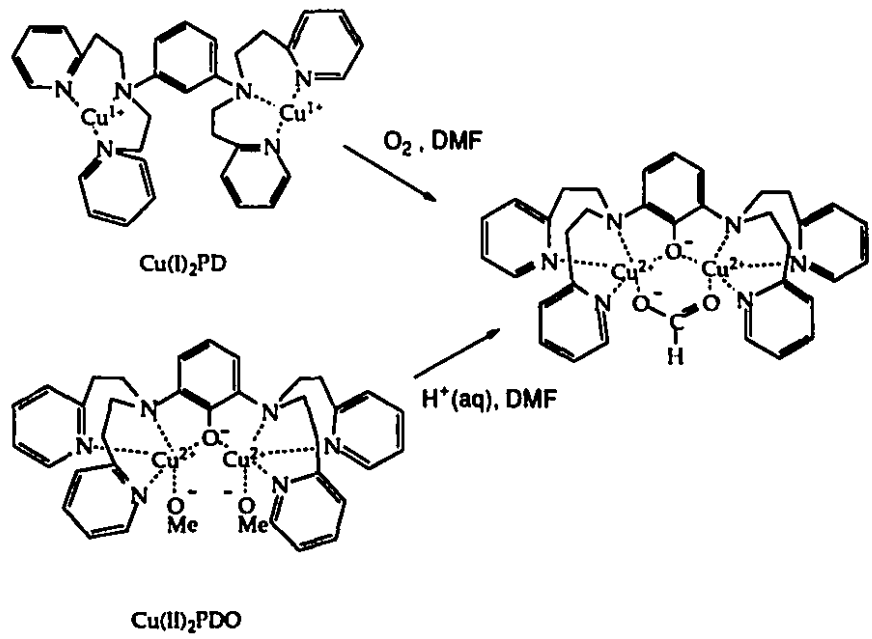

Figure 1.23. Amide hydrolysis effected by a dinuclear copper(II) complex.[70]

Interestingly a crystal structure of a dinuclear copper(II) complex ($Cu(II)_2XYLO$) bridging BNPP has been determined as shown in Figure 1.24.[71] There has been no reactivity reported for phosphate ester hydrolysis activated by this complex. The crystal structure is a clear indication of the complex's ability to provide double Lewis acid activation, a strategy that has demonstrated its effectiveness for hydrolyzing RNA substrates. It is possible that under suitable reaction conditions $Cu(II)_2XYLO$ could cleave RNA, or an RNA analog.

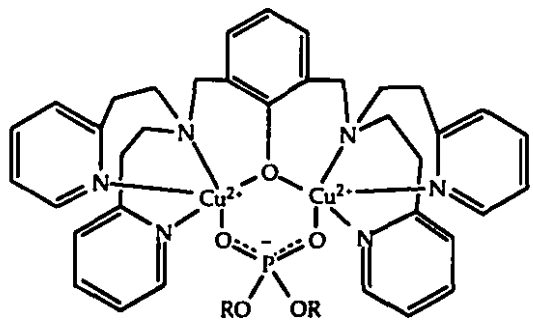

Figure 1.24. A crystal structure of the dinuclear copper(II) complex, $Cu(II)_2XYLO$, bridging a phosphate diester has been determined.[71] (R = 4-nitrophenyl).

A dinuclear system is not required to demonstrate the efficacy of double Lewis acid activation for hydrolyzing phosphate diesters. In fact the most reactive transition metal complex to date for hydrolyzing ApA is copper(II)neocuproine (Cu(II)neo).[47] Cu(II)neo (10 mM) at pH 7.0 and 25 °C provided ~10^8 fold rate acceleration over the background rate for cleaving RNA. Linkletter and Chin proposed that the mechanism of cleavage proceeded by double Lewis acid activation through chelation of the substrate to the metal complex (Figure 1.25).

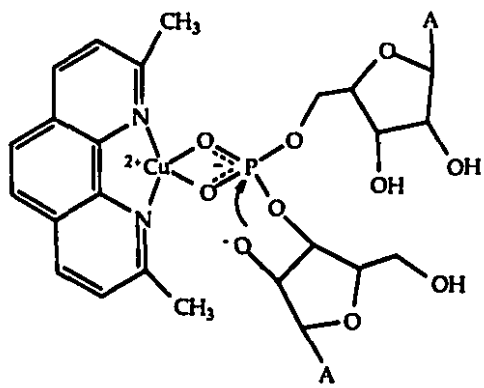

Figure 1.25. Cu(II)neocuproine promoted cleavage of ApA.[47]

1.4.3.2. Sequence Specific Hydrolytic Cleavage of RNA.

A target of the antisense strategy, sequence specific cleavage of RNA, has been achieved with varying degrees of success by four different research groups. All the researchers employed a common strategy to achieve their goal, a complementary single-stranded oligodeoxyribonucleotide was conjugated to a chemical cleaving moiety. The following metal complexes were used to achieve cleavage: Cu(II)(2,2':6',2''-terpyridine) (Cu(II)ter),[72] Eu(III)texaphyrin (Eu(III)tex),[73] Lu(III)iminodiacetate (Lu(III)ida),[74] and a europium(III) complex of a terpyridine derivative (Eu(III)terp)[50] (Figure 1.26). A summary of the results obtained are shown in Table 1.1.

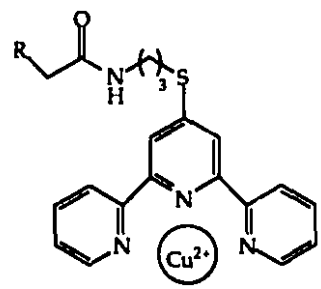

Cu(II)ter

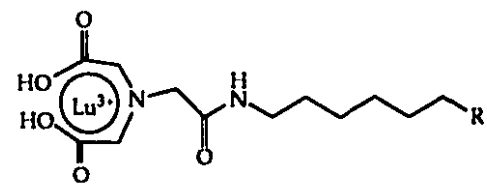

Lu(III)ida

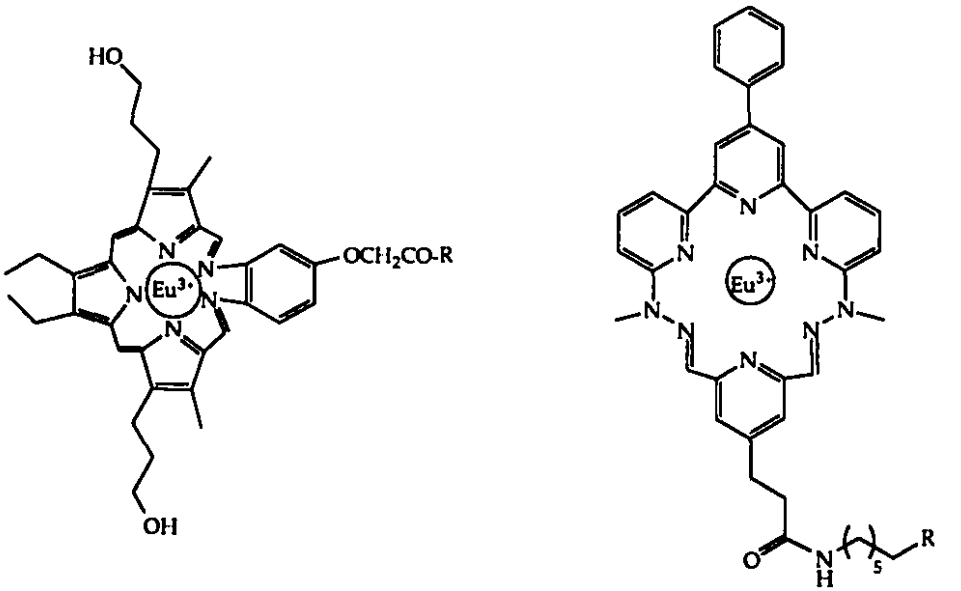

Eu(III)tex Eu(III)terp

Figure 1.26. Sequence selective RNA cleavage agents.[50,72-74] R represents the complementary oligodeoxyribonucleotide strand.

Table 1.1. Sequence Specific cleavage of RNA.

complex	RNA substrate	cleaving agent	pH	T (°C)	Time (h)	% target cleavage	~ half-life (h)
Cu(II)ter[72]	10 nM (159-mer)	5 μM (17-mer)	7.5	45	72	18-25	173-250
Eu(III)tex[73]	1 nM (30-mer)	25 nM (20-mer)	7.5	37	18-24	30	35-47
Lu(III)ida[74]	300 nM (39-mer)	10 μM (15-mer)	8.0	37	8	17	30
Eu(III)terp[50]	10 nM (29-mer)	400 nM (20-mer)	7.5	37	16	88	5

These are significant studies since they clearly demonstrate the ability of synthetic nucleases to effect sequence-specific hydrolytic cleavage of RNA. Their reactivities however fall far short of natural enzymes and therefore more reactive synthetic sequence-selective ribonucleases are still required. Of

the four complexes in Table 1.1 only one complex, Cu(II)ter, has been shown in a previous study to cleave an RNA substrate.[47,75] Cu(II)ter (10 mM, 25 °C) cleaves ApA with a half life of 10 hours at pH 8.[47] The antisense strategy provides a rational approach towards designing drugs for gene therapy. The design of the cleaving agent for possible antisense applications should be equally rational. In order to improve the efficacy of sequence-specific synthetic ribonucleases a detailed understanding of the mechanism of cleavage by the cleavage component and the binding interactions of the recognition component is required. The systems in Table 1.1 provide a strong basis for further developing sequence specific synthetic ribonucleases and hopefully in the future the reactivities can be improved.

1.4.3.3. DNA Hydrolysis Mediated by Metal Ions and Metal Complexes.

The metal promoted hydrolysis of DNA by nonenzymatic systems represents a difficult challenge considering the stability of the phosphoester linkage. As a result the literature has relatively few examples of synthetic nucleases that promote the hydrolysis of DNA, as compared to those that hydrolyze RNA. Tremendous rate acceleration ($\sim 10^{11}$) has been observed for the hydrolysis of a deoxyribonucleotide, dApdA, by cerium(III) ion (20 mM) in the presence of molecular oxygen at pH 8.2 and 37 °C[48] and by Ce(IV) ion (10 mM) at pH 7 and 50 °C [49]. The proposed mechanism by Takasaki and Chin for hydrolysis incorporated a peroxide bound nucleophile attacking the bridging substrate (Figure 1.27).[48] Cerium(IV) ion promoted hydrolysis is approaching the rate acceleration necessary for antigene agents, unfortunately the metal ions provide no handle for a recognition component to be covalently linked for sequence selection.

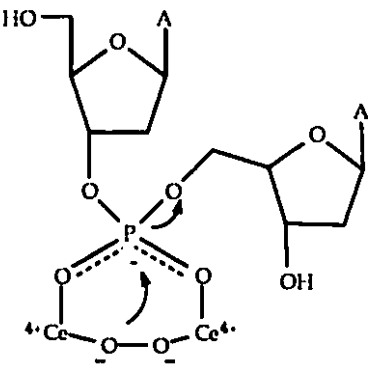

Figure 1.27. Proposed mechanism for reactivity of Ce(IV) ion upon deoxyribonucleotide, dApdA.[48]

Two-metal ion activated hydrolysis was investigated using a dinuclear cobalt(III) complex of 1,4,7-triazacyclononane (tacn) that can be isolated with a doubly coordinated phosphate diester (P).[76,77] The complex, $Co(III)_2(tacn)_2(OH^-)_2(P)$, does not undergo rapid substitution enabling the effect of the dinuclear complex alone on the hydrolysis of phosphate diesters to be studied. A DNA analog, methyl 4-nitrophenyl phosphate (MPNPP), was hydrolyzed with a 10^{12} acceleration over the background rate by $Co(III)_2(tacn)_2(OH^-)_2(P)$ through a mechanism suggested to involve double Lewis acid activation and the attack of a bridging nucleophilic oxo ligand (Figure 1.28).[76] Double Lewis acid activation alone was shown to provide ~ 4 $\times 10^5$ fold rate acceleration (25 °C) by substituting an RNA analog, 2-hydroxypropyl phenyl phosphate (HPPP), for the DNA analog.[77]

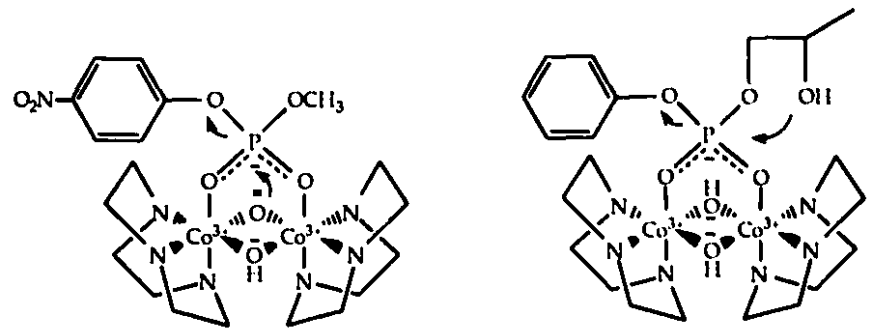

Figure 1.28. Proposed mechanism of cleavage of a DNA analog and an RNA analog by $Co(III)_2(tacn)_2(OH^-)_2(P)$.[76,77]

The hydrolysis of DNA by a ruthenium(II) octahedral (Ru(II)DIP) complex has been reported by Basile *et al.* (Figure 1.29).[78] After 5 hours a 30% conversion was reported of form I supercoiled DNA, a more reactive form of DNA than linear DNA, to nicked form II DNA under the following reaction conditions: 7 μM Ru(II)DIP, 160 μM Zn(II) ion, (or Cd(II) ion or Pb(II) ion), 37 °C, and pH 8.5. The reactivity was proposed to result from a metal-hydroxide nucleophile (of Zn(II), Cd(II) or Pb(II)) being delivered to the substrate by Ru(II)DIP, a complex that strongly binds DNA.

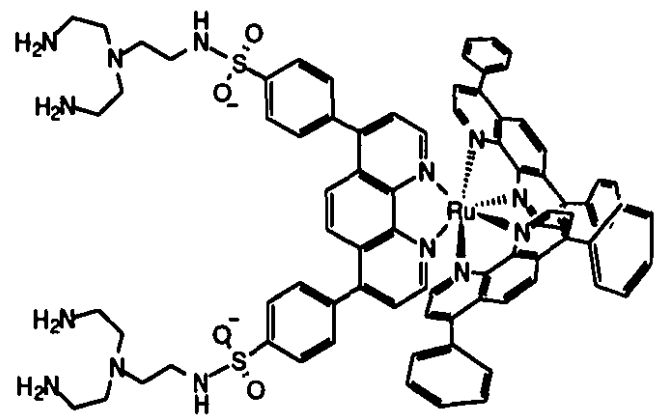

Figure 1.29. Double-stranded DNA cleaving agent Ru(II)DIP.[78]

Reactive synthetic hydrolytic nucleases have been developed, however more reactive systems are required if the desired goal is to match the efficiency of nature's nucleases. This efficiency is necessary if synthetic nucleases are to be applied to either molecular biology or the antisense and antigene fields.

1.5. Plan of Study.

Two independent studies have been designed with the objective to develop and understand the mechanism of activation of simple transition metal complexes that mediate the hydrolysis of phosphate diesters.

The first study was designed to compare the reactivities of metal-hydroxides to metal-alkoxides for cleaving phosphate diesters. This study is relevant to the proposed metal-alkoxide attack of serine in alkaline phosphatase and of guanosine during group I intron ribozyme cleavage.[16,27] Two novel copper(II) complexes that contained pendant alcohol groups were prepared. The reactivities and mechanisms of cleavage of an activated phosphate diester by the two copper(II) complexes, with pendant alcohol groups, are compared to that of the corresponding copper(II) complex without a pendant alcohol group. From these results a relationship between the structure of the copper(II) complex and the reactivity for cleavage of the phosphate diester is proposed.

The second study was designed to examine the advantage of a dinuclear transition metal complex, that bridges phosphate diesters through both metal centers, for cleaving RNA to a mononuclear transition metal complex. This study was inspired by previous dinuclear metal systems[69,79] that effectively mediated the cleavage of RNA analogs and also by the many phosphoesterases [26-28,55,80] that require two or more metals for activation. For this study a novel dinuclear copper(II) complex is synthesized and its activity for cleaving a diribonucleotide and the cyclic phosphate intermediate is tested. The mechanism of the RNA activation by the dinuclear metal complex is investigated and compared to the corresponding mononuclear metal complex.

Chapter 2. Metal-Alkoxide Versus Metal-Hydroxide Reactivity for Cleaving an Activated Phosphate Diester.

2.1. Introduction.

The role of metal ions as nucleophilic catalysts in the hydrolysis of phosphodiester bonds has been extensively studied in enzymatic and non-enzymatic systems. Numerous model studies have shown that the metal-hydroxide nucleophile provides relatively large rate accelerations over the base-catalyzed hydrolysis of phosphate diesters at physiological pH.[3,59] This is understandable considering that in the absence of metals the ionization of water, to produce OH^- and H^+, requires 21.6 kcal/mol at room temperature in aqueous solution.[81] In the presence of metals this energy demand is reduced due to electrostatic stabilization of the negative charge. Many hydrolytic metalloenzymes in nature use metal-hydroxide nucleophiles to promote phosphate ester hydrolysis, however the metal-hydroxide nucleophile is not exclusive. Enzymes such as alkaline phosphatase[27] and group 1 intron ribozymes[16] use metals to promote nucleophilic attack of an alcohol, or alkoxide, upon the phosphate substrate. Alkaline phosphatase is a hydrolytic metalloenzyme that cleaves phosphate monoesters under basic conditions. The accepted mechanism of catalytic action of alkaline phosphatase is outlined in Figure 2.1.[27] Of interest is the covalent intermediate that forms between serine 102 from the peptide chain of alkaline phosphatase and the substrate. The guanosine cofactor present in group 1 intron ribozymes promotes self-cleavage through two consecutive transesterification steps

(Figure 1.11).[16] The advantage for these metalloenzymes to use a metal-alkoxide nucleophile instead of a metal-hydroxide nucleophile has not been established. There have been many model studies exemplifying the rate enhancement of phosphoester hydrolysis by a metal bound hydroxide, however there have been relatively few model studies demonstrating the effect of a metal bound alkoxide on the rate of hydrolysis.

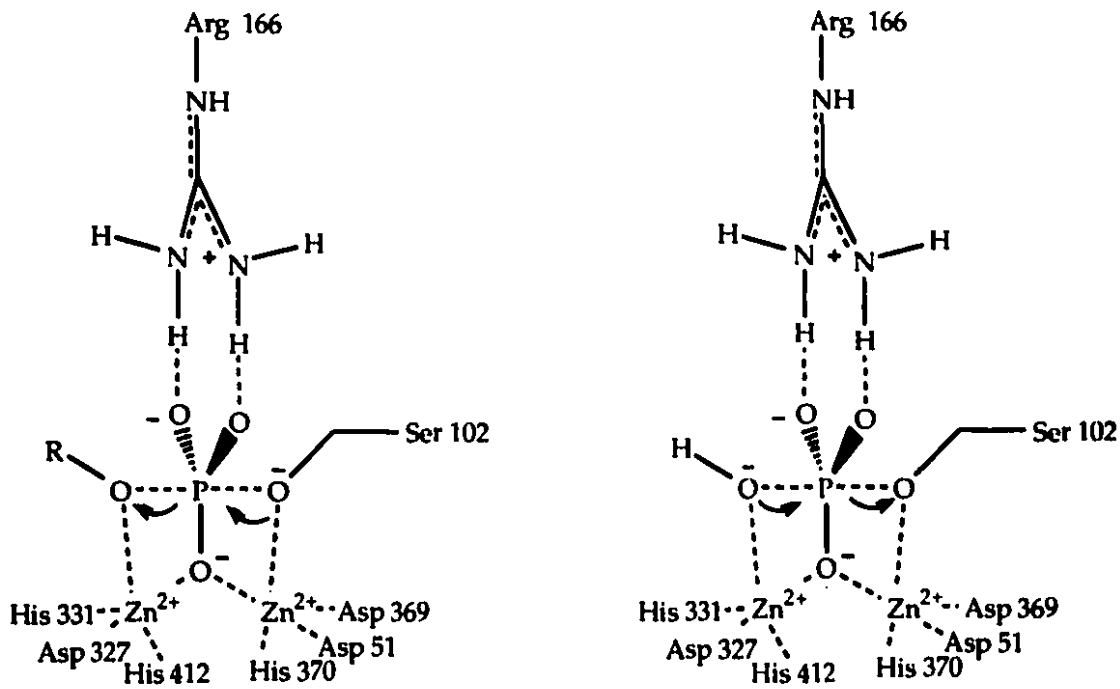

Figure 2.1. Proposed mechanism of cleavage of phosphate monoesters by Alkaline Phosphatase.[27] Cleavage occurs through two consecutive transesterification steps.

Kimura *et al.* have reported a study that compared the reactivity of three zinc(II) complexes; Zn(II)cyclen, Zn(II)((S)-1-hydroxy-2-phenylethyl)cyclen) (Zn(II)hphcyclen) and Zn(II)(N-methylcyclen) (Zn(II)mcyclen) for cleaving BNPP (Figure 2.2).[82] The second order rate constants of BNPP cleavage at 35 °C by Zn(II)cyclen, Zn(II)hphcyclen, and Zn(II)mcyclen are given in Table 2.1.

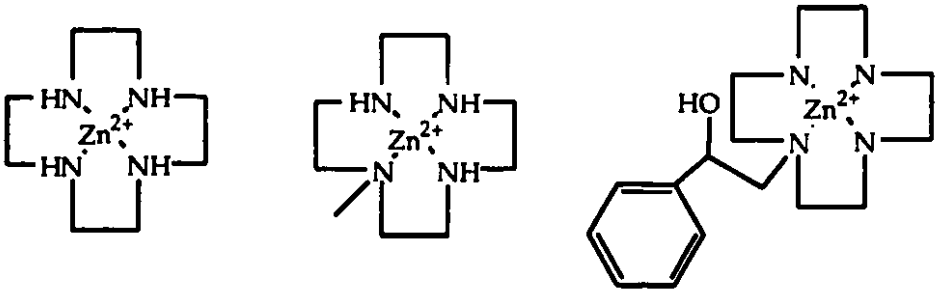

Zn(II)cyclen Zn(II)mcyclen Zn(II)hphcyclen

Figure 2.2. The complex, Zn(II)hphcyclen, promoted the cleavage of a phosphate diester at a greater rate than Zn(II)cyclen or Zn(II)mcyclen.[82]

Table 2.1. Comparison of the phosphodiester bond cleavage rate constants by Zn(II)cyclen, Zn(II)hphcyclen and Zn(II)mcyclen.

Catalyst	Rate Constant[82] ($M^{-1}s^{-1}$)
Zn(II)cyclen	2.1×10^{-5}
Zn(II)mcyclen	5.2×10^{-6}
Zn(II)hphcyclen	6.5×10^{-4}

The pH rate profiles of the complexes had a sigmoidal shape with an inflection occurring at the pK_a of each of the complexes, indicating that either the metal-hydroxide or the metal-alkoxide was the active species. Zn(II)hphcyclen was ~27 times more reactive than Zn(II)cyclen and ~125 times more reactive than Zn(II)mcyclen for cleaving BNPP. The difference in reactivity was attributed to the greater nucleophilicity of metal-alkoxide than metal-hydroxide. Elemental analysis and ^{1}H, ^{13}C, and ^{31}P NMR confirmed that Zn(II)hphyclen cleaved BNPP through transesterification rather than hydrolysis.

Morrow *et al.* have documented a 10^7 rate enhancement of BNPP at 25 °C and pH 7.4 in the presence of 1 mM europium(III)(1,4,7-10-tetrakis(2-hydroxyethyl)-1,4,7,10-tetraazacyclododecane) (Eu(III)THED) (Figure 2.3).[83] The pH-rate profile had a sigmoidal shape with an inflection occurring at 7.4, the pK_a of the complex. Analysis of the products of the reaction between BNPP and Eu(III)THED by ^{31}P NMR, HPLC, and analytical analysis was consistent with metal-alkoxide attack on the phosphate diester resulting in transesterification. No explanation was offered by the authors regarding the benefit of the metal-alkoxide nucleophile.

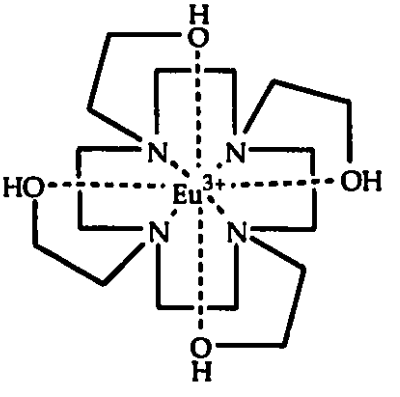

Figure 2.3. Eu(III)THED.

The aforementioned studies are relevant to the role of the serine in alkaline phosphatase and guanosine in group I intron ribozymes because they demonstrate the potential of a metal-alkoxide to be a more reactive nucleophile than a metal-hydroxide for cleaving phosphate bonds. To the best of our knowledge the studies reported by Kimura *et al.*,[82] Morrow *et al.*,[83] and our study[84] represent the only documented examples of metal-alkoxide nucleophilic attack upon a phosphate diester in a model system.

Our study concentrated on comparing the reactivities and mechanisms of copper(II) complexes of bis(2-pyridylmethyl)amine (bpa), N-(2-

hydroxyethyl)bis(2-pyridylmethyl)amine (hebpa), and N-(3-hydroxypropyl)bis(2-pyridylmethyl)amine (hpbpa) for cleaving bis(2,4-dinitrophenyl) phosphate (BDNPP) (Figure 2.4). For this system a novel structure-reactivity relationship is proposed that accounts for the observed differences in reactivities and mechanisms between the metal-hydroxide and metal-alkoxide nucleophiles for cleaving the phosphate diester.

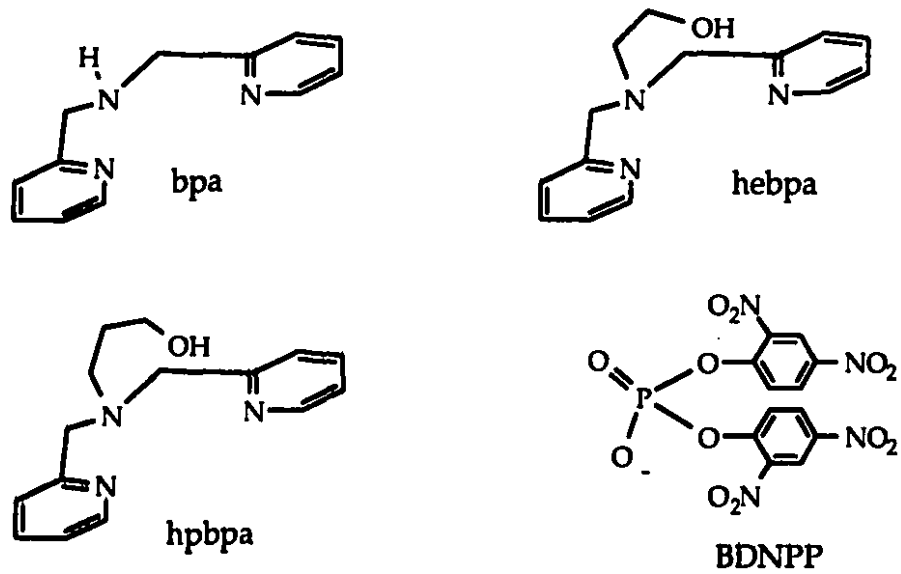

Figure 2.4. Structures of bpa, hebpa, hpbpa, and BDNPP.

2.2. Results and Discussion.

2.2.1. Activated Substrates.

Many studies of phosphate ester hydrolysis have used activated phosphate esters with good leaving groups as models of biologically relevant unactivated phosphate esters with poor leaving groups. A relationship has been demonstrated between the second-order rate constant for the base-catalyzed hydrolysis of phosphate diesters at 25 °C and the basicity of the leaving group (Figure 2.5).[3] The plot, which spans 12 orders of magnitude in the basicity of the leaving group including both alkyl and aryl leaving groups, indicates that substrates are hydrolyzed by the same base-catalyzed mechanism.

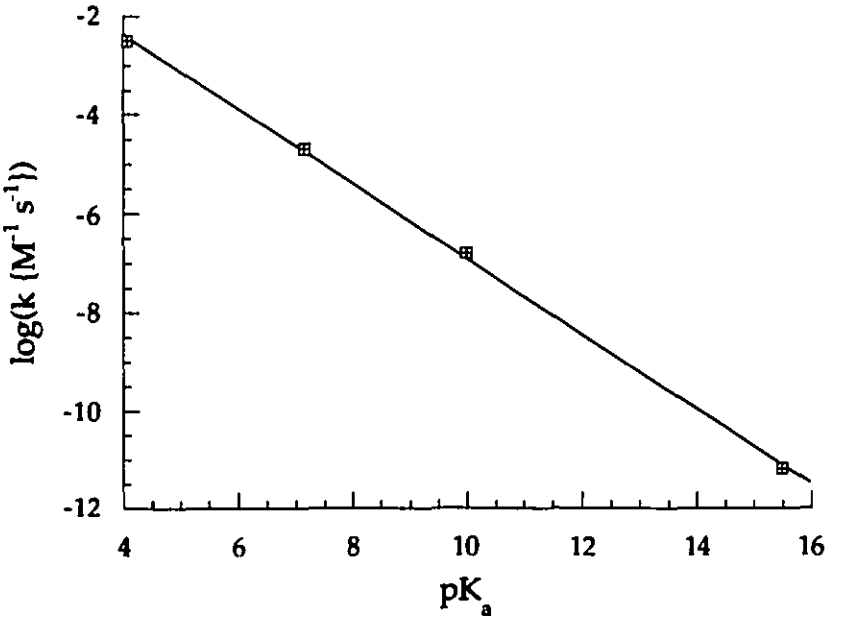

Figure 2.5. Linear free-energy relationship between the second-order rate constants for base-catalyzed hydrolysis of phosphate diesters at 25°C and the pK_a of the conjugate acid of the leaving group.[3]

The use of activated substrates as models of biological substrates has received criticism from Menger and Ladika, who have labeled the shortcomings of activated substrates as the p-nitrophenyl ester syndrome.[85] Undeniably the rate accelerations observed for the cleavage of activated phosphate esters and unactivated phosphate esters in model systems are not always consistent. For example Co(III)cyclen provides comparable rate-accelerations for hydrolyzing BNPP[3] and dimethyl phosphate,[86] however Cu(II)(2,2':6',2"terpyridine) provides a greater rate-acceleration for hydrolyzing 2'3'-cyclic AMP than for hydrolyzing BNPP.[87] The use of activated phosphate diesters with good leaving groups, even though they may not always be good models of unactivated phosphate diesters with poor leaving groups, might be

justified if the role of the metal ions in stabilizing the leaving group in many of nature's phosphatases is considered.

The *Tetrahymena* ribozyme catalyzes the cleavage of RNA or DNA substrates in the presence of magnesium(II) or manganese(II) ions to yield 3'OH and 5'PO_4 products. Piccirilli *et al.* synthesized a DNA substrate that had the 3'oxygen at the cleavage site replaced by a sulfur atom (Figure 2.6).[80] In the presence of magnesium(II) ion the 3'-sulfur substrate was cleaved 10^3 times more slowly than the corresponding unmodified substrate, presumably due to magnesium(II) ion's low affinity for sulfur.[80]

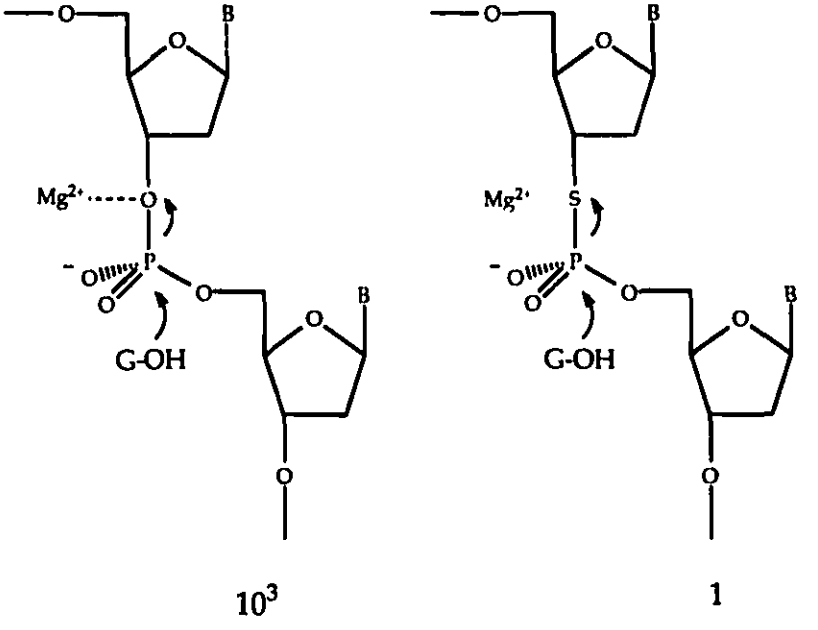

10^3 1

Figure 2.6. Leaving group activation in the *Tetrahymena* ribozyme.[80] The relative rates of cleavage of the two substrates in the presence of magnesium(II) by the ribozyme are given.

These results indicated that the metal ion contributed to catalysis by coordinating to the 3'oxygen atom in the transition state, thus stabilizing the developing negative charge of the leaving group. Coordination of the

leaving group oxygen to a metal ion has been similarly proposed in the hydrolysis of DNA by the 3'5'-exonuclease activity of *Escherichia coli* DNA polymerase I and the cleavage of phosphate monoesters by alkaline phosphatase.[26,27] The role of the metal ion, by coordinating the oxyanion leaving group, can be viewed as converting a poor leaving group into a good leaving group. If we can consider activated substrates with good leaving groups as the equivalent of poor leaving groups coordinated to a metal then activated substrates can be considered as relevant models of biological substrates.

2.2.3. Synthesis and Structure.

The ligands bis(2-pyridylmethyl)amine (bpa)[88] and N-(2-hydroxyethyl)bis(2-pyridylmethyl)amine (hebpa)[89] were prepared by the literature methods. The novel ligand N-(3-hydroxypropyl)bis(2-pyridylmethyl)amine (hpbpa) was prepared under reductive amination conditions according to Figure 2.7.

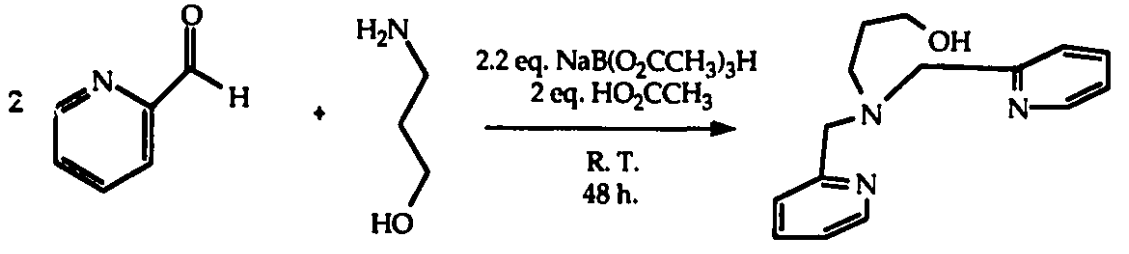

hpbpa

Figure 2.7. Synthesis of N-(3-hydroxypropyl)bis(2-pyridylmethyl)amine (hpbpa).

In water the copper(II) chloride complexes of bpa, hebpa, and hpbpa should form the square pyramidal dicationic species Cu(II)bpa, Cu(II)hebpa,

and Cu(II)hpbpa, respectively (Figure 2.8). The solvent water molecules are expected to reversibly displace the coordinated pendant alcohol groups in Cu(II)hebpa and Cu(II)hpbpa to varying degrees.

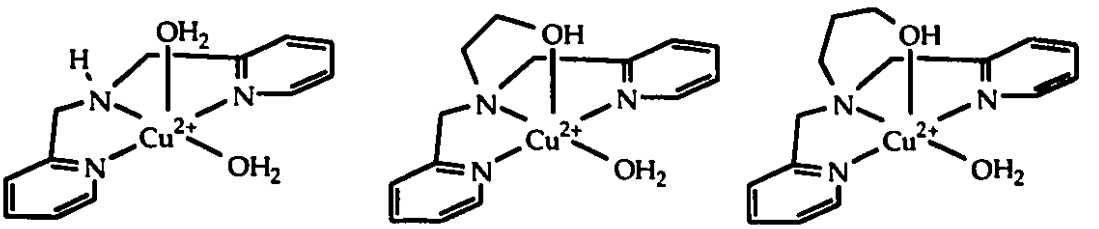

Cu(II)bpa Cu(II)hebpa Cu(II)hpbpa

Figure 2.8. Structures of Cu(II)bpa, Cu(II)hebpa, and Cu(II)hpbpa.

Crystal structure data[84] of two analogs were compared in order to gain insight into the structures of Cu(II)bpa, Cu(II)hebpa, and Cu(II)hpbpa. Bis(2-benzimidazolylmethyl)amine (bba) and N-(2-hydroxyethyl)bis(2-benzimidazolylmethyl)amine (hebba) are considered respective analogs of bpa and hebpa. The pyridine groups in bpa and hebpa are replaced with benzimidazole groups in the two analogs. Crystallographic studies show that [Cu(II)bba(OP(O)(OCH_3)$_2$)($HOCH_3$)]Cl and (Cu(II)hebbaCl)Cl (abbreviated as Cu(II)bba(P) and Cu(II)bba, respectively) are square pyramidal in structure with the alcohol groups coordinated at the apical position (Figure 2.9).

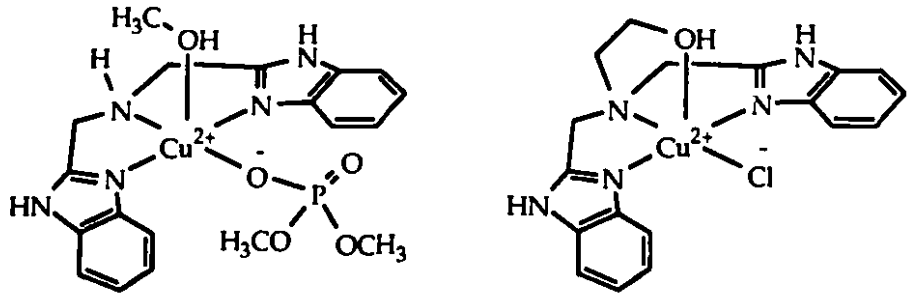

Cu(II)bba(P) Cu(II)hebba

Figure 2.9. Structures of Cu(II)bba(P) and Cu(II)hebba.

2.2.4. Potentiometric Titrations.

Potentiometric titrations of Cu(II)bpa, Cu(II)hebpa, and Cu(II)hpbpa gave one titratable proton each with pK_a values between 8.7 and 8.8. It is not clear whether the observed pK_a values are due to the metal bound alcohol groups or the metal bound water molecules. The constancy of the pK_a values suggests that the titratable protons in the three complexes are from the coordinated water molecules at the equatorial position. The coordinated water molecules at the equatorial position should be more acidic than the coordinated water molecules at the apical position since the equatorial water-to-copper bond lengths are expected to be shorter than the apical water-to-copper or alcohol-to-copper bond lengths.[90-93] For example, the apical chloride-to-copper bond length in Cu(II)bba (2.60 27(22) Å) is significantly longer than the equatorial chloride-to-copper bond length (2.26 74(21) Å) in the same complex (Figure 2.10).[79]

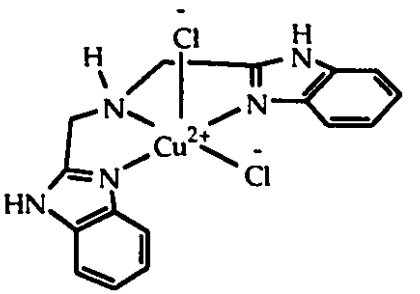

Cu(II)bba

Figure 2.10. Structure of Cu(II)bba.

2.2.5. Binding of Phosphate Diesters to Copper(II) Complexes.

The equilibrium constants of a phosphate diester, dimethyl phosphate (DMP), to Cu(II)bpa, Cu(II)hebpa, and Cu(II)hpbpa were determined by potentiometric titrations. The observed acid dissociation constant of the metal bound water of the copper(II) complex changes in the presence of differing concentrations of DMP according to equation 2.1 (Figure 2.11).

$$1/[H^+]_{midpoint} = 1/C(([DMP]/K_dK_a) + 1/K_a) \qquad \text{equation 2.1}$$

In equation 2.1, $[H^+]_{midpoint}$ represents the proton concentration at the observed K_a, C is a constant (see appendix B), K_a represents the true acid dissociation constant of the water bound to the metal complex, and K_d represents the dissociation constant of the phosphate from the copper(II) complex.

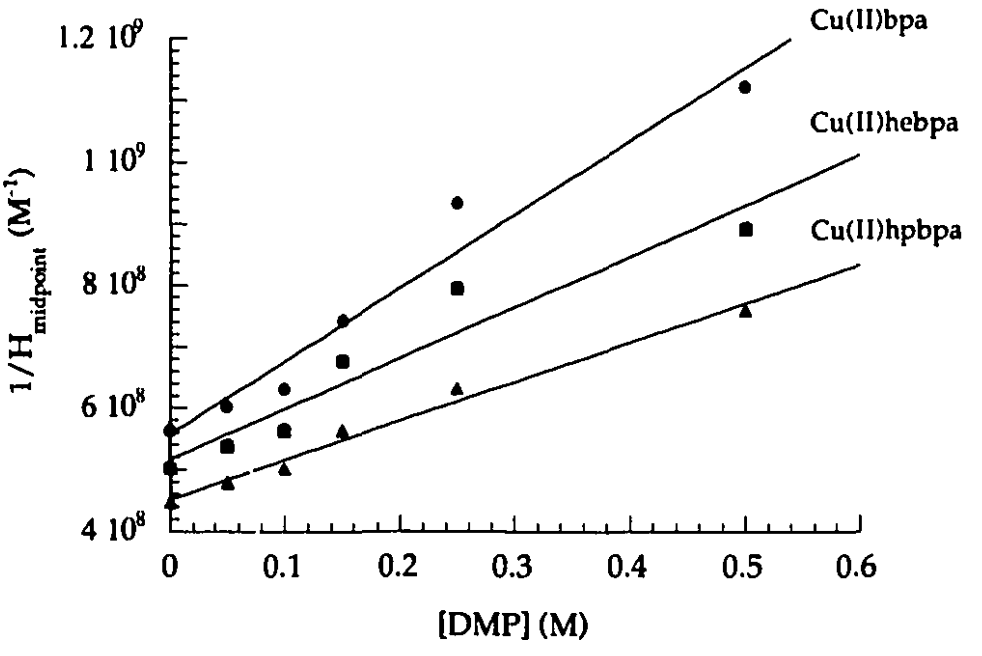

Figure 2.11. Determination of the binding constants of a phosphate diester to Cu(II)bpa, Cu(II)hebpa, and Cu(II)hpbpa. {R(equation 2.1)= 0.98 (Cu(II)bpa), 0.96 (Cu(II)hebpa), 0.99 (Cu(II)hpbpa)}.

The equilibrium constants ($K_{association}$) for the binding of DMP to the three copper(II) complexes and the acid dissociation constants (pK_a) of the water bound to the metal complex, as determined using a non-linear least-squares analysis, from the fit of equation 2.1 to Figure 2.11 are given in Table 2.2.

Table 2.2. The values and errors of $K_{association}$ and pK_a as determined from the observed pK_a dependence upon the concentration of DMP as shown in Figure 2.11.

complex	$K_{association}$ (M^{-1}) $K_{association} = 1/K_d$	pK_a
Cu(II)bpa	2.1 ± 0.3	8.8 ± 0.04
Cu(II)hebpa	1.6 ± 0.3	8.8 ± 0.03
Cu(II)hpbpa	1.4 ± 0.1	8.8 ± 0.03

The equilibrium constant for a phosphate diester coordinating to copper(II)(2,2'-bipyridine) has been reported to be ~20 M^{-1}.[94] The value reported by Morrow and Trogler is large compared to the values that were measured for Cu(II)bpa, Cu(II)hebpa, and Cu(II)hpbpa. The value obtained by Morrow *et al.* appears too large if the association constants of Co(III)trpn, Co(III)tren, and Co(III)cyclen to DMP are considered. The binding constants of DMP to the three cobalt(III) complexes were measured by ^{31}P NMR at 4 ± 1 M^{-1} for all three cobalt(III) complexes.[3] The equilibrium constant of binding of $-OP(O)(OH)_2$ to $Co(III)(NH_3)_5(OH_2)$ was also measured at 8 M^{-1}.[95] Cobalt(III) is a stronger Lewis acid than copper(II) and therefore it is reasonable to assume that the equilibrium constant of binding of a phosphate diester should be greater to a cobalt(III) complex than to a copper(II) complex. The association constant of a phosphate diester to copper(II)(2,2'-bipyridine) as quoted by Morrow and Trogler appears too high if the previously determined association constants of phosphate diesters to cobalt(II) complexes are considered.

Recently Kady *et al.* reported a study that compared the reactivity of zinc(II) complexes of 2,6-bis(aminomethyl)pyridine (Zn(II)bamp) and of a hydroxyethyl derivative of 2,6-bis(aminomethyl)pyridine (Zn(II)hebamp) for

promoting the hydrolysis of a phosphate triester (Figure 2.12).[96] At pH 8.6 and 25 °C, Zn(II)hebamp (2 mM) was reported to accelerate the cleavage of diethyl 4-nitrophenyl phosphate (DENPP) with a 10^4 fold greater rate enhancement than Zn(II)bamp (2 mM). ^{31}P NMR studies indicated that Zn(II)hebamp promoted the cleavage of DENPP through transesterification whereas Zn(II)bamp promoted the hydrolysis of DENPP.

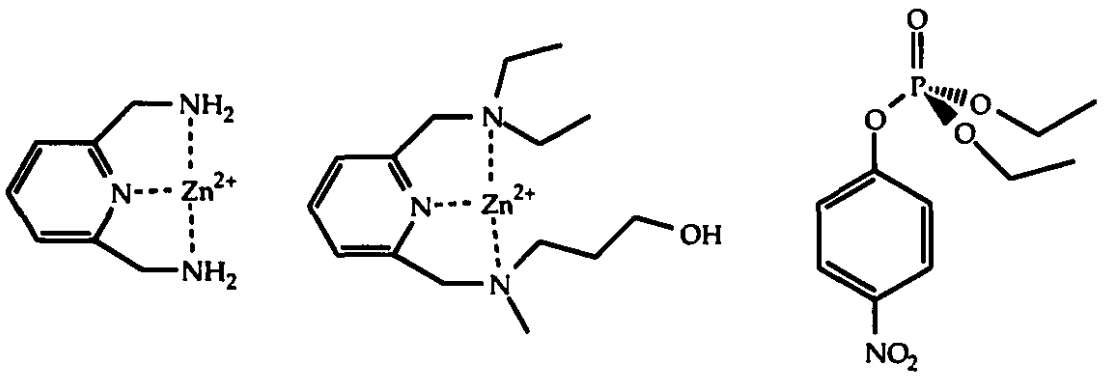

Zn(II)bamp Zn(II)hebamp DENPP

Figure 2.12. Zn(II)hebamp cleaved a phosphate triester (DENPP) 10^4 times faster than Zn(II)bamp according to Kady *et al.*[96]

The results reported by Kady *et al.* are interesting for two reasons; the substrate used in the study was a phosphate triester and that the difference in rate enhancement between the two complexes for cleaving DENPP was so remarkable. Phosphate triesters are not expected to have as large an affinity for metal complexes as phosphate diesters since they are neutral molecules and as a result the rate enhancement of metal promoted hydrolysis of phosphate triesters is typically not as great as that observed for phosphate diesters.[97] In order to explore the potential of Zn(II)hebamp we attempted to repeat the studies reported by Kady *et al.* Under the identical conditions reported by Kady *et al.* (2 mM complex, 10 mM TAPS, pH 8.6, 25 °C, and 0.2 M

$NaClO_4$) it was observed that Zn(II)hebamp did not cleave DENPP with any significant rate acceleration. The source of the discrepancy between the results reported by Kady *et al.* and our results using Kady's compound is unclear.

2.2.5. Cleavage of BDNPP.

The ability of cis-diaquo metal complexes to efficiently hydrolyze phosphate diesters has been well documented.[3,86,98,99] The mechanism of hydrolysis has been proposed to involve the coordination of the phosphate diester to the metal (M) complex followed by intramolecular metal-hydroxide attack on the coordinated phosphate (Figure 2.13).

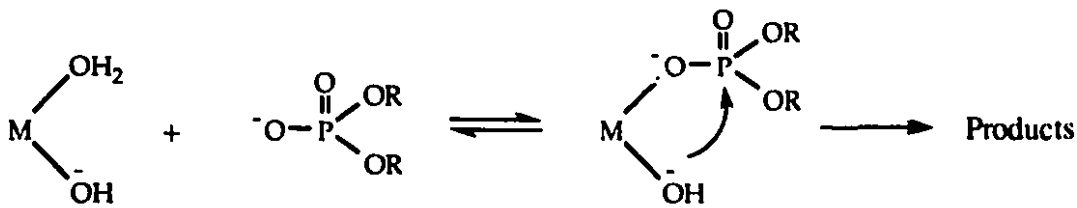

Figure 2.13. Mechanism of cleavage of phosphate diesters by cis-diaquo metal complexes

It is the cis-aquo hydroxo form of the metal complex that is the active species for hydrolyzing phosphate diesters. The cis-aquo hydroxo metal complex may also form inactive dimers at high concentrations (Figure 2.14).[100-102]

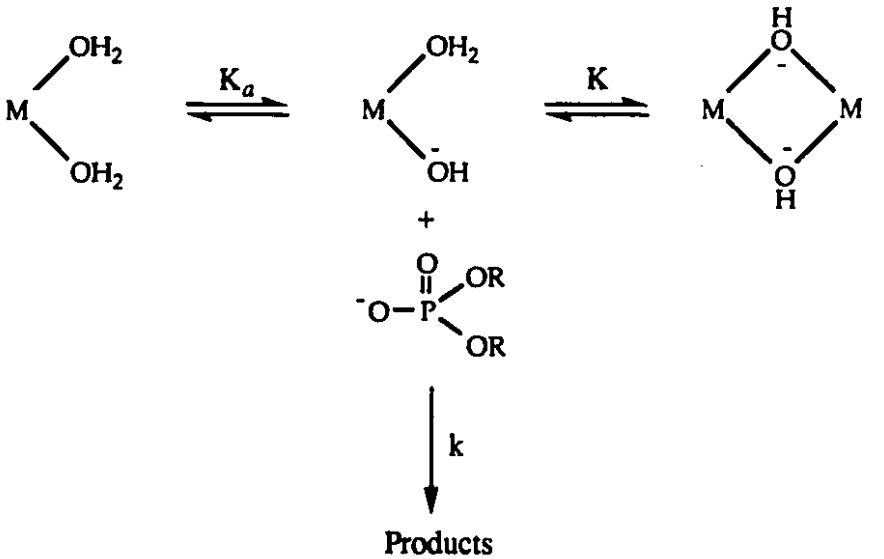

Figure 2.14. The metal complex can exist in three different forms depending upon the pH. The cis-aquo hydroxo form of the metal complex is the active species for hydrolyzing phosphate diesters.

A term for the observed rate constant (k_{obs}) for hydrolysis of a phosphate diester by a cis-diaquo metal complex, according to Figure 2.14, is given in equation 2.2. In equation 2.2 $[Cu]_T$ represents the total copper(II) complex concentration and $[H^+]$ represents the proton concentration

$$k_{obs} = k\{((1 + [H^+]/K_a)^2 + 8K[Cu]_T)^{1/2} - (1 + [H^+]/K_a)\}/4K \qquad \text{equation 2.2}$$

The equation (2.2) should also be applicable for cis-aquo alcohol metal complexes since they too may cleave phosphate diesters and form dimers with bridging alkoxides or hydroxides.

The copper complexes, Cu(II)bpa, Cu(II)hebpa, and Cu(II)hpbpa, all cleave BDNPP with concomitant release of 1 equivalent of 2,4-dinitrophenolate. The complexes (10 mM), Cu(II)bpa, Cu(II)hebpa, and Cu(II)hpbpa, did not cleave the monoester, 2,4-dinitrophenyl phosphate

(DNPP) (5×10^{-5} M), at pH 8.8 and 25 °C with any significant rate acceleration. None of the three complexes (10 mM, pH 10) were observed to lose reactivity for cleaving BDNPP to any significant extent after 1.5 h. The rate of Cu(II)bpa, Cu(II)hebpa, and Cu(II)hpbpa promoted cleavage of BDNPP was monitored by following the increase in the visible absorbance at 400 nm due to the release of 2,4-dinitrophenolate. A typical UV-vis experiment is shown in Figure 2.15 depicting Cu(II)bpa, Cu(II)hebpa, and Cu(II)hpbpa promoted cleavage of BDNPP.

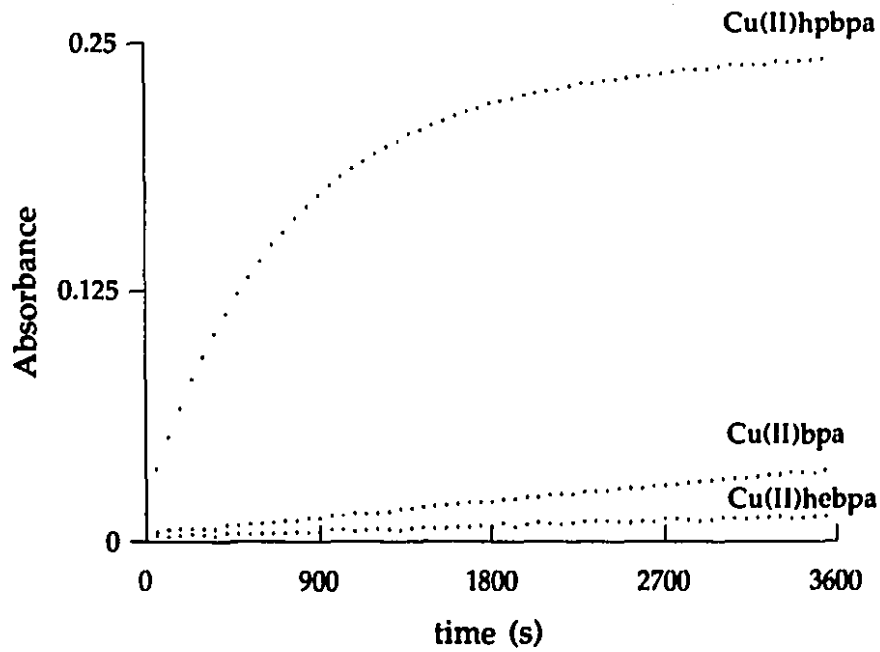

Figure 2.15. Typical UV-vis chromatographs monitoring the release of 2,4-dinitrophenolate at 400 nm upon reaction of the copper(II) complexes (3 mM, pH 8.8, 25 °C) with BDNPP.

The rate of cleavage of BDNPP initially increased linearly with increase in the concentrations of the metal complexes but gradually deviated from linearity (Figure 2.16 and Figure 2.17). The concentration-rate profiles were fit

according to equation 2.2. The best fit for equilibrium constants (K) for apparent dimerization and second order rate constants (k) were determined from a non-linear least-squares analysis of Figures 2.16 and 2.17 (Table 2.3).

Table 2.3. The values and errors of K and k as determined from the fit of equation 2.2 to the data in Figures 2.16 and 2.17.

complex pH 8.8, 25 °C	K (M^{-1})	k ($M^{-1}s^{-1}$)
Cu(II)bpa	45 ± 7	$(2.0 \pm 0.1) \times 10^{-2}$
Cu(II)hebpa	56 ± 14	$(9.5 \pm 0.5) \times 10^{-3}$
Cu(II)hpbpa	83 ± 8	$(7.2 \pm 0.2) \times 10^{-1}$

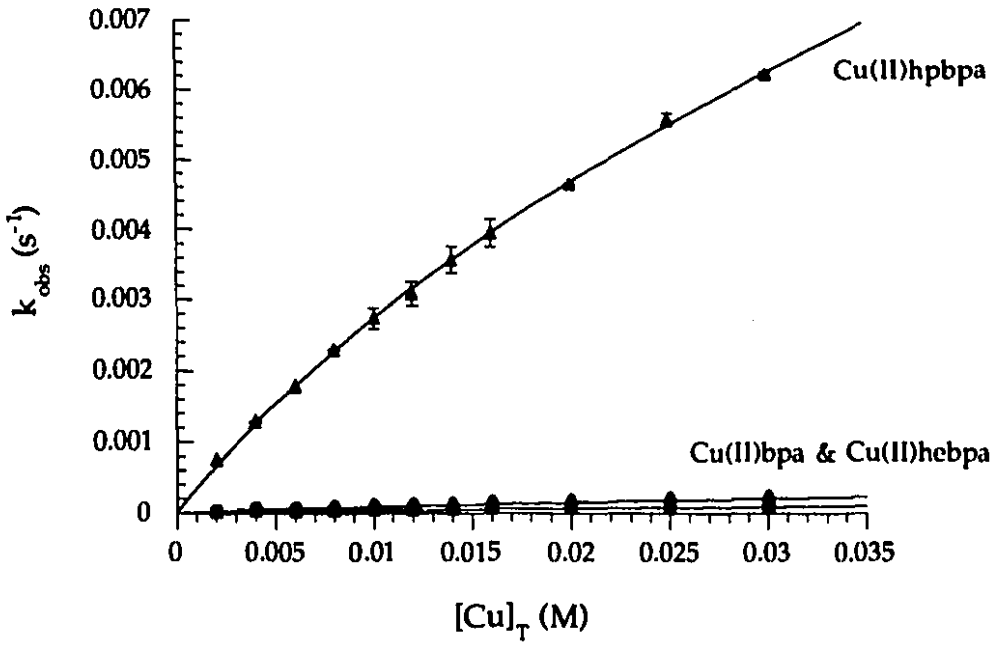

Figure 2.16. Rate-concentration (of copper(II) complex) profiles for the cleavage of BDNPP (5×10^{-5} M) by Cu(II)bpa, Cu(II)hebpa, and Cu(II)hpbpa at 25 °C and pH 8.8. {R(equation 2.2) = 0.99 (Cu(II)bpa), 0.98 (Cu(II)hebpa), 0.99 (Cu(II)hpbpa)}. Error bars indicate ± one standard deviation based upon duplicate runs. The rate-concentration profiles of Cu(II)bpa and Cu(II)hebpa are shown again in Figure 2.17.

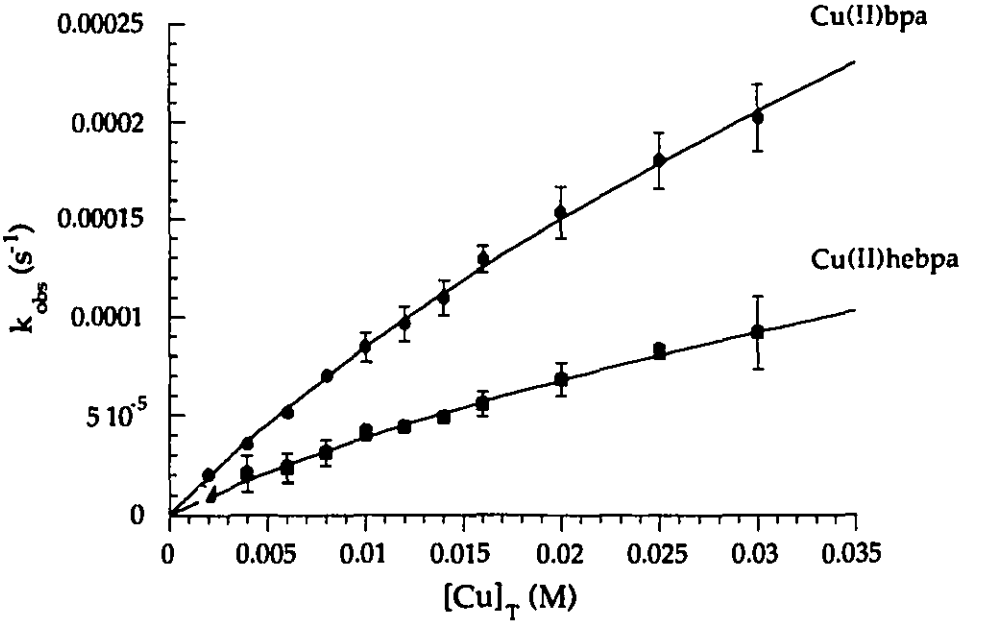

Figure 2.17. Rate-concentration (of copper(II) complex) profiles for cleavage of BDNPP (5×10^{-5} M) by Cu(II)bpa and Cu(II)hebpa at 25 °C and pH 8.8. (R(equation 2.2) = 0.99(Cu(II)bpa), 0.98 (Cu(II)hebpa)). Error bars indicate ± one standard deviation based upon duplicate runs.

The rates of BDNPP cleavage in the presence of Cu(II)bpa, Cu(II)hebpa, and Cu(II)hpbpa increased with increasing pH but leveled off above the pK_a of the copper bound water molecules (Figure 2.18). The pH-rate profiles were fit according to equation 2.2 using the K values determined from the concentration-rate profiles (Figures 2.16 and 2.17) and $[Cu]_T$ = 10.0 mM. The best fit for the pK_a and k values were determined from a non-linear least-square analysis of the pH rate profile data and are listed in Table 2.4.

Table 2.4. The values and errors of k and pK_a as determined from the fit of equation 2.2 to the data in the pH-rate profiles (Figure 2.18).

complex (10 mM) 25 °C	k ($M^{-1}s^{-1}$)	pK_a
Cu(II)bpa	$(3.0 \pm 0.1) \times 10^{-2}$	9.0 ± 0.1
Cu(II)hebpa	$(1.4 \pm 0.1) \times 10^{-2}$	8.9 ± 0.1
Cu(II)hpbpa	$(1.1 \pm 0.03) \times 10^{0}$	8.8 ± 0.05

The pK_a values obtained from the pH-rate profiles are in reasonably good agreement with those obtained from potentiometric titrations. The k values obtained for the pH-rate profiles are also in agreement with those obtained from the concentration-rate profiles.

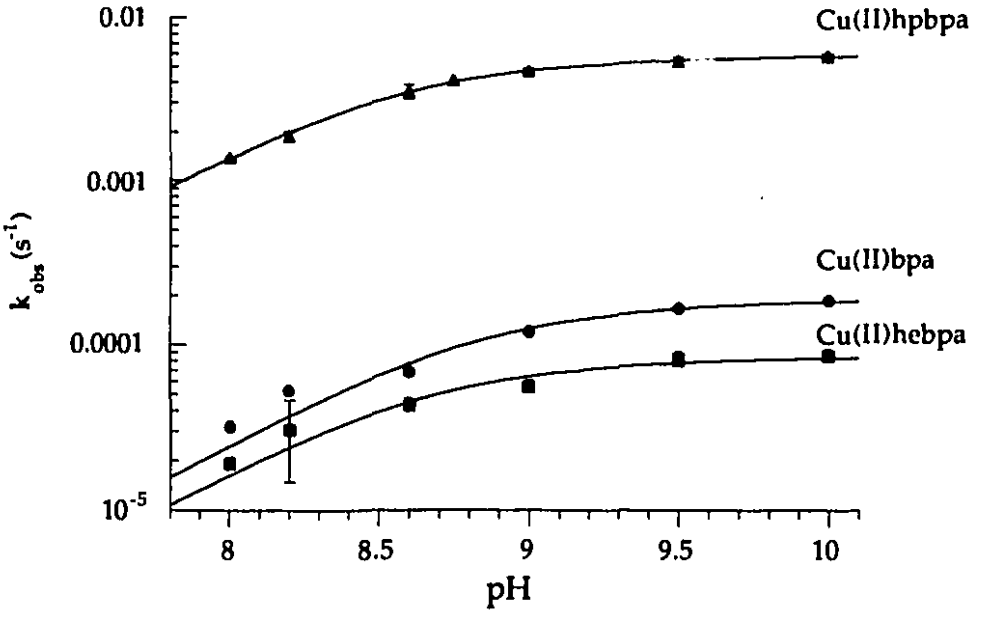

Figure 2.18. pH rate profiles for cleavage of BDNPP (5×10^{-5} M) with 10 mM solutions of Cu(II)bpa, Cu(II)hebpa, and Cu(II)hpbpa at 25 °C. {R(equation 2.2) = 0.99 (Cu(II)bpa), 0.98 (Cu(II)hebpa), 0.99 (Cu(II)hpbpa)}. Error bars indicate ± one standard deviation based upon duplicate runs.

2.2.6. Cleavage of BNPP.

The reactivity pattern for cleavage of BNPP ($5 \times 10\text{-}5\ M^{-1}$) by Cu(II)bpa and Cu(II)hpbpa (3 mM copper(II) complex) at 50 °C and pH 8.8 differed from that observed for BDNPP at 25 °C. The rates were impractically slow to measure however qualitatively it was observed that Cu(II)hpbpa does not promote BNPP cleavage at a much greater rate than Cu(II)bpa. It appears that the basicity of the leaving group must be considerably lower than that of the metal-alkoxide nucleophile for the metal-alkoxide mechanism to be operating.

2.2.7. Zinc(II) Complexes.

Many of nature's hydrolytic enzymes, including alkaline phosphatase, require one or more zinc(II) ions for activation.[27] The zinc(II) complexes of bpa, hebpa, and hpbpa have been prepared because it is important to extend model studies to include biologically relevant metals. The zinc(II) complexes, Zn(II)bpa, Zn(II)hebpa, and Zn(II)hpbpa, each had one titratable proton between pH 9 and 9.1. The reactivity of the complexes for cleaving BDNPP is shown in Table 2.5. Interestingly, the three zinc(II) complexes demonstrated the same reactivity pattern for cleaving BDNPP as the corresponding copper(II) complexes. As was observed with the copper(II) complexes, Zn(II)bpa, Zn(II)hebpa, and Zn(II)hpbpa were unreactive for cleaving the monoester DNPP (10 mM zinc(II) complex, pH 9, 25 °C).

Table 2.5. Pseudo-first order rate constants for the cleavage of BDNPP (5×10^{-5} M) by Zn(II)bpa, Zn(II)hebpa, and Zn(II)hpbpa at 25 °C and pH 9.

complex (10 mM)	k_{obs} (s^{-1})
Zn(II)bpa	3.7×10^{-4}
Zn(II)hebpa	2.1×10^{-4}
Zn(II)hpbpa	2.8×10^{-3}

2.2.8. Covalent Intermediate.

Cu(II)hpbpa was observed to be approximately thirty-five times more reactive than Cu(II)bpa and approximately eighty times more reactive than Cu(II)hebpa for cleaving BDNPP. HPLC analyses (Figure 2.20) indicated that Cu(II)bpa cleaved BDNPP hydrolytically to give the phosphate monoester DNPP and 2,4-dinitrophenolate while Cu(II)hebpa and Cu(II)hpbpa cleaved the phosphate diester by hydrolysis and by transesterification to give the phosphate monoester, 2,4-dinitrophenolate and the transesterified products (hebpaP and hpbpaP) as shown in Figure 2.19.

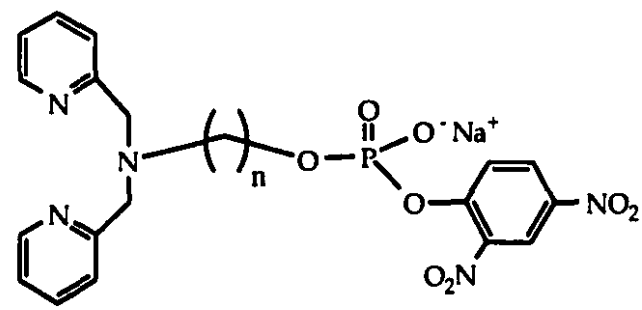

n = 2 : Cu(II)hebpaP
n = 3 : Cu(II)hpbpaP

Figure 2.19. Structure of transesterified products.

The transesterified products were first detected by HPLC, isolated by preparative chromatography, and characterized by ^{1}H and ^{31}P NMR as well as by HPLC and mass spectrometry. The HPLC analyses indicated that the copper(II) complex with the hydroxypropyl group (Cu(II)hpbpa) cleaves BDNPP predominantly be transesterification (95% $\pm$ 3%) whereas the copper(II) complex with hydroxyethyl group (Cu(II)hebpa) cleaves the

phosphate diester predominantly by hydrolysis (90% $\pm$ 5%). The errors quoted are based on duplicate runs.

Figure 2.20. HPLC analyses for cleavage of BDNPP with (a) Cu(II)bpa, (b) Cu(II)hebpa, and (c) Cu(II)hpbpa: (■)2,4-dinitrophenyl phosphate; (▼) BDNPP; (◆) hebpaP; (●) hpbpaP.

2.2.9. Mechanism.

We propose that Cu(II)hpbpa cleaves BDNPP by first coordinating the phosphate diester followed by intramolecular metal-alkoxide attack (Figure 2.21).

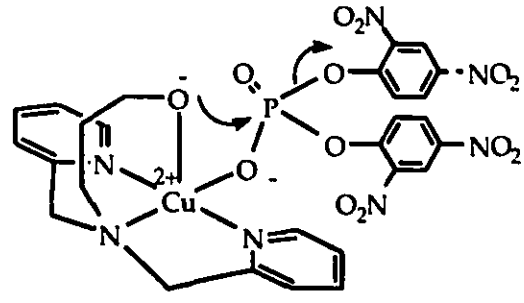

Figure 2.21. Proposed mechanism of cleavage of BDNPP by Cu(II)hpbpa.

This implies that the aquo-alkoxy form of the metal complex rather than the thermodynamically more stable hydroxo-alcohol form of the metal complex is the active species for cleaving the phosphate diester. Since the ratio of the concentration of the aquo-alkoxy form of the metal complex to that of the hydroxo-alcohol form of the metal complex is independent of pH, the pH-rate profile (Figure 2.18) cannot be used to identify the active species. The structure in Figure 2.21 may be compared with the crystal structure of Cu(II)bba(P) (Figure 2.9).[84] In both structures, a phosphate diester is coordinated at the equatorial position and an alkoxide or an alcohol is coordinated at the apical position. The nucleophilic attack by the metal-alkoxide on the coordinated phosphate diester (Figure 2.21) should be facilitated by a decrease in the O-Cu-O bond angle. The propyl group in Cu(II)hpbpa should expand the alkyl amine N-Cu-O bond angle thereby decreasing the O-Cu-O bond angle.

Cu(II)bpa may hydrolyze the diester by intramolecular metal-hydroxide attack on the coordinated phosphate diester by a mechanism similar to the Cu(II)hpbpa promoted cleavage of BDNPP (Figure 2.22).

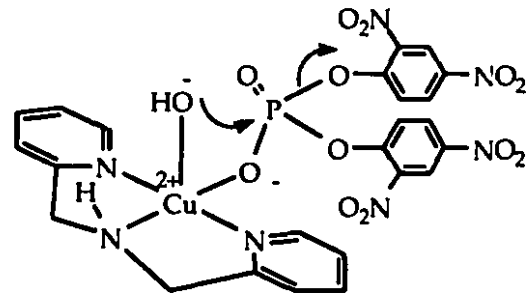

Figure 2.22. Proposed mechanism of cleavage of BDNPP by Cu(II)bpa.

The greater reactivity of Cu(II)hpbpa compared to Cu(II)bpa may be due to the greater value of the O-Cu-O bond angle in the latter complex (Figure 2.23). In a related study, it has been shown that the reactivity of *cis*-diaquo tetraamine Co(III) complexes for hydrolyzing phosphate diesters increases with decreasing O-Co-O bond angle which can be achieved by increasing the N-Co-N bond angle opposite the O-Co-O bond angle.[3,103]

When the propyl bridging group in Cu(II)hpbpa was replaced with the ethyl bridging group (Cu(II)hebpa) the reactivity of the metal complex for cleaving BDNPP decreased by about two orders of magnitude. It appears that the metal-alkoxide of Cu(II)hebpa cannot easily reach the phosphate due to the increased O-Cu-O bond angle and the decreased alkyl amine N-Cu-O bond angle (Figure 2.23). Indeed the O-Cu-Cl bond angle in Cu(II)hebba (102.65(7)°) is significantly greater than the O-Cu-O bond angle in Cu(II)bba(P) (95.70(14)°) presumably because the alkyl amine N-Cu-O bond angle in Cu(II)hebba (78.20(21)°) is much smaller than that in Cu(II)bba(P) (99.34(15)°).[84]

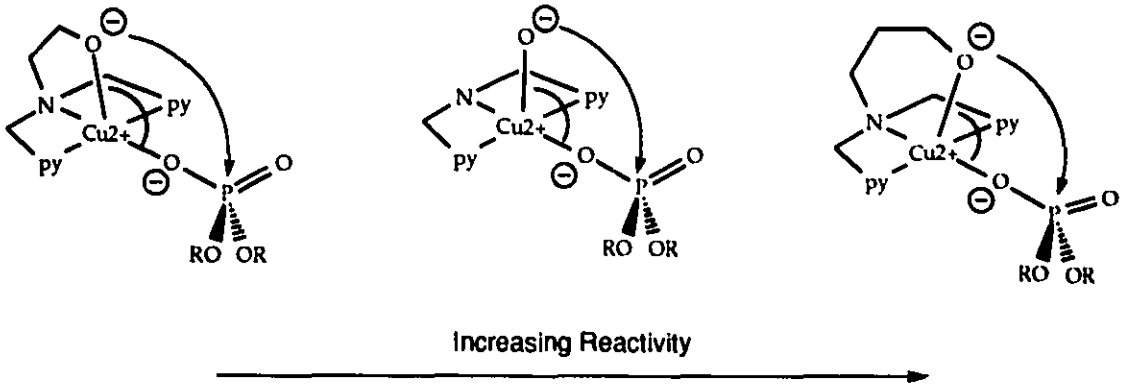

Figure 2.23. The difference in the O-Cu-O bond angle between the metal complexes possibly affects the rate of attack of the metal-hydroxide or -alkoxide upon the substrate. The closer the approach between the nucleophile and the substrate, the more reactive the complex. (py = pyridyl; R = 2,4-dinitrophenyl).

The complex Cu(II)hebpa was about two orders of magnitude less reactive than Cu(II)hpbpa and about half as reactive as Cu(II)bpa. Furthermore, Cu(II)hebpa cleaves the diester predominantly by hydrolysis rather than by transesterification. It appears that the more active form of Cu(II)hebpa is formed by displacement of the coordinated alkoxide by hydroxide. The metal-hydroxide can then attack the coordinated phosphate diester much like with Cu(II)bpa (Figure 2.22). Although it is possible that the metal-hydroxide or metal-alkoxide in Cu(II)bpa or Cu(II)hebpa may be acting as an intramolecular general base catalyst, it seems unlikely that the mechanistic role of the metal-hydroxide in Cu(II)bpa would be different from the mechanistic role of the metal-alkoxide in Cu(II)hpbpa.

2.3. Conclusion.

In summary, three copper(II) complexes (Cu(II)bpa, Cu(II)hebpa, and Cu(II)hpbpa) have been prepared in order to investigate the reactivities of metal-alkoxides and metal-hydroxides for cleaving an activated phosphate diester. The copper(II) complex with the hydroxypropyl group (Cu(II)hpbpa) is observed to be about eighty times more reactive than the Cu(II) complex with the hydroxyethyl group (Cu(II)hebpa) and over thirty-five times more reactive than the Cu(II) complex without any pendant alcohol groups (Cu(II)bpa) for cleaving BDNPP. The pattern of reactivity for cleaving BDNPP is likewise observed for the corresponding zinc complexes, Zn(II)bpa, Zn(II)hebpa, and Zn(II)hpbpa. The equilibrium constants for the binding of a phosphate diester to Cu(II)bpa, Cu(II)hebpa, and Cu(II)hpbpa are measured to be $2 \pm 1\ M^{-1}$ for all the complexes. HPLC analyses provided direct evidence that the three copper(II) complexes did not cleave BDNPP by the same mechanism. Cu(II)bpa cleaved the diester by direct hydrolysis. Cu(II)hebpa cleaved the diester predominantly by hydrolysis but some transesterification was also be detected. Cu(II)hpbpa cleaved the diester mainly by transesterification. Based on crystallographic data of two analogs (Cu(II)bba(P) and Cu(II)hebba) the differences in the reactivities and mechanisms of the three copper(II) complexes have been proposed to be due to the differences in their structures. These results demonstrate how subtle changes in the structure of simple metal complexes can influence their reactivity. A possible advantage for an enzyme to employ a metal-alkoxide instead of a metal-hydroxide may be the preferential positioning of the nucleophile. In conclusion, it has been shown that a simple metal complex with a pendant alcohol group can efficiently cleave a phosphate diester by transesterification

similar to the proposed mechanism of action for alkaline phosphatase catalyzed cleavage of phosphate monoesters and *Tetrahymena* ribozyme catalyzed self-cleavage.

2.4. Experimental.

2.4.1. General Information.

Infrared spectra were obtained on a Bruker IFS FTIR spectrophotometer and an Analect AQS spectrophotometer. All elemental analyses were performed by Guelph Chemical Laboratories. Mass spectra were obtained on a Kratos MS25RFA mass spectrometer by Nadim Saade of McGill University.

NMR. ^{1}H NMR (299.3 MHz), ^{13}C NMR (75.4 MHz) and ^{31}P NMR (121.4 MHz) spectra were obtained on a Varian XL-300 FT spectrophotometer. ^{1}H NMR (199.975 MHz) and ^{13}C NMR (50.289 MHz) were obtained on a Varian Gemini 200 spectrophotometer. Data are reported in parts per million (ppm).

Titrations. Titrations were performed with a Radiometer PHM63 pH meter equipped with a Radiometer TTT80 titration controller and an ABU80 automatic burette. Standardized NaOH solutions purchased from Aldrich were used as titrant. The pH was measured with a Radiometer K-4040 calomel reference electrode and a G-2040C glass electrode. Temperature was maintained using a Lauda RM6 water bath.

UV-vis measurements. Kinetic UV measurements and spectra were taken with a HP8452A diode array spectrophotometer equipped with a water jacketed 7 cell transport. Temperatures were controlled with a Lauda RM6 water bath. Data were collected on an IBM PC using HP software and analyzed on an Apple Macintosh computer with KaleidaGraph 3.0.1 software.

Buffers. 4-(2-hydroxyethyl)-1-piperazineethanesulfonic acid (HEPES, pKa = 7.4), 2-(cyclohexylamino)ethanesulfonic acid (CHES, pKa = 9.3), N-ethylmorpholine (NEM, pKa = 7.7) and 3-((tris(hydroxymethyl)methyl)amino)-1-propanesulfonic acid (TAPS, pKa =

8.4) were purchased from Aldrich. All were used without further purification.

2.4.2. Materials.

Bis(4-nitrophenyl) phosphate (sodium salt) (BNPP), 2-pyridinecarboxaldehyde, 2-aminopropanol, sodium triacetoxyborohydride, copper(II) chloride, zinc(II) chloride, and EDTA (disodium salt) were purchased from Aldrich and used without further purification. Diethyl 4-nitrophenyl phosphate (DENPP) was purchased from Sigma. Bis(pyridylmethyl)amine (bpa),[104] N-(2-hydroxyethyl)bis(2-pyridylmethyl)amine (hebpa),[89] 2,4-dinitrophenyl phosphate (2,6-lutidine salt) (DNPP),[105] and bis(2,4-dinitrophenyl) phosphate (pyridinium salt) (BDNPP)[106] were prepared by previously reported methods.

The ligand, hebamp, was prepared by a co-worker, Mark Wall. Dimethylphosphate (sodium salt) (DMP) was prepared by a co-worker, Barry Linkletter.

2.4.3. Synthesis of Ligand and Metal Complexes.

N-(3-hydroxypropyl)-bis(2-pyridylmethyl)amine (hpbpa).

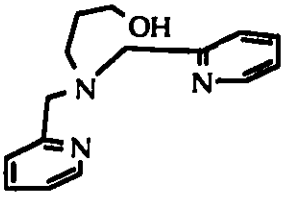

2-pyridinecarboxaldehyde (9.6 g, 0.09 mol), 3-aminopropanol (3.4 g, 0.045 mol), and acetic acid (5.1 mL, 0.09 mol) were mixed together in dry THF. Sodium triacetoxyborohydride (25.4 g, 0.12 mol) was added to the above solution and stirred at room temperature for 48 hours under nitrogen. After removing the solvent *in vacuo*, the product was dissolved in CH_2Cl_2 and washed with an aqueous solution saturated with

sodium bicarbonate. The product was distilled to give a pale yellow oil (yield: 6.7 g, 58%; b.p. 130 °C, 0.03 mm Hg). IR (neat) 3200-3500, 2950, 2809, 1593, 1571, 1474, 1436, 1050 cm^{-1}. ^1H NMR (299.3 MHz, $CDCl_3$, (TMS)) δ 1.82 (2H, m), 2.78 (2H, t, J = 6.0 Hz), 3.73 (2H, t, J = 4.9 Hz), 3.84 (4H, s), 7.17 (2H, t, J = 6.1 Hz), 7.41 (2H, d, J = 7.8. Hz), 7.64 (2H, t, J = 7.7 Hz), 8.55 (2H, d, J = 7.7 Hz). ^{13}C NMR (75.4 MHz, $CDCl_3$, 1,4-dioxane (66.7 ppm)) δ 28.5, 52.4, 59.6, 61.9, 121.7, 122.7, 136.2, 148.7, 158.6. MS (EI, ion source 200 °C, 70 eV, direct inlet 100 °C), [m/z(relative intensity)] : 257($M^{+\cdot}$,2), 165(74), 135(32), 93(100).

Cu(bpa)Cl_2.

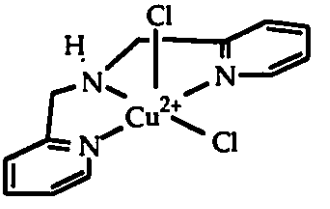

The complex Cu(bpa)Cl_2 was prepared according to previously reported procedures.[88,108] Anal. Calcd. $C_{12}H_{13}N_3Cl_2Cu$: C, 43.19; H, 3.93; N, 12.59. Found: C, 43.36; H, 3.97; N, 12.37.

Cu(hebpa)Cl_2.

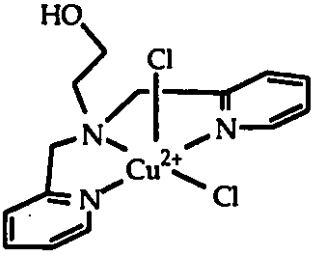

A solution of $CuCl_2$ (0.207 g, 1.54 mmol) in 100% ethanol (10 mL) was added to a solution of hebpa (0.375 g, 1.54 mmol) in 100% ethanol (10 mL). After 2 hours the total volume of the mixture was reduced to 10 mL. A blue precipitate that appeared after addition of ether (5 mL) was filtered and washed with cold 100% ethanol. The complex was dried overnight *in vacuo*. (0.390 g, 67% yield). IR (neat) 3100-3500, 2960, 2880, 1610, 1570, 1480, 1440, 1380, 1350, 1300, 1290, 1070, 1040, 1030, 990 cm^{-1}. UV-vis (H_2O, pH 6): 254 nm (ε = 1.15 x 10^4 cm^{-1} M^{-1}); 678 nm (ε = 84 cm^{-1} M^{-1}). Anal. Calcd. for $C_{14}H_{17}N_3OCuCl_2$: C, 44.51; H, 4.50; N, 11.12; Cl, 18.77; Cu, 16.82. Found: C, 44.67; H, 4.61; N, 11.03; Cl, 19.06; Cu, 16.51.

Cu(hpbpa)Cl_2.

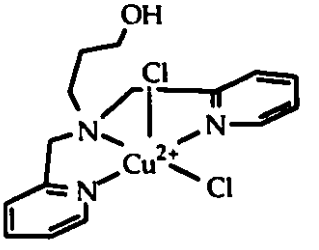

A solution of $CuCl_2$ (0.605 g, 4.5 mmol) in 100% ethanol (10 mL) was added to a solution of hpbpa (1.16, 4.5 mmol) in 100% ethanol (10 mL). A blue precipitate that formed within minutes was filtered and washed with cold ethanol. The complex was dried overnight *in vacuo* (1.137 g, 64% yield). IR (neat) 3100-3500, 3070, 2870, 1610, 1570, 1480, 1440, 1380, 1300, 1280, 1100, 1050, 975 cm^{-1}. UV-vis (H_2O, pH 6): 254 nm ($\varepsilon = 1.34 \times 10^4$ cm^{-1} M^{-1}); 658 nm ($\varepsilon = 108$ cm^{-1} M^{-1}). Anal. Calcd for $C_{15}H_{19}N_3OCuCl_2$: C, 45.99; H, 4.89; N, 10.77; Cl, 18.10; Cu, 16.22. Found: C, 46.06; H,5.05; N, 10.75; Cl, 18.35; Cu, 16.50.

Zn(bpa)Cl_2.

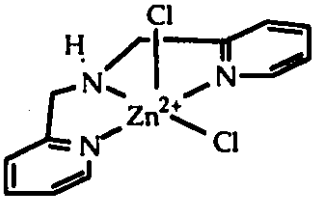

A solution of $ZnCl_2$ (0.158 g, 4.5 mmol) in 100% ethanol (8 mL) was added to a solution of bpa (0.231 g, 1.2 mmol) in 100% ethanol (8 mL). A white precipitate that formed immediately was filtered and washed with cold 100% ethanol. The complex was dried overnight *in vacuo* (0.321 g, 83% yield). Anal. Calcd. for $C_{12}H_{13}N_3Cl_2Zn$: C, 42.96; H, 3.91; N, 12.52. Found: C, 42.95; H, 3.76; N, 12.31.

Zn(hebpa)Cl_2.

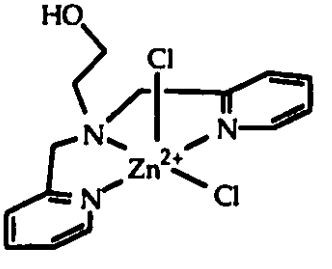

A solution of $ZnCl_2$ (0.207 g, 1.52 mmol) in 100% ethanol (10 mL) was added to a solution of hebpa (0.371 g, 1.52 mmol) in 100% ethanol (10 mL). A white precipitate that formed immediately was

filtered and washed with cold 100% ethanol. The complex was dried overnight *in vacuo* (0.439 g, 76% yield). Anal. Calcd for $C_{14}H_{17}N_3Cl_2OZn$: C, 44.30; H, 4.51; N, 11.07. Found: C, 44.54; H, 4.61; N, 10.86.

Zn(hpbpa)Cl_2.

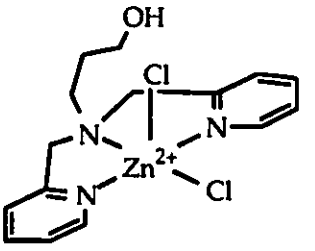

A solution of $ZnCl_2$ (0.199 g, 1.46 mmol) in ethanol (10 mL) was added to a solution of hebpa (0.376 g, 1.46 mmol) in ethanol (10 mL). A white precipitate that formed immediately was filtered and washed with cold ethanol. The complex was dried overnight *in vacuo* (0.403 g, 70% yield). Anal. Calcd for $C_{15}H_{19}N_3Cl_2OZn$: C, 45.77; H, 4.87; N, 10.68. Found: C, 45.78; H,4.85; N, 10.50.

Zn(hebamp)Cl_2.

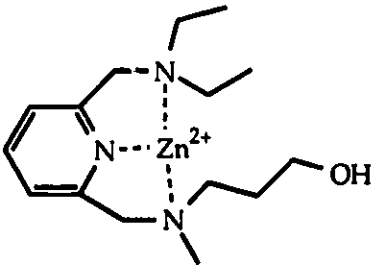

The Zn(II)hebamp complex was prepared *in situ* due to difficulty in obtaining an analytically pure isolated sample. Kady *et al.* reported to have isolated the complex as a dimer under basic conditions in aqueous methanol.[96] Their analytical analysis was calculated (found) for $C_{28}Cl_2H_{22}N_6O_{10}Zn_2$: C, 41.84 (41.69); H, 2.74 (2.75); N, 10.46 (10.48), however the formula quoted is incorrect for the number of hydrogens by at least 25 hydrogens. Under similar conditions to Kady *et al.* we obtained only precipitated metal salts, according to the analytical analysis. Anal. Calcd. for $C_{28}H_{48}N_6Cl_2O_{10}Zn_2$ (dimer): C, 40.84; H, 5.83; N, 10.12. Found: C, 1.49; H, 0.25; N, 0.15. Repeated attempts to isolate Zn(II)hebamp as a monomer were unsuccessful.

Evidence for formation of the complex *in situ* is provided through titration studies. A 0.01 M NaOH (0.1 M $NaNO_3$) titrant was standardized using potassium hydrogen phthalate. A 2 mM solution (2.5 mL, 25 °C, 0.1 M $NaNO_3$) of the complex was prepared from the addition of one equivalent of $ZnClO_4$ (from a 10 mM standardized solution) to one equivalent of hebamp [^{1}H NMR (199.99 MHz, $CDCl_3$, (TMS)) δ 1.05 (6H, 7.2), 2.36 (3H, s), 2.64 (6H, m), 3.65 (2H, t, 5.1 Hz), 3.75 (4H, s), 7.20 (1H, d, J = 7.7 Hz), 7.40 (1H, d, J = 7.7 Hz), 7.66 (1H, t, J = 7.7 Hz). ^{13}C NMR (50.289 MHz, $CDCl_3$, 1,4-dioxane (66.7 ppm)) δ 12.07, 42.53, 47.2, 58.5, 58.7, 59.1, 62.6, 120.0, 120.3, 135.7, 156.3, 158.5. MS (CI, ion source 200 °C, 70 eV, direct inlet 150 °C), [m/z(relative intensity)] : 252(MH^+, 16), 180(100), 106(39)]. The titration from pH 4-10 of 1 equivalent of hebamp and 1 equivalent of $Zn(II)(ClO_4)_2$ (2 mM complex) indicated the equivalent of 4 titratable protons, as was reported by Kady *et al.*[96] There is a shift in the first pK_a of the ligand to a slightly lower pH (~0.5 pH unit) in the presence of 1 equivalent of zinc(II) metal.

2.4.4. Potentiometric Titrations.

A 3 mL (15 mM) solution of Cu(II)bpa, Cu(II)hebpa, Cu(II)hpbpa, Zn(II)bpa, Zn(II)hebpa, or Zn(II)hpbpa in water (25°C) was titrated with a 0.1 M NaOH solution. The ionic strength was maintained at 0.1 M with $NaNO_3$.

2.4.5. Dimethyl Phosphate Binding to Copper(II) Complexes.

A 5 mM solution of Cu(II)bpa, Cu(II)hebpa, or Cu(II)hpbpa and dimethyl phosphate (0 - 500 mM) in water (10 mL, 25°C) was titrated with a 0.1 M NaOH solution. All solutions were prepared in 0.1 M with $NaNO_3$.

2.4.6. Kinetic Studies.

Hydrolysis of BDNPP was monitored by following the visible absorbance change at 400 nm due to the release of 2,4-dinitrophenolate anion. One equivalent of 2,4-dinitrophenolate was released for each reaction. In a typical kinetics experiment 5 μL of a freshly prepared BDNPP stock solution in dimethyl sulfoxide (10 mM) was added to a freshly prepared copper(II) complex solution (2 to 30 mM, 1 mL) at 25°C. The copper(II) complex and zinc(II) complex solutions were buffered with CHES (10 mM, pH 8.6-10) or NEM (10 mM, pH 7-8.2). The pH of the solutions were adjusted using concentrated NaOH or $HClO_4$ solutions.

The rate constants for Cu(II)bpa, Cu(II)hebpa, Zn(II)bpa and Zn(II)hebpa promoted hydrolysis of BDNPP were obtained by the initial rate method. First-order rate constants were calculated from the slopes of the linear portion of the plots of the UV-vis chromatograph (≤ 5% of reaction) versus time by converting to concentration units and dividing by the initial phosphate ester concentration.

The rate constants for Cu(II)hpbpa and Zn(II)hpbpa promoted hydrolysis of BDNPP were obtained by fitting the first three half lives of the reaction according to a first-order kinetics equation.

2.4.6. Product Analysis.

The products for Cu(II)bpa, Cu(II)hebpa, and Cu(II)hpbpa promoted cleavage of BDNPP were analyzed by HPLC. In a typical experiment, the metal complex (2.4×10^{-4} mol) was reacted with an equivalent amount of BDNPP in water (25 mL) at room temperature (20-24 °C). The pH of the reaction solution was maintained between 8.5 and 9.5 with sodium hydroxide. After 2 to 7 h, EDTA (2.4×10^{-3} mol) was added to complex the copper. The reaction

mixture was injected (5 μL) onto the HPLC column and eluted for 5 min with $NH_4H_2PO_4$ (0.2 M at pH 5.5) followed by a 0-100% linear gradient of the ammonium phosphate and methanol/water (3/2) solutions over 20 min with a flow rate of 0.5 mL/min. For the cleavage of BDNPP with Cu(II)bpa, the HPLC peak (at 254 nm) due to the diester (retention time: 17.9 min) decreased with concomitant increase in the peaks due to the monoester DNPP (1.6 min) and 2,4-dinitrophenol (8.7 min). For the cleavage of the diester with Cu(II)hebpa and Cu(II)hpbpa, the decrease in the diester peak was accompanied by an increase in the peaks due to the monoester as well as the transesterified products (hebpaP, 18.4 min; hpbpaP, 18.8 min) and 2,4-dinitrophenol.

The ratio of transesterified product to hydrolysis product of Cu(II)hebpa and Cu(II)hpbpa promoted cleavage of BDNPP was determined by converting integration of the peaks of the HPLC chromatograph (Figure 2.20) into concentration as determined from the isolated samples.

2.4.7. Isolation of Covalent Intermediates.

Isolation of hpbpaP. The EDTA quenched reaction mixture for the cleavage of BDNPP by Cu(II)hpbpa (as described in section 2.4.6) was extracted into dichloromethane. After removing the dichloromethane *in vacuo*, the extract was chromatographed on a 6 cm x 30 cm reversed-phase C-18 column and eluted with methanol/water (1/4) until all of 2,4-dinitrophenol had eluted. A linear gradient from methanol/water (1/4) up to methanol/water (3/2) was used to elute hpbpaP. Further purification was performed by extracting hpbpaP into water from dichloromethane giving a yellow solid upon lyophilization (yield: 26%). HPLC analysis of the yellow solid indicated a single peak with a retention time of 18.8 min (using HPLC conditions

described in section 2.4.6). ^1H NMR (200 MHz, D_2O, (DSS)): δ 1.96 (2H, m), 2.73 (2H, t, J = 7.4 Hz), 3.62 (4H, s), 4.03 (2H,m), 7.30 (2H, t, J = 7.7 Hz), 7.41 (2H, d, J = 7.8. Hz), 7.62 (1H, d, 9.2 Hz), 7.78 (2H, t, J = 7.7 Hz), 8.4 (3H, m), 8.80 (1H, d, J = 2.8 Hz). ^{13}C NMR (50.289 MHz, D_2O, 1,4-dioxane (66.7ppm)) δ 27.4, 50.7, 59.5, 65.8, 121.1, 121.9, 122.3, 123.4, 128.63, 137.0, 147.1, 156.58. ^{31}P NMR (121 MHz, D_2O, (trimethyl phosphate)) δ -8.8. MS (FAB, NBA matrix, 7 kV) [m/z(relative intensity)] 679, 0.8% $(C_{21}H_{21}N_5NaO_8P + NBA + H)^+$; 526, 1.5% $(C_{21}H_{21}N_5NaO_8P + H)^+$; 504, 6.2% $(C_{21}H_{23}N_5NaO_8P)^+$.

Isolation of hebpaP. The product hebpaP was isolated under the same experimental conditions for isolating hpbpaP. HPLC analysis of hebpaP indicated a single peak with a retention time of 18.4 min (using HPLC conditions described in section 2.4.6). ^1H NMR (200 MHz, D_2O, (DSS)): δ 2.86 (2H, t, J= 6.9 Hz), 3.75 (4H, s), 4.12 (2H, m), 7.25 (2H, t , J= 6.4 Hz), 7.44 (2H, d, J= 7.8 Hz), 7.72 (3H, m), 8.35 (3H, m), 8.78 (1H, d, J= 2.9 Hz). ^{13}C NMR (50.289 MHz, D_2O, 1,4-dioxane (66.7ppm)) δ 54.0, 59.9, 61.5, 122.0, 122.7, 123.0, 124.4, 129.6, 137.0, 148.0, 156.58. ^{31}P NMR (121 MHz, D_2O, (trimethyl phosphate)) δ -8.8. MS (FAB, NBA matrix, 7 kV) [m/z(relative intensity)] 512, 0.8% $(C_{20}H_{19}N_5NaO_8P+ H)^+$; 490, 3.1% $(C_{20}H_{21}N_5NaO_8P)^+$.

APPENDIX 2A. Tables of data from Chapter 2.

Table 2A.1. Potentiometric titration to determine the binding constant of dimethyl phosphate to the three copper(II) complexes based upon the dependence of the observed pK_a upon the concentration of DMP. The standard error for pK_a measurements is ~ ± 0.02 pH units.

[DMP] (M) 25 °C	Observed pK_a* [Cu(II)bpa)] (5 mM)	Observed pK_a* [Cu(II)hebpa)] (5 mM)	Observed pK_a* [Cu(II)hpbpa)] (5 mM)
0.0	8.75	8.70	8.65
0.050	8.78	8.73	8.68
0.100	8.80	8.75	8.70
0.150	8.87	8.83	8.75
0.250	8.97	8.90	8.80
0.500	9.05	8.95	8.88

*Observed pKa = $-\log [H^+]_{midpoint}$

Table 2A.2. Concentration-rate profile data. The observed rate constants are the average of duplicate runs (unless no error indicated) and the error is quoted as ± 1 standard deviation.

[complex] (mM) pH 8.8	k_{obs} (s^{-1}) Cu(II)bpa	k_{obs} (s^{-1}) Cu(II)hebpa	k_{obs} (s^{-1}) Cu(II)hpbpa
2.0	$(2.03 \pm 0.07) \times 10^{-5}$	$(1.12 \pm 0.36) \times 10^{-5}$	7.45×10^{-4}
4.0	$(3.52 \pm 0.004) \times 10^{-5}$	$(2.06 \pm 0.91) \times 10^{-5}$	$(1.27 \pm 0) \times 10^{-3}$
6.0	$(5.11 \pm 0.13) \times 10^{-5}$	$(2.34 \pm 0.72) \times 10^{-5}$	1.78×10^{-3}
8.0	6.99×10^{-5}	$(3.10 \pm 0.65) \times 10^{-5}$	$(2.30 \pm 0.001) \times 10^{-3}$
10.0	$(8.42 \pm 0.75) \times 10^{-5}$	$(4.07 \pm 0.34) \times 10^{-5}$	$(2.73 \pm 0.14) \times 10^{-3}$
12.0	$(9.62 \pm 0.87) \times 10^{-5}$	$(4.38 \pm 0.19) \times 10^{-5}$	$(3.09 \pm 0.18) \times 10^{-3}$
14.0	$(1.10 \pm 0.09) \times 10^{-4}$	$(4.87 \pm 0.59) \times 10^{-5}$	$(3.57 \pm 0.19) \times 10^{-3}$
16.0	$(1.29 \pm 0.07) \times 10^{-4}$	$(5.53 \pm 0.63) \times 10^{-5}$	$(3.94 \pm 0.12) \times 10^{-3}$
20.0	$(1.53 \pm 0.13) \times 10^{-4}$	$(6.80 \pm 0.83) \times 10^{-5}$	$(4.65 \pm 0.04) \times 10^{-3}$
25.0	$(1.80 \pm 0.14) \times 10^{-4}$	$(8.22 \pm 0.36) \times 10^{-5}$	$(5.59 \pm 0.01) \times 10^{-3}$
30.0	$(2.02 \pm 0.17) \times 10^{-4}$	$(9.17 \pm 0.19) \times 10^{-5}$	$(6.24 \pm 0.03) \times 10^{-3}$

Table 2A.3. pH-rate profile data. The observed rate constants are the average of duplicate runs (unless no error indicated) and the error is quoted as ± 1 standard deviation.

pH	k_{obs} (s^{-1}) Cu(II)bpa (10 mM)	k_{obs} (s^{-1}) Cu(II)hebpa (10 mM)	k_{obs} (s^{-1}) Cu(II)hpbpa (10 mM)
8.0	3.19×10^{-5}	1.93×10^{-5}	$(1.39 \pm 0.72) \times 10^{-3}$
8.2	5.29×10^{-5}	$(3.05 \pm 0.99) \times 10^{-5}$	1.88×10^{-3}
8.6	$(6.83 \pm 0.31) \times 10^{-5}$	$(4.31 \pm 0.16) \times 10^{-5}$	3.51×10^{-3}
8.8			4.10×10^{-3}
9.0	$(1.18 \pm 0.02) \times 10^{-4}$	$(5.55 \pm 0.06) \times 10^{-5}$	$(4.67 \pm 0.22) \times 10^{-3}$
9.5	$(1.65 \pm 0.02) \times 10^{-4}$	$(8.11 \pm 0.66) \times 10^{-5}$	$(5.40 \pm 0.26) \times 10^{-3}$
10.0	1.85×10^{-4}	8.52×10^{-5}	$(5.81 \pm 0.27) \times 10^{-3}$

APPENDIX 2B Derivation of equations in Chapter 2.

Derivation of equation 2.1.

Determining the equilibrium constant of binding of dimethyl phosphate (DMP) to the copper(II) complex through potentiometric titrations.

Cu(DMP) represents DMP bound to copper(II) complex.

Cu represents the copper(II) complex in the diaquo form.

$Cu(OH^-)$ represents the copper(II) complex in the mono hydroxo form.

$Cu(OH^-)_2Cu$ represents the copper(II) complex as the dihydroxo bridge form.

$[Cu]_T$ represent the total copper(II) ion concentration.

$$Cu(DMP) \overset{K_d}{\rightleftharpoons} Cu + DMP \overset{K_a}{\rightleftharpoons} Cu(OH^-) + H^+ \overset{K}{\rightleftharpoons} Cu(OH^-)_2Cu$$

K_d represents the dissociation constant of DMP from Cu.

K_a represents the acid dissociation constant of the metal bound water.

K represents dimerization constant of the mono-hydroxo form of complex.

$$K_d = [Cu][DMP]/[CuDMP] \qquad 2B.1$$

$$K_a = [Cu(OH^-)][H^+]/[Cu] \qquad 2B.2$$

$$K = [Cu(OH^-)_2Cu]/[Cu(OH^-)]^2 \qquad 2B.3$$

$$[Cu]_T = [Cu(DMP)] + [Cu] + [Cu(OH\text{-})] + 2[Cu(OH^-)_2Cu] \qquad 2B.4$$

Substitute (2B.1), (2B.2), and (2B.3) into (2B.4);

$$[Cu]_T = [Cu(OH^-)]\{[DMP][H+]/(K_dK_a) + [H+]/Ka + 1 + 2K[Cu(OH^-)]\} \qquad 2B.5$$

At midpoint of potentiometric titration;

$$1/2[Cu]_T - 2[Cu(OH^-)_2Cu] = [Cu(OH^-)]$$

Substitute (2B.5) into (2B.6);

$1/[H^+]_{midpoint} = 1/C\{[DMP]/(K_dK_a) + K_a\}$ equation 2.1

where $C = \{2[Cu(OH^-)] + 4[Cu(OH^-)2Cu]/[Cu(OH^-)]\} - 2K[Cu(OH-)] - 1$ 2B.7

C is a numerical value calculated using previously determined K. The value of C does not affect K_d in equation 2.1, only K_a. $[Cu(OH^-)]$ and $[Cu(OH^-)_2Cu]$ in (2B.7) determined by substituting (2B.6) into (2B.3);

$K = [Cu(OH^-)_2Cu]/[Cu(OH^-)]^2 = [Cu(OH^-)_2Cu]/(1/2[Cu]_T - 2[Cu(OH^-)_2Cu])$

Derivation of rate equation 2.2.

Cu represents the copper(II) complex in the diaquo form.

$Cu(OH^-)$ represents the copper(II) complex in the mono hydroxo form.

$Cu(OH^-)_2Cu$ represents the copper(II) complex as the dihydroxo bridge form.

$[Cu]_T$ represent the total copper(II) ion concentration.

$$Cu \overset{K_a}{\rightleftharpoons} Cu(OH^-) + H^+ \overset{K}{\rightleftharpoons} Cu(OH^-)_2Cu$$

$$\downarrow +\ BDNPP \xrightarrow{k} Products$$

$K_a = [Cu(OH^-)][H^+]/[Cu]$ 2B.8

$K = [Cu(OH^-)_2Cu]/[Cu(OH^-)]^2$ 2B.9

Rate equation;

$rate = k[Cu(OH^-)][BDNPP]$ 2B.10

Under pseudo-first order conditions in (2B-10);

$k_{obs} = k[Cu(OH^-)]$ 2B.11

Total copper concentration;

$[Cu]_T = [Cu] + [Cu(OH^-)] + 2[Cu(OH^-)_2Cu]$ 2B.12

Substitute (2B.8) and (2B.9) into (2B.11);

$[Cu]_T = [Cu(OH^-)][H^+]/K_a + [Cu(OH^-)] + 2K[Cu(OH^-)]^2$ 2B.13

Use quadratic formula to solve (2B.13) for $[Cu(OH^-)]$;

$0 = 2K[Cu(OH-)]^2 + ([H^+]/Ka + 1)[Cu(OH^-)] - [Cu]_T$

$[Cu(OH^-)] = -([H^+]/Ka + 1) + (([H^+]/Ka + 1)^2 + 8K[Cu]_T)^{1/2}/4K$ 2B.14

Substitute (2B.14) into (2B.11)

$kobs = k\{((1 + [H^+]/K_a)^2 + 8K[Cu]_T)^{1/2} - (1 + [H^+]/K_a)\}/4K$ equation 2.2

Chapter 3. Dinuclear Copper(II) Cleavage of RNA.

3.1 Introduction.

The development of efficient synthetic ribonucleases is currently an active area of research due to their potential antisense application as novel antiviral and anticancer therapeutic agents.[38] Sequence-specific cleavage of RNA has been achieved by attaching various chemical cleaving agents to an oligodeoxyribonucleotide,[50,72-74] however improvement is still necessary since the complexes' cleaving efficiencies were far less than that of natural ribonucleases. In nature there are many phosphatases that require two or more metals in the active site; including alkaline phosphatase,[27] purple acid phosphatase,[55] the 3'5'-exonuclease activity of *Escherichia coli* DNA polymerase I,[26] RNase H from HIV reverse transcriptase,[28] and group I intron ribozymes[109] . Recently model studies of reactive dinuclear metal systems that demonstrate cooperativity between two metal ions for hydrolyzing phosphate esters have been reported.[48,69,110,111]

Chapman and Breslow have compared the reactivities of a mononuclear zinc(II) complex to three different dinuclear zinc(II) complexes for cleaving a diribonucleotide, uridyl(3'-5')uridine (UpU), and other substrates.[111] The metal binding sites of the dinuclear zinc(II) complexes were separated by rigid spacer groups of differing lengths and geometries; 1,4-phenyl ($Zn(II)_2$tn1,4ph), 1,3-phenyl ($Zn(II)_2$tn1,3ph) and 4,4'-biphenyl ($Zn(II)_2$tn4,4ph) (Figure 3.1).

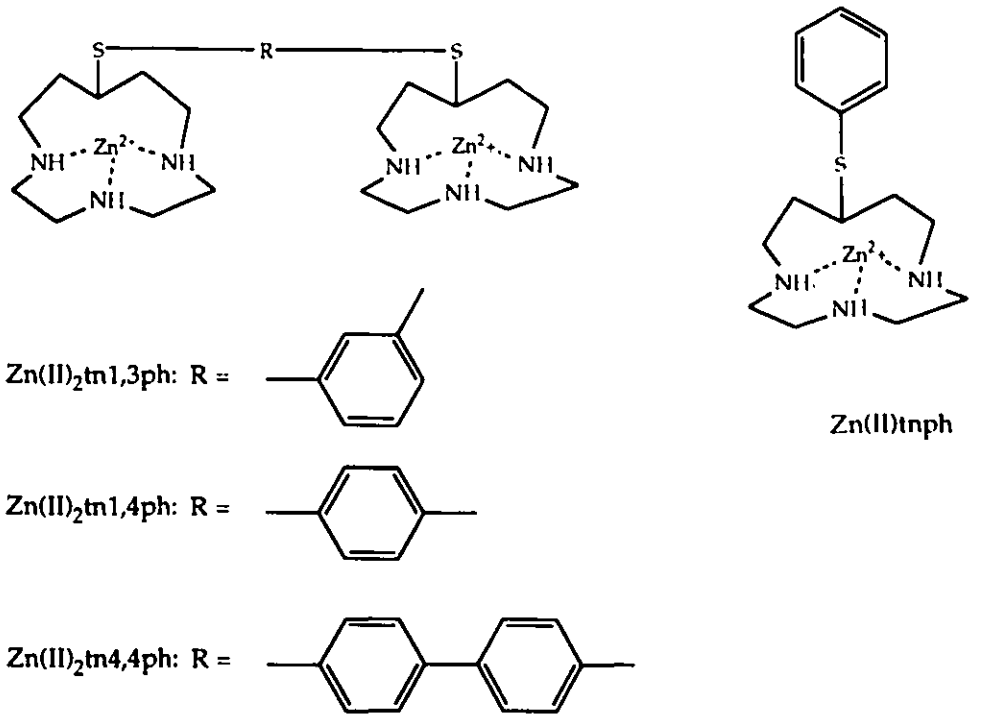

Figure 3.1. Structures of the dinuclear zinc(II) complexes ($Zn(II)_2$tn1,3ph, $Zn(II)_2$tn1,4ph, and $Zn(II)_2$tn4,4ph) and the mononuclear zinc(II) complex (Zn(II)tnph) prepared by Chapman and Breslow for cleaving UpU.[111]

The conditions for the kinetic runs were 227 mM in dimer ($Zn(II)_2$tn1,3ph, $Zn(II)_2$tn1,4ph or $Zn(II)_2$tn4,4ph) and UpU and 454 mM in monomer (Zn(II)tnph) prepared in 20% DMSO solutions at 41 °C and pH 8.36. The observed rate constants and the relative rates of reaction between the various dinuclear zinc(II) complexes and the monomer complex are given in Table 3.1. Although the complexes were not very reactive for cleaving UpU Chapman and Breslow observed that the rates of UpU cleavage varied between the various dinuclear zinc(II) complexes with different spacer groups and also that the mononuclear complex was less reactive than the dinuclear zinc(II) complexes for cleaving the substrate.

Table 3.1. Kinetic data for the zinc(II) complexes at pH 8.4, 41 °C in 20% DMSO and 80% 50 mM Tris buffer.[111]

complex pH 8.36	[complex] (mM)	k_{obs} (s^{-1})	half life (days)	relative rate
$Zn(II)_2$tn4,4phtn	227	3.8×10^{-7}	~ 21	4.2
$Zn(II)_2$tn1,4phtn	227	1.8×10^{-7}	~ 45	2
$Zn(II)_2$tn1,3phtn	227	9×10^{-8}	~ 89	1
Zn(II)tnph	454	9×10^{-8}	~ 89	1

Komiyama *et al.* have prepared a dinuclear zinc(II) complex of N,N,N',N'-tetrakis((2-pyridyl)methyl)-2-hydroxy-1,3-diaminopropane (tpp).[112] The complex $Zn(II)_2$tpp (2.5 mM) cleaved ApA (0.1 mM) with a half life of 10 hours at pH 7 and 50 °C. Although no mechanistic details were provided the authors proposed a mechanism for the cleavage of ApA (Figure 3.2) that parallels the proposed mechanism of DNA cleavage by the 3'5'-exonuclease activity of *E. coli.* DNA polymerase I (Figure 1.9).

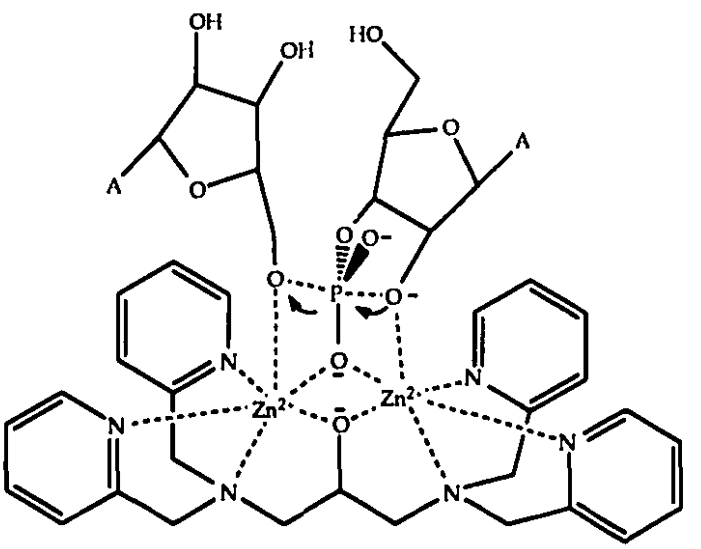

Figure 3.2. Proposed mechanism of cleavage of ApA by $Zn(II)_2$tpp.[112]

In an interesting study Vance and Czarnik prepared a novel cobalt(III) cyclen dimer (see Figure 3.3) with a rigid anthracene backbone and compared its reactivity to the monomer, cobalt(III)cyclen (Co(III)cyclen), for hydrolyzing the phosphate diester BNPP and the monoester 4-nitrophenyl phosphate (NPP).[110] The dinuclear complex (4 mM) was found to be 10 times more reactive for hydrolyzing NPP and 0.7 fold as reactive for hydrolyzing BNPP than the mononuclear Co(III)cyclen (2 mM) at 25 °C and pH 7.

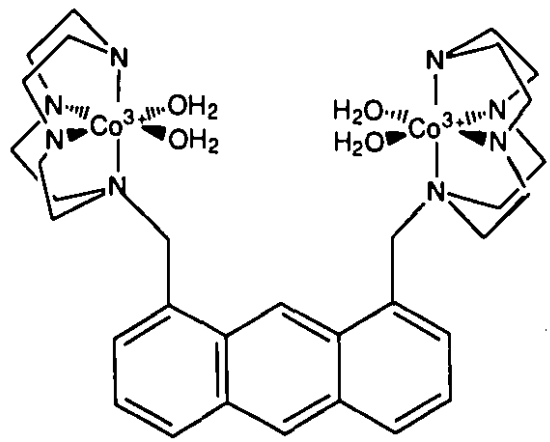

Figure 3.3. Structure of dinuclear cobalt(III) complex, designed by Vance and Czarnik, used to cleave a phosphate diester and a phosphate monoester.[110]

In our study, a novel dinuclear copper(II) complex of 1,8-bis(1,4,7-triazacyclononyl-N-methyl)naphthalene (tntn) was prepared and its ability to cleave an RNA diribonucleotide, ApA, was studied. The dinuclear copper(II) complex, ($Cu(II)_2$tntn), was structurally similar to that prepared by Vance and Czarnik[110] to study BNPP and NPP hydrolysis (Figure 3.4). Dinuclear metal complexes have provided tremendous rate acceleration for RNA model substrates[69,79] but not for RNA itself. The reactivity of the dinuclear copper(II) complex is compared to the reactivity of the mononuclear

copper(II) complex of 1,4,7-triazacyclononane for cleaving ApA and 2'3'-cAMP.

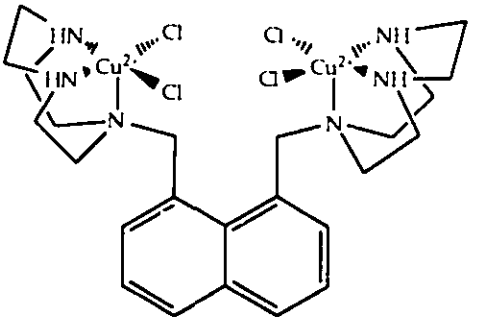

$Cu(II)_2tntn$

Figure 3.4. Structure of dinuclear copper(II) complex used in study to cleave RNA.

3.2. Results and Discussion.

3.2.1. Syntheses and Structures of Complexes.

The ligand, 1,8-bis(1,4,7-triazacyclononyl-N-methyl)naphthalene (tntn), was synthesized by reacting 2 equivalents of the orthoamide protected triazacyclononane with one equivalent of 1,8-bis(bromomethyl)naphthalene in DMSO, followed by removal of the protecting group under basic conditions (Figure 3.5).

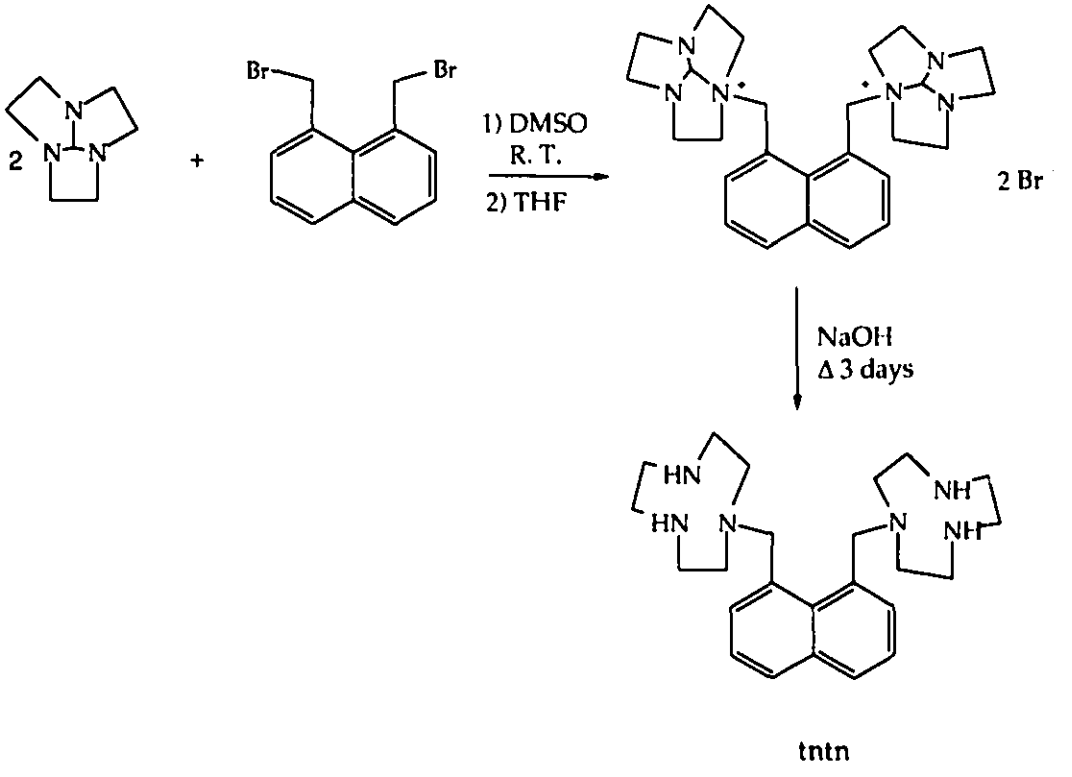

Figure 3.5. Method of synthesis of 1,8-bis(1,4,7-triazacyclononyl-N-methyl)naphthalene (tntn).

The copper(II) complexes of 1,4,7-triazacyclononane and tntn, Cu(II)tacn and $Cu(II)_2$tntn respectively, were prepared by adding ethanolic

solutions of the ligand to ethanolic solutions of copper(II) chloride (Figure 3.6).

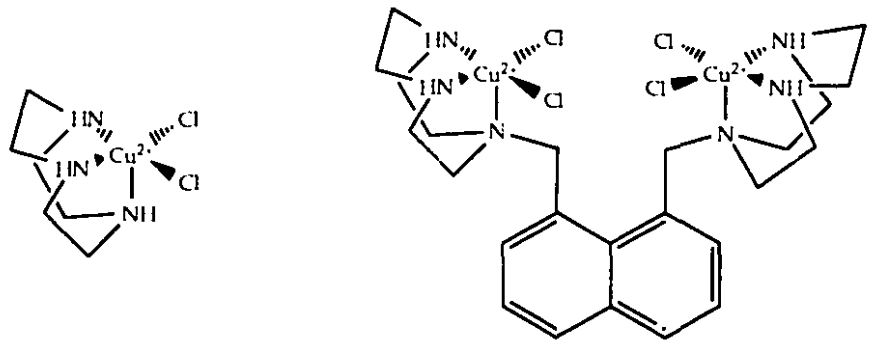

Cu(II)tacn Cu(II)$_2$tntn

Figure 3.6. Structure of copper(II) complexes of 1,4,7-triazacyclononane (tacn) and tntn.

In water the metal-bound chlorides of Cu(II)tacn and Cu(II)$_2$tntn are expected to be replaced by water molecules. Cu(II)$_2$tntn provides a binding site for the substrate that has restricted motion which is considered an essential feature in the design. Other researchers have designed dinuclear metal complexes with flexible backbones but their reactivities for promoting phosphate ester hydrolysis were often not much greater than that of the mononuclear complexes.[111,113] Chapman and Breslow determined that a dinuclear zinc(II) complex (227 mM, pH 8.4) with 1,5-pentane as a backbone was about 2 times faster than the corresponding mononuclear zinc(II) complex (454 mM, pH 8.4) for promoting the cleavage of HPNPP, and slightly less reactive for promoting the cleavage of BNPP (Figure 3.7).[111] The reduction in freedom of motion of the binding site in Cu(II)$_2$tntn is considered an important feature of the design.

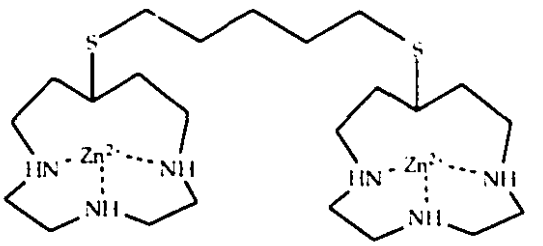

Figure 3.7. Example of a dinuclear metal complex a with a flexible backbone that was not much more effective than two equivalents of the corresponding mononuclear metal complex for promoting phosphate ester hydrolysis.[111]

3.2.2. Potentiometric Titrations.

Potentiometric titrations of Cu(II)tacn determined that there is one titratable proton with a pK_a of 7.5. The potentiometric titration of $Cu(II)_2$tntn showed two equivalents of titratable protons that both appear to occur together. The potentiometric data have been fit to equation 3.1 and based on a non-linear least-squares analysis pK_1 and pK_2 are determined to be 6.5 ± 0.5 and 6.4 ± 0.5, respectively (Figure 3.8). In equation 3.1, V represents the volume of titrant being added, V_O is the original volume of water in the titration cell, $[H^+]$ is the proton concentration, K_a is the acid dissociation constant of the strong acid used to lower the pH initially, F_a is the original concentration of strong acid, K_b is the base dissociation constant of the titrant, F_b is the concentration of titrant being added, K_1 is the first metal bound water acid dissociation constant of $Cu(II)_2$tntn, K_2 is the second metal bound water acid dissociation constant of $Cu(II)_2$tntn, and M represents the original concentration of $Cu(II)_2$tntn.

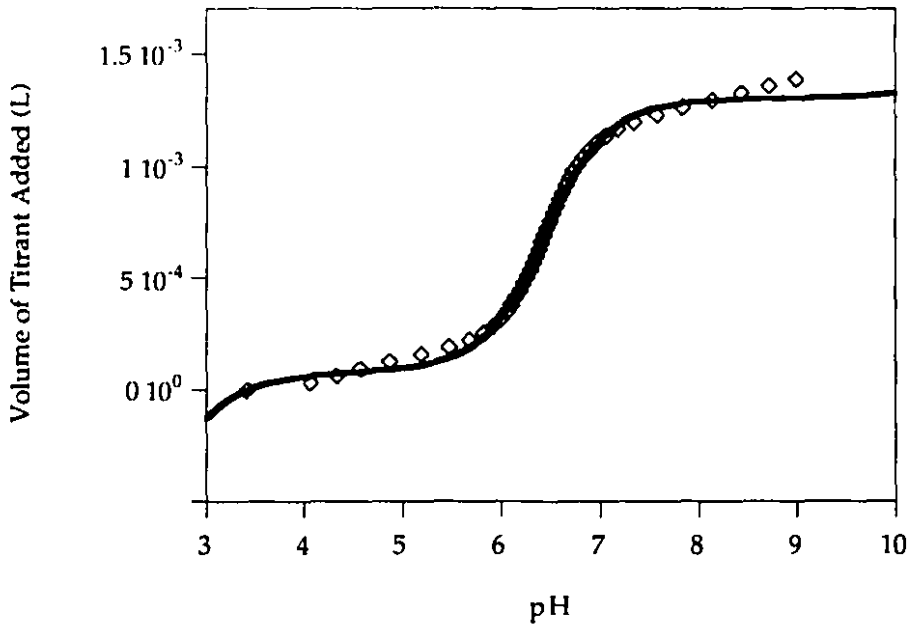

Figure 3.8. The best fit of equation 3.1 to the potentiometric titration data of $Cu(II)_2$tntn. R(equation 3.1) = 0.99.

Volume of titrant being added (V) =

$$Vo\{\underline{Kw/[H+] + KaFa/([H+] + Ka) - [H+] + M(2K_1K_2 + K_1[H+]/([H+]^2 + K_1[H+] + K_1K_2)}\}$$
$$(K_bF_b[H^+]/K_b[H^+] + K_w + [H^+] - K_W/[H^+]$$

equation 3.1

Potentiometric titrations have been determined of the ligand (tntn) in the absence and in the presence of copper(II) ion, and copper(II) ion in the absence of ligand, that demonstrate complete metal binding under the experimental conditions. Hexaamine ligands with flexible backbones can effectively encapsulate a single metal ion rather than coordinate two metal ions.[114-116] The titration curves are shown in Figure 3.9. From these curves it can be seen that the solution containing only copper(II) chloride (Figure 3.9-A) has 2 equivalents of titratable protons occurring at neutral pH,

corresponding to the $Cu(II)(OH^-)_2$ species. The ligand (tntn) has no titrable protons around neutral pH (Figure 3.9-B). The solution containing one equivalent of ligand and one equivalent of copper(II) ion has the equivalent of one titratable proton around neutral pH (Figure 3.9-C) and the solution containing one equivalent of ligand and two equivalents of copper(II) ion has the equivalent of two titratable protons at neural pH (Figure 3.9-D). If the second metal was not binding then three equivalents of titratable protons would be expected in the 1:2 ligand:metal solution (Figure 3.9-D) since the 1:1 ligand:metal solution (Figure 3.9-C) showed one titratable proton at neutral pH. If the ligand tntn was not binding either metal ion then four titrable protons would be expected in Figure 3.9-D.

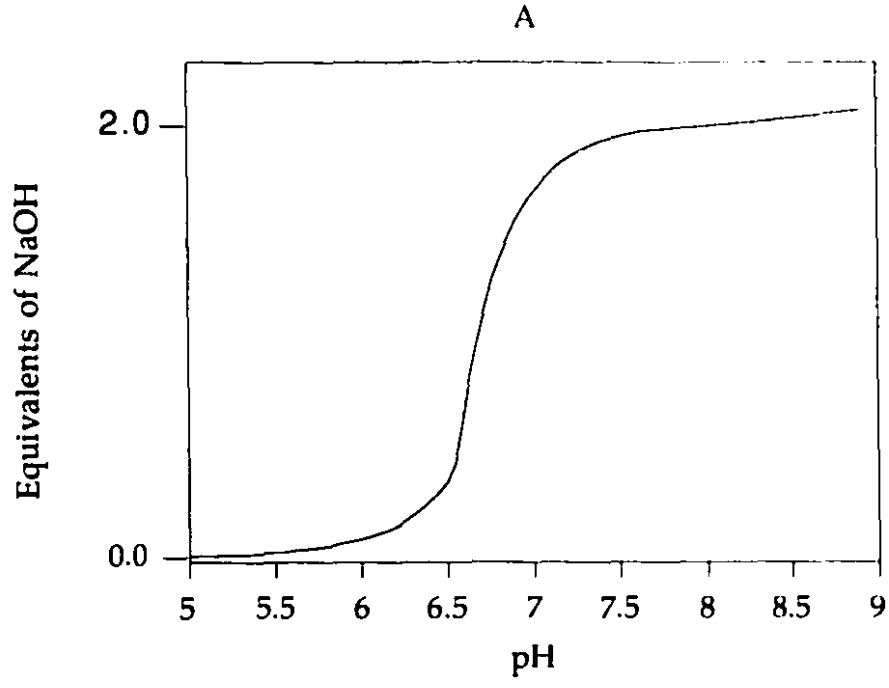

B

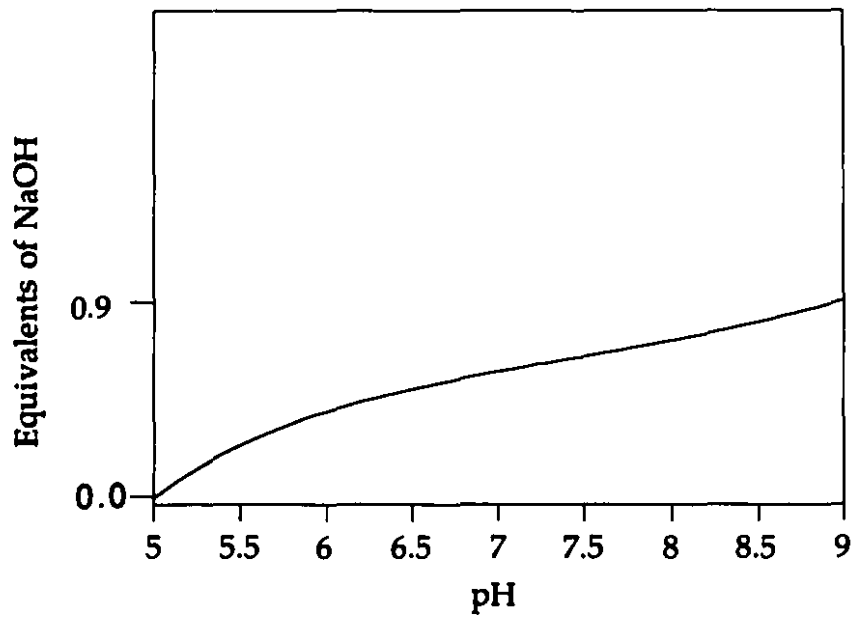
Equivalents of NaOH
0.9
0.0
5
5.5
6
6.5
7
7.5
8
8.5
9
pH

C

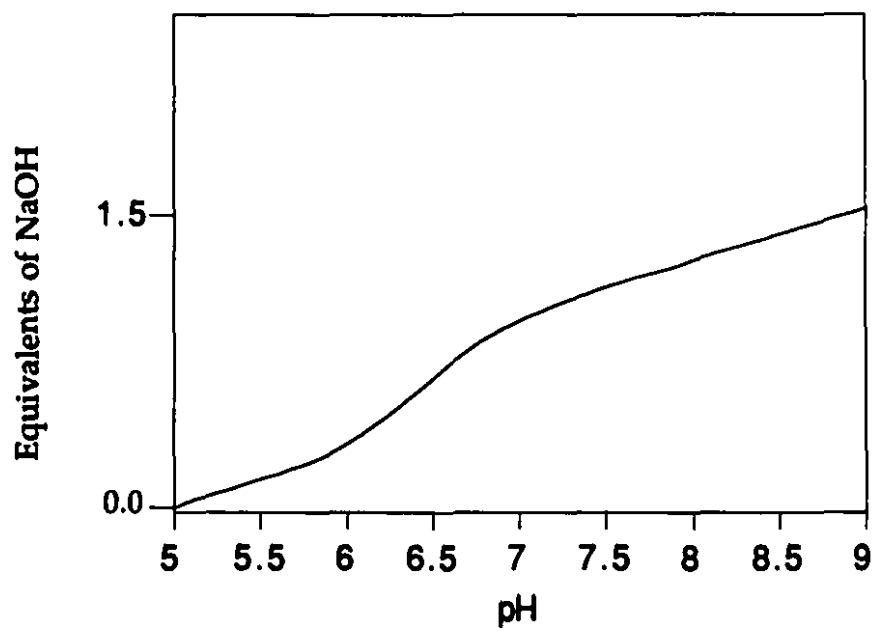
Equivalents of NaOH
1.5
0.0
5
5.5
6
6.5
7
7.5
8
8.5
9
pH

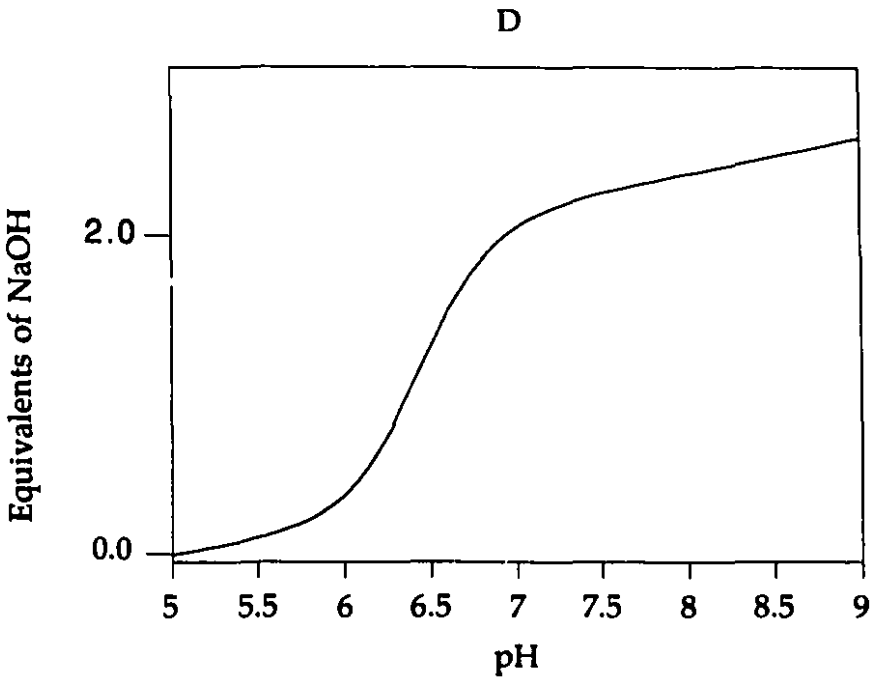

Figure 3.9. Potentiometric titrations of mixed solutions of $CuCl_2$ and tntn demonstrating that tntn binds 2 equivalents of metals in aqueous solution. A) 5 μmol $CuCl_2$; B) 5 μmol tntn; C) 5 μmol CuCl2 and 5 μmol tntn; and D) 10 μmol and 5 μmol tntn with 0.01 M NaOH titrant at 25 °C. The ionic strength was maintained with 0.1 M $NaNO_3$.

3.2.3. Dinuclear Cleavage of ApA and 2'3'-cAMP.

Base-catalyzed hydrolysis of ApA involves two steps (Figure 3.10). In the first step the ionized 2'OH of ApA attacks the phosphorus center, liberating adenosine and producing the 2'3'-cyclic-adenosine monophosphate (2'3'-cAMP). In the second step the 2'3'-cAMP is hydrolyzed forming both the 3'phosphate (3'-AMP) and the 2'adenosine monophosphate (2'-AMP).

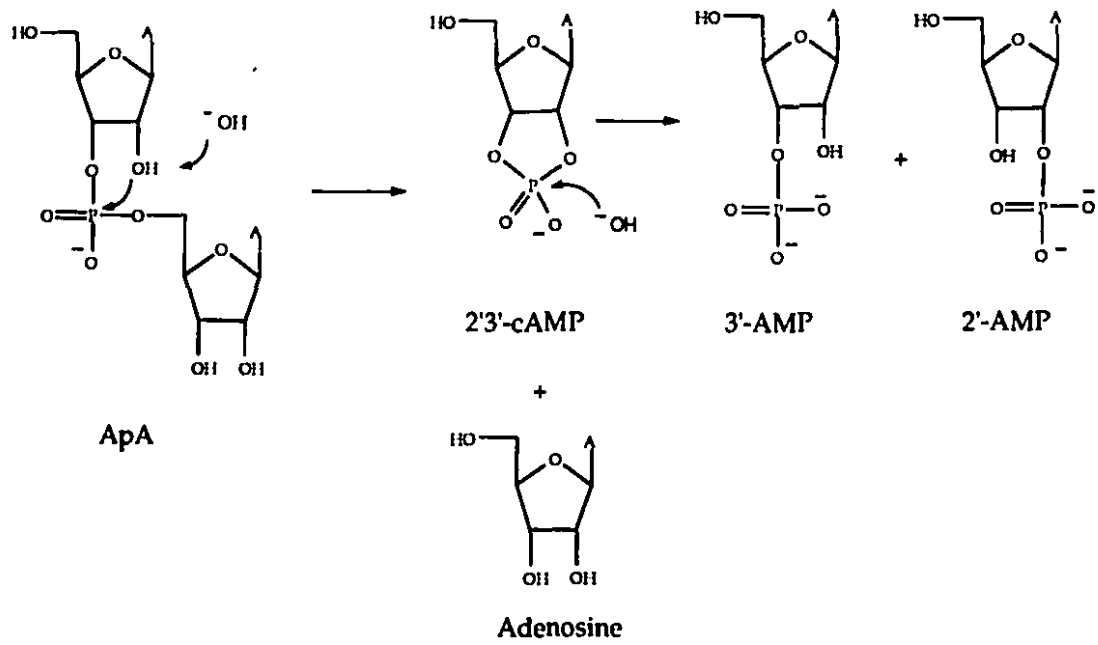

Figure 3.10. Base-catalyzed hydrolysis of ApA.

For the rate studies, solutions of $Cu(II)_2$tntn (2.0 mM) and ApA (50 °C, 0.05 mM), or 2'3'cAMP (25 °C, 0.05 mM), were buffered using MES (10 mM). Cleavage of ApA to adenosine, 2'-AMP and 3'-AMP was monitored by HPLC, as was for the cleavage of 2'3-cAMP to 2'-AMP and 3'-AMP. The complex, $Cu(II)_2$tntn, appeared to be stable at 25 °C (10 mM MES, pH 6) considering there was no significant change in the UV-vis absorbance spectrum from 350-800 nm over a period of 7 hours. Solutions of $Cu(II)_2$tntn at pH greater than 6 and 50 °C gradually lost reactivity with time, presumably due to precipitation of copper(II)$(OH^-)_2$. A typical HPLC plot for $Cu(II)_2$tntn promoted cleavage of ApA (0.05 mM) at pH 6.0 and 50 °C is shown in Figure 3.11.

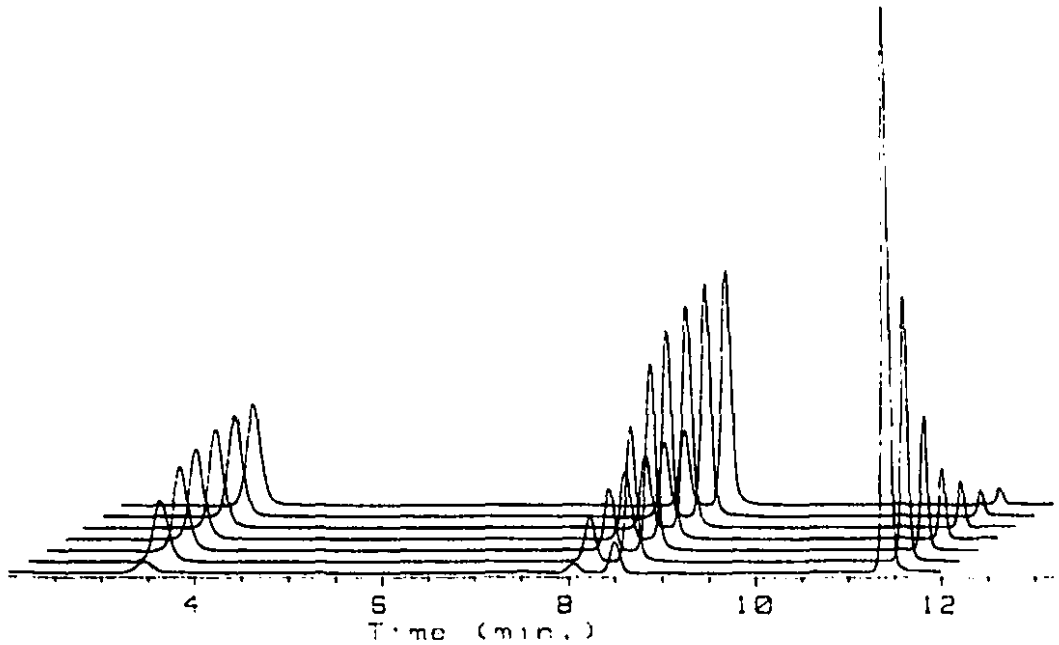

Figure 3.11. HPLC traces of $Cu(II)_2$tntn (2 mM) promoted cleavage of ApA (0.05 mM) at 50 °C, pH 6.0 (10 mM) MES. Retention times are as follows: 3'AMP = 3.5 min; 2'3'-cAMP = 7.5 min; 2'AMP = 8 min; adenosine = 8.5 min; ApA = 11 .4 min. Reaction times are from foreground to background 20, 100, 180, 260, 340, 420 and 500 min.

There was no accumulation of 2'3'cAMP during the ApA cleavage reaction, however it is evident from the HPLC plot that the cleavage reaction occurs hydrolytically, producing adenosine, 3'-AMP, and 2'-AMP. Oxidative cleavage typically occurred at the ribose and results in degradation of the sugar.[42] A typical HPLC plot for $Cu(II)_2$tntn promoted cleavage of 2'3'-cAMP (0.05 mM) at pH 6.0 and 25 °C is shown in Figure 3.12.

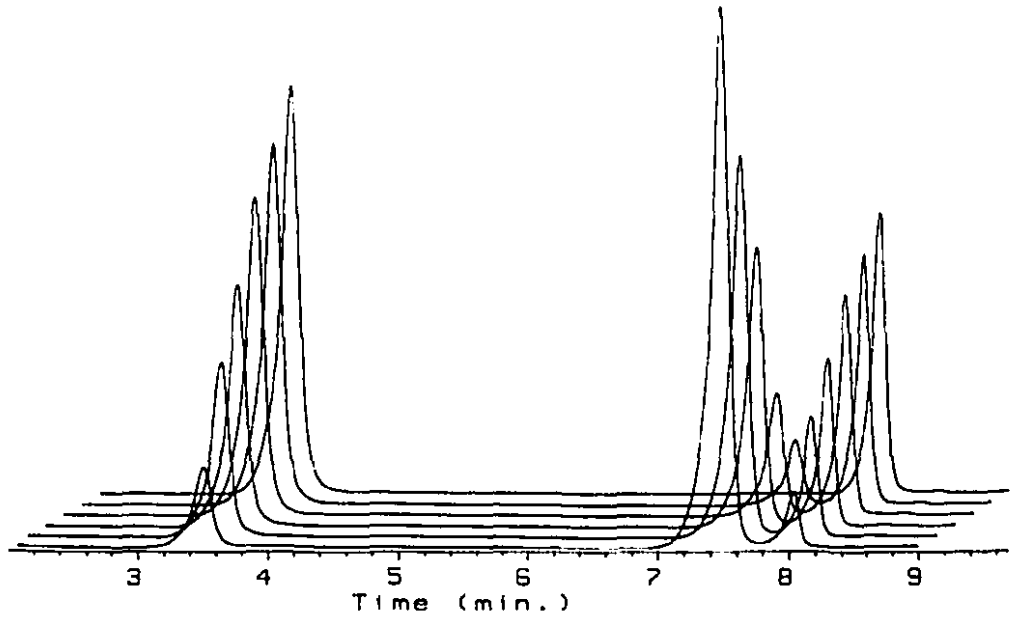

Figure 3.12. HPLC traces of $Cu(II)_2$tntn (2 mM) promoted cleavage of 2'3'-cAMP (0.05 mM) at 25 °C, pH 6.0 (10 mM) MES. Retention times are as follows: 3'-AMP = 3.5 min; 2'3'-cAMP = 7.5 min; and 2'-AMP = 8 min. Reaction times are from foreground to background 1, 3, 5, 10, 15 and 60 min.

The optimal reactivity of $Cu(II)_2$tntn for cleaving ApA and 2'3'-cAMP was reached about pH 6. The pH-rate profile of $Cu(II)_2$tntn accelerated cleavage of ApA (50 °C) and 2'3-cAMP (25 °C) is shown in Figure 3.13.

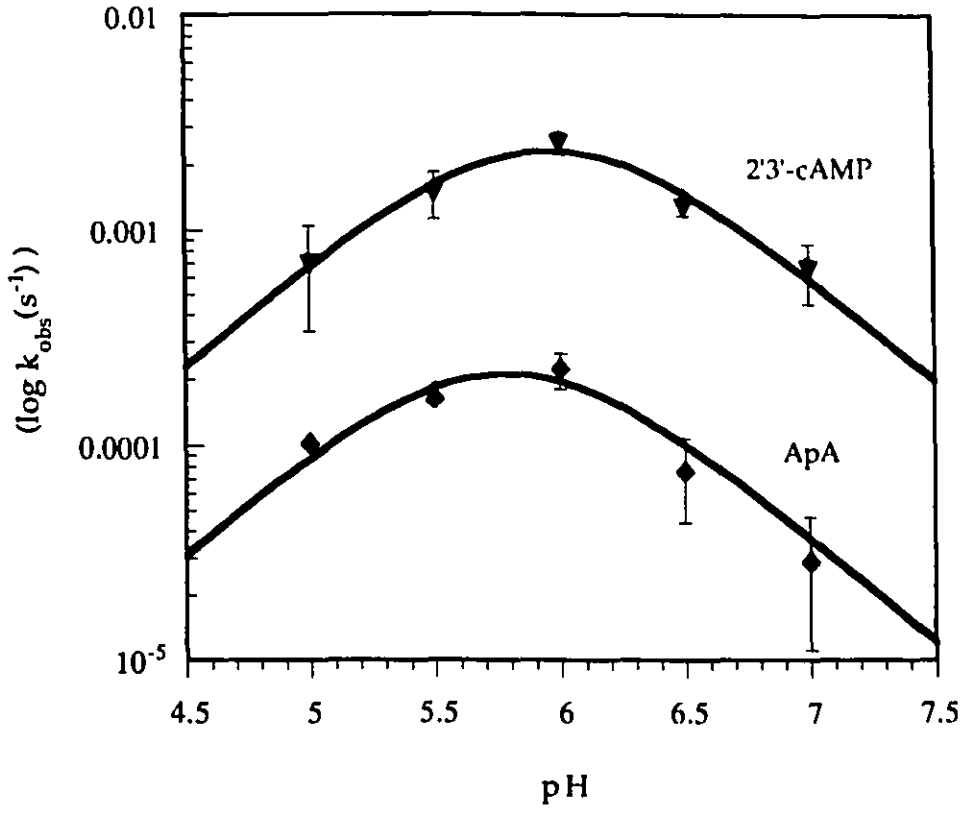

Figure 3.13. pH-rate profiles for $Cu(II)_2$tntn promoted cleavage of 2'3'-cAMP (0.05 mM) at 25 °C and ApA (0.05 mM) at 50 °C. (R(equation 3.2) = 0.96 (ApA) and 0.98 (2'3'-cAMP)). Error bars represent ± one standard deviation based on triplicate runs.

The pH rate profiles (Figure 3.13) were fit based on a non-linear least-squares analysis to equation 3.2, where $[Cu(II)_2tntn]_T$ represents the total concentration of complex, $[H^+]$ is the proton concentration, K_{a1} and K_{a2} are the first and second acid dissociation constants of the metal bound waters, and k is the second-order rate constant for the mono-hydroxo form of $Cu(II)_2$tntn promoted cleavage of ApA or 2'3'-cAMP. The values from the fit of equation 3.2 (with K_{a1} fixed equal to K_{a2}) to the pH-rate profiles of Figure 3.12 are presented in Table 3.2.

$$k_{obs} = k\,[Cu(II)_2tntn]_T\,/(1 + [H^+]/K_{a1} + K_{a2}/[H^+]) \qquad \text{equation 3.2}$$

Table 3.2. The values and errors of K_{a1}, K_{a2} and k as determined from the non-linear least-squares fit of equation 3.2 to the pH rate-profiles (Figure 3.12).

$Cu(II)_2tntn$ (2 mM)	K_{a1}	K_{a2}	k ($M^{-1}s^{-1}$)
ApA (50 °C)	$(1.6 \pm 0.3) \times 10^{-6}$	$(1.6 \pm 0.3) \times 10^{-6}$	$(3.2 \pm 0.3) \times 10^{-1}$
2'3'-cAMP (25 °C)	$(1.0 \pm 0.1) \times 10^{-6}$	$(1.0 \pm 0.1) \times 10^{-6}$	$(3.4 \pm 0.2) \times 10^{0}$

3.2.4. Mononuclear Cleavage of ApA and 2'3'cAMP.

The pseudo-first order rate constants for the cleavage of ApA (50 °C, 0.05 mM) and 2'3'cAMP (25 °C, 0.05 mM) by Cu(II)tacn (4.0 mM) were investigated using HPLC analyses over the pH range of 7.0 to 7.6. The optimal reactivity for Cu(II)tacn cleavage for both ApA and 2'3-cAMP was reached at approximately pH 7.3. In Table 3.3 the pseudo-first order rate constants for cleavage of ApA (50 °C) and 2'3'-cAMP (25 °C) promoted cleavage by Cu(II)tacn and $Cu(II)_2tntn$ are compared at their optimal reactivities. The dinuclear metal complex $Cu(II)_2tntn$ is observed to be a few hundred times more reactive than the mononuclear metal complex Cu(II)tacn per metal center for cleaving ApA or 2'3-cAMP.

Table 3.3. Comparison of pseudo-first order rate constants (s^{-1}) for cleavage of ApA (50 °C) and 2'3'-cAMP (25 °C) by Cu(II)tacn (4.0 mM) and $Cu(II)_2$tntn (2.0 mM). The optimal reactivity of Cu(II)tacn was reached at pH 7.3 (10 mM HEPES) while the optimal reactivity of $Cu(II)_2$tntn was reached at pH 6.0 (10 mM MES). Errors are quoted as ± one standard deviation based on triplicate runs.

Substrate	k_{obs} (s^{-1}) Cu(II)tacn	k_{obs}(s^{-1}) $Cu(II)_2$tntn	kobs-$Cu(II)_2$tntn/ kobs-Cu(II)tacn
ApA	$(4.2 \pm 0.8) \times 10^{-7}$	$(2.2 \pm 0.4) \times 10^{-4}$	$\sim 5 \times 10^2$
2'3'cAMP	$(8.7 \pm 0.6) \times 10^{-6}$	$(2.5 \pm 0.3) \times 10^{-3}$	$\sim 3 \times 10^2$

The original studies of $Cu(II)_2$tntn promoted cleavage of ApA and 2'3'-cAMP were compared to the mononuclear complex Cu(II)tacn. More recently the mononuclear complex Cu(II)(N-benzyl-1,4,7-triazacyclononane) (Cu(II)btacn) has been prepared and its reactivity for cleaving 2'3'-cAMP has been investigated. The complex, Cu(II)btacn, was prepared according to Figure 3.14. Cu(II)btacn has one titrable proton with a pK_a of 7.6. The pseudo-first order rate constants for the cleavage of 2'3'cAMP (25 °C, 0.05 mM) by Cu(II)btacn (4.0 mM) was investigated by HPLC analysis over the pH range of 7.0 to 8.0. The optimal reactivity for Cu(II)btacn (4.0 mM, pH 7.3, 25 °C) promoted cleavage of 2'3-cAMP (0.05 mM) was reached at approximately pH 7.3 with a pseudo-first order rate constant measured at $(1.5 \pm 0.6) \times 10^{-6}$ s^{-1}. (The error quoted is ± 1 standard deviation based on triplicate runs). The reactivity of Cu(II)btacn appeared insignificantly different than Cu(II)tacn for cleaving 2'3'cAMP. The complexes, Cu(II)tacn and Cu(II)btacn, appeared stable at 25 °C (10 mM HEPES, pH 7.3) considering there were no significant changes in their UV-vis absorbance spectra from 350-800 nm over a period of 7 hours.

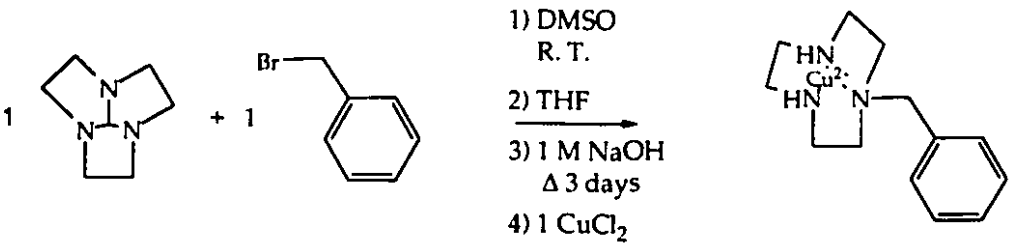

Figure 3.14. Preparation of copper(II)(N-benzyl-1,4,7-triazacyclononane), Cu(II)btacn.

3.2.5. Mechanism.

Two dinuclear copper(II) complexes systems recently been shown to greatly accelerate the cleavage of an RNA analog, HPNPP.[69,79] Their reactivities were proposed to result from double Lewis acid activation through bridging of the phosphate diester to the two metal centers. In contrast to a mononuclear metal complex that provides single Lewis activation, a dinuclear metal complex that bridges a phosphate diester provides additional stabilization during RNA transesterification since the negative charge develops next to the positively charged metal ion (Figure 3.15). In the mononuclear metal system the negative charge transferred to the phosphate during RNA transesterification receives no such additional stabilization. The dinuclear metal complexes that cleaved HPNPP were however unreactive for cleaving RNA itself. The lack of reactivity is possibly due to the complexes' steric bulk interfering with a bridging RNA phosphate diester.

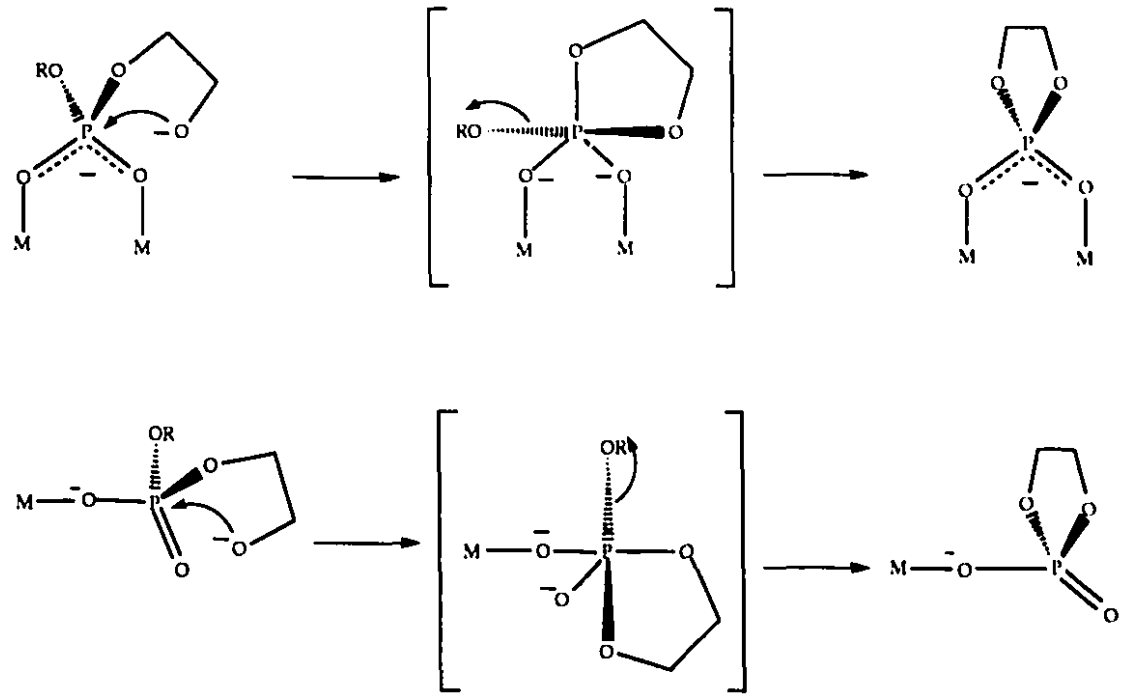

Figure 3.15. Stabilization of the transition state during RNA transesterification by double Lewis acid activation (top) and single Lewis acid activation (bottom). Notice that during double Lewis acid activation there is an additional stabilizing interaction between the metal and the developing negative charge.

The reactivity of $Cu(II)_2$tntn for cleaving RNA is proposed to result from bridging of the phosphate diester to the two metal centers. Crystals of $Cu(II)_2$tntn grown in the presence of diphenyl phoshinate, a substrate analog, gave $[Cu_2(O_2PPh_2)_2(tntn)](ClO_4)_2$. The structure was determined by X-ray crystallography (Figures 3.16 and 3.17).

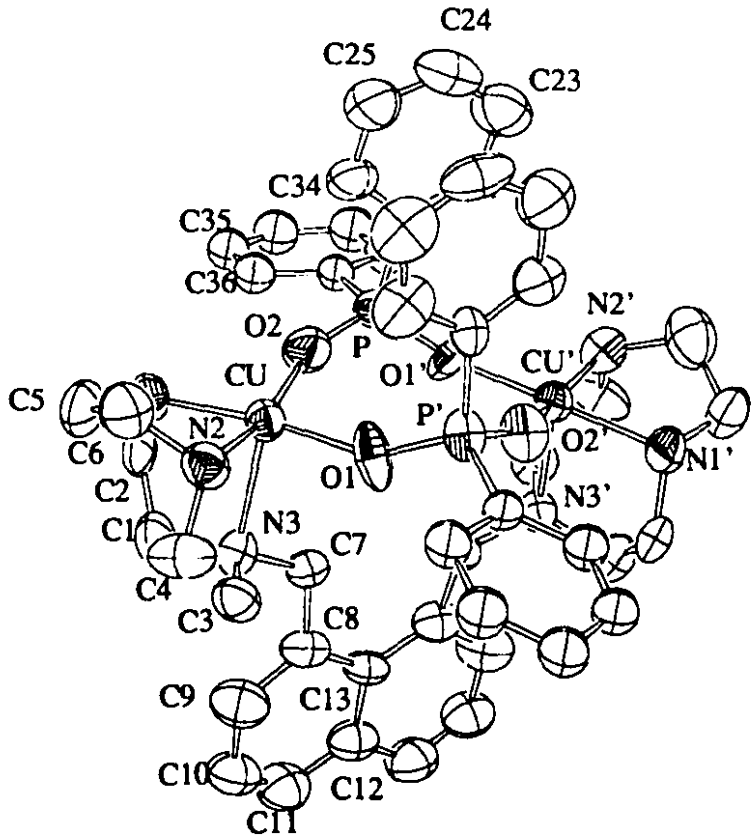

Figure 3.16. ORTEP diagram of $[Cu_2(O_2PPh_2)_2(tntn)](ClO_4)_2 \cdot 1.5MeOH$. ORTEP showing at 30% probability ellipsoids.

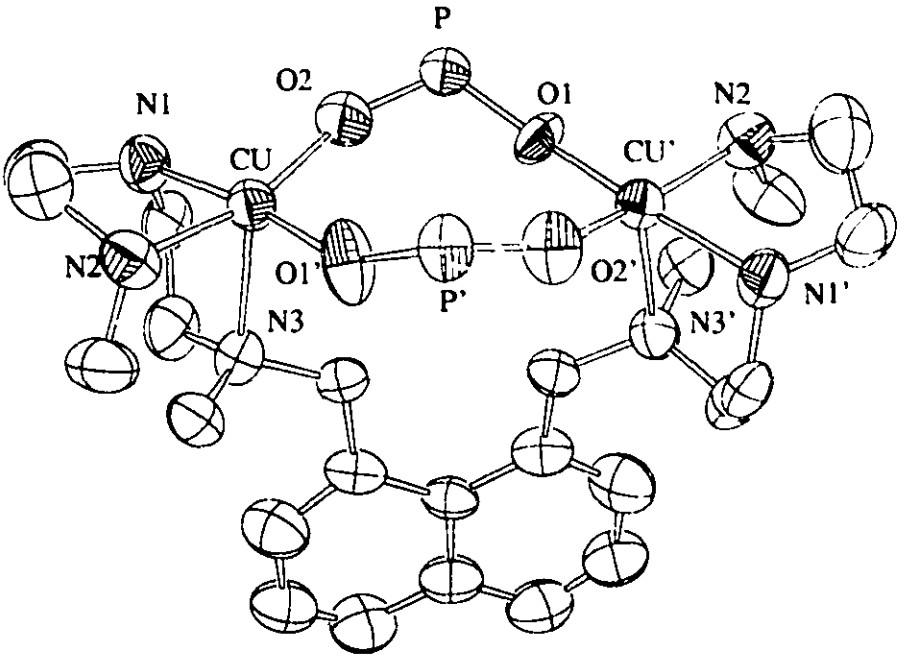

Figure 3.17. Modified ORTEP diagram of $[Cu_2(O_2PPh_2)_2(tntn)](ClO_4)_2 \cdot 1.5MeOH$ with the four phenyl groups of the two diphenylphosphinates removed in order to clearly view the bridging of the phosphinates to the two metal centers. ORTEP showing at 30% probability ellipsoids.

Table 3.4. Selected bond lengths and angles for $[Cu_2(O_2PPh_2)_2(tntn)](ClO_4)_2 \cdot 1.5MeOH$. Symmetry transformations used to generate equivalent atoms: #1 x ,-y+1/2,-z+1/4.

Atoms	Distance (Å)	Atoms	Distance (Å)
Cu-O(1)	1.908(6)	Cu-N(3)	2.342(7)
Cu-O(2)	1.925(6)	P-O(2)#1	1.496(7)
Cu-N(1)	2.006(7)	P-O(1)	1.521(6)
Cu-N(2)	2.006(7)	Cu-Cu	5.050(3)

Atoms	Angles (°)	Atoms	Angles (°)
O(1)-Cu-O(2)	97.0(3)	O(1)-Cu-N(3)	92.7(3)
O(1)-Cu-N(1)	72.6(3)	O(2)-Cu-N(3)	109.8(3)
O(2)-Cu-N(1)	89.9(3)	N(1)-Cu-N(3)	82.5(3)
O(1)-Cu-N(2)	90.8(3)	N(2)-Cu-N(3)	84.0(3)
O(2)-Cu-N(2)	163.6(3)	O(2)#1-P-O(1)	116.8(4)
N(1)-Cu-N(2)	83.1(3)		

The X-ray analysis supports the proposal that $Cu(II)_2$tntn cleaves phosphate diesters by providing double Lewis acid activation. The observation that $Cu(II)_2$tntn is 200-500 times more reactive than Cu(II)tacn or Cu(II)btacn per metal center for cleaving ApA and 2'3'-cAMP represents a tremendous cooperation between the two metal centers. $Cu(II)_2$tntn is not the most reactive complex for cleaving RNA,[47] however it does represent the first example of a simple dinuclear metal complex whose metal centers cooperatively cleave the phosphate diester bonds of both RNA and 2'3'-cAMP. The bell shaped pH-rate profiles indicate that the mono-hydroxo form of $Cu(II)_2$tntn, or its kinetic equivalent, is the active species for cleaving ApA and hydrolyzing 2'3'-cAMP. The products of ApA cleavage, adenosine, 2'-AMP and 3'-AMP, indicate that the internal 2'hydroxyl is acting as nucleophile to promote transesterification of the diribonucleotide. The active

form of $Cu(II)_2$tntn, the mono-hydroxide form, appears to be acting as a general base in promoting the cleavage of ApA. With the 2'3'-cAMP substrate the active form of $Cu(II)_2$tntn may be acting as a general base, or alternatively the metal-hydroxide may be acting as a nucleophile.

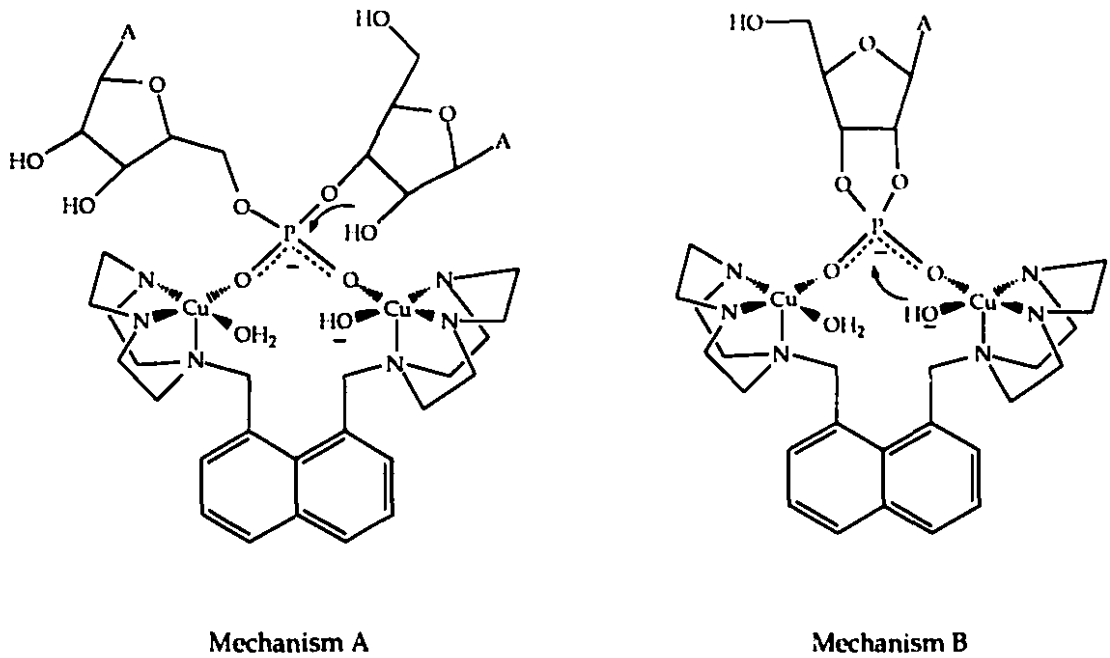

Mechanism A Mechanism B

Figure 3.18. Possible pathways available to $Cu(II)_2$tntn for accelerating the cleavage of RNA. The copper-hydroxide in the active species of $Cu(II)_2$tntn may act as a general base (mechanism A) or as a nucleophile (mechanism B).

It is important to understand the relative rates of the background base-catalyzed hydrolysis of ApA and 2'3'-cAMP for interpreting the data from the $Cu(II)_2$tntn system. It is not intuitively obvious which is more susceptible to base-catalyzed cleavage. The internal nucleophile of RNA has been estimated to destabilize the phosphate ester linkage by 10^7 fold compared to that of DNA while the 2'3'-cAMP intermediate is a 5-membered cyclic phosphate. Westheimer *et al.* have demonstrated that the base-catalyzed hydrolysis of a 5-membered cyclic phosphate diester, ethylene phosphate, is 10^8 fold faster

than the acyclic phosphate diester, dimethyl phosphate.[6,117] The rates of base catalyzed diribonucleotide cleavage and 2'3'-cAMP have been extensively studied by Lönnberg *et al.* and Abrash *et al.*, respectively.[5,118] The second order rate constants for hydroxide-catalyzed hydrolysis of ApA at 60 °C and 2'3'-cAMP at 30 °C has been estimated to be 3.3×10^{-3} $M^{-1}s^{-1}$ and 1.5×10^{-3} $M^{-1}s^{-1}$.[5,118] Upon extrapolation of these values of base catalyzed hydrolysis of ApA and 2'3'-cAMP as well as other values[5,118] to the same temperature and pH the rates of base-catalyzed cleavage appear to have similar values (within one order of magnitude). A similar rate for the base-catalyzed hydrolysis of UpA and 2'3'-cUMP has also been proposed by Thompson *et al.*[119] If the base-catalyzed rate at pH 6 is compared to the dinuclear copper(II) complex rate at pH 6 it is observed that $Cu(II)_2$tntn provides approximately 5 orders of magnitude rate acceleration for cleaving ApA and 8 orders of magnitude rate acceleration for hydrolyzing 2'3'-cAMP. The difference in the rate-accelerations provided by $Cu(II)_2$tntn for cleaving ApA and 2'3'-cAMP suggests that the metal-hydroxide of the active-form of the complex is acting as a nucleophilic catalyst rather than as a general base catalyst for cleaving 2'3'-cAMP (Figure 3.18). Intramolecular general base catalysis is typically limited to an effective molarity of 10 M or less and therefore does not account for the observed differences in rate acceleration.[64]

3.3 Conclusion.

A novel dinuclear copper(II) complex ($Cu(II)_2$tntn) has been prepared that demonstrates remarkable cooperativity between the two metal centers for cleaving RNA. $Cu(II)_2$tntn is observed to be approximately 500 times more reactive per metal center than the mononuclear complex Cu(II)tacn for cleaving ApA and between 200-300 times more reactive than the mononuclear complexes, Cu(II)tacn and Cu(II)btacn, for cleaving 2'3'-cAMP. The observed reactivity of the dinuclear copper(II) complex is proposed to result from the bridging of a phosphate diester through both metal centers. This proposal is supported by a crystal structure of the complex bridging a substrate analog, diphenyl phosphinate. The difference in rate-accelerations provided by $Cu(II)_2$tntn for cleaving ApA and 2'3'-cAMP suggests that the active form of the dinuclear copper(II) complex cleaves these substrates by two different mechanisms.

3.4 Experimental.

3.4.1. General Information.

All elemental analyses were performed by Guelph Chemical Laboratories. Mass spectra were obtained on a Kratos MS25RFA mass spectrometer by Nadim Saade of McGill University.

NMR. ^{1}H NMR (299.3 MHz), ^{13}C NMR (75.4 MHz) and ^{31}P NMR (121.4 MHz) spectra were obtained on a Varian XL-300 FT spectrophotometer. ^{1}H NMR (199.975 MHz) and ^{13}C NMR (50.289 MHz) were obtained on a Varian Gemini 200 spectrophotometer. Data are reported in parts per million (ppm).

Titrations. Titrations were performed with a Radiometer PHM63 pH meter equipped with a Radiometer TTT80 titration controller and an ABU80 automatic burette. Standardized NaOH solutions purchased from Aldrich were used as titrant. The pH was measured with a Radiometer K-4040 calomel reference electrode and a G-2040C glass electrode. Temperature was maintained using a Lauda RM6 water bath.

UV-vis measurements. UV-vis measurements were taken with a HP8452A diode array spectrophotometer equipped with a water jacketed 7 cell transport. Temperatures were controlled with a Lauda RM6 water bath.

HPLC Measurements. All HPLC measurements were performed on a HP 1090m HPLC equipped with a temperature controlled autosampler compartment equipped. A 2.1x100 mm 5 μm ODS Hypersil C18 reverse-phase column maintained at 40 °C was used. Data were collected and integrated using an HP9153c computer and analyzed using Microsoft Excel and KaleidaGraph software on a Macintosh computer. Peaks were observed with a diode array UV detector at 254 nm and were identified by their retention times which had been determined by injections of authentic samples.

Injection volumes ranged from 1 to 25 μL depending on the concentration of the sample.

Buffers. 4-(2-hydroxyethyl)-1-piperazineethanesulfonic acid (HEPES, pKa = 7.4) and 4-morpholineethanesulfonic acid monohydrate (MES, pKa = 6.1) were purchased from Aldrich. All were used without further purification.

Danger. Metal complexes isolated as perchlorate salts are potentially explosive therefore caution should be exercised. They should be prepared only in small quantities and appropriate precautions taken in their handling.

3.4.2. Materials.

Benzyl bromide, copper(II) chloride, copper(II) perchlorate, diphenylphosphinic acid, and EDTA (disodium salt) were purchased from Aldrich and were used without further purification. ApA (free acid), 2'-AMP (free acid), 3'-AMP (free acid), adenosine and 2'3'-cAMP (sodium salt) were purchased from Sigma and were used without further purification. 1,8-bis(bromomethyl)naphthalene[120,121], 1,4,7-triazacyclononane[122,123] and 1,4,7-triazacyclononane orthoamide[124] were prepared by previously reported methods.

3.4.3. Synthesis of Ligands and Metal Complexes.

[1-bromomethyl-8-((N-orthoamide)-1,4,7-triazacyclononyl-N-methyl)naphthalene] bromide. (tnBr)

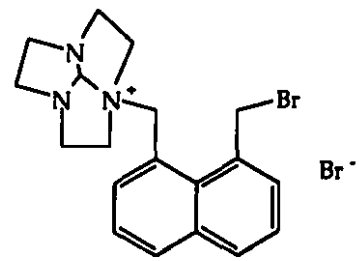

1,4,7-Triazacyclononane orthoamide (0.1348 g, 9.68×10^{-4} mol) was added to 1,8-bis(bromomethyl)naphthalene(0.3041 g, 9.68×10^{-4} mol) in dry THF (30 mL). The reaction was stirred at room temperature for 12 hours, the product filtered, washed with dry THF, and the solvent was removed *in vacuo*. Yield: 0.390 g (89%). ^{1}H NMR (DMSO-d_6) δ 3.4 (4H, m), 3.8 (8H, m), 5.35 (2H, s), 5.42 (2H, s), 6.59 (1H, s), 7.5 - 7.9 (4H, m), 8.12 (2H, m). ^{13}C NMR (DMSO-d_6, 1,4-dioxane(66.7 ppm)) δ 51.9, 55.5, 58.1, 60.1, 124.9, 125.6, 127.6,128.4, 130.4, 131.3, 132.8, 133.0, 135.1, 139.0.

[1,8-Bis(N-orthoamide-1,4,7-triazacyclononyl-N-methyl)naphthalene] dibromide. (tntnBr$_2$)

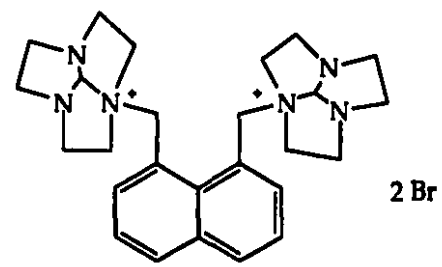

1,4,7-Triazacyclononane orthoamide (0.095 g, 6.82×10^{-4} mol) was added to tnBr (0.302 g, 6.67×10^{-4} mol) in DMSO (10 mL). After stirring at room temperature for 20 minutes dry THF (100 mL)was added. The product was filtered, washed with THF and dried *in vacuo*. Alternatively tntnBr$_2$ was prepared by 1,4,7-triazacyclononane (2 equivalents) to 1,8-bis(bromomethyl)naphthalene (1 equivalent) in DMSO, followed by addition of dry THF after 20 minutes. The workup was completed as previously

described. Yield: 0.379 g (96%). ^{1}H NMR (DMSO-d_6) δ 3.9 - 3.5 (24H, m), 5.35 (2H, s), 5.05 (4H, s), 6.68 (2H, s), 7.7 (4H, m), 8.09 (2H, d).

1,8-Bis(1,4,7-triazacyclononyl-N-methyl)naphthalene. (tntn)

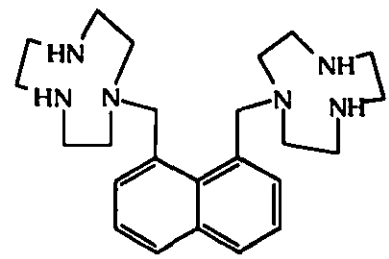

The compound, tntnBr_2 (0.350 g, 5.9 x 10^{-4} mol), was heated to ~90°C in 1 M NaOH (125 mL) for 3.5 days. The reaction mixture was cooled, the product was extracted into chloroform, and the solvent removed *in vacuo*. The product was dissolved in 100% ethanol/ether (3:1) mixture, HCl gas was passed through the solution, and the acid salt of the product was filtered and washed with 100% ethanol. The acid salt was recrystallized in an acetone/methanol (1:1) mixture. The product was obtained upon extraction under basic conditions into chloroform (3 × 150 mL) and removing the solvent in vacuo. Yield: 0.172 g (71 %). ^{1}H NMR (CDCl3, TMS) δ 2.27 (8H, t), 2.65 (16H, m), 4.42 (4H, s), 7.35 (2H, t, J = 8.3 Hz)), 7.52 (2H, d, J = 6.5 Hz)), 7.79 (2H, d, J = 8.3 Hz)). ^{13}C NMR ($CDCl_3$, 1,4-dioxane(66.7 ppm)) δ 46.1, 46.3, 52.7, 63.5, 123.7, 128.6, 129.6. MS (EI, ion source 200 °C, 70 eV, direct probe 250 °C), [m/z(relative intensity)] : 411($M^{+\cdot}$,1), 182(100), 153(65). HRMS(EI, 70ev, direct probe 100°C) calcd. for $C_{24}H_{38}N_6$, found m/z 410.31520 (M+·).

N-benzyl-(N-orthoamide)-1,4,7-triazacyclononane bromide. (btacnBr)

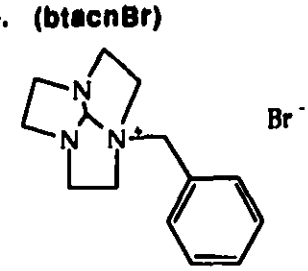

Benzyl bromide (0.30 mL, 2.3 mmol) was added to a solution of 1,4,7-triazacyclononane orthoamide (0.35 g, 2.5 mmol) in dry THF (20 mL). The solution was stirred for 3 hours at room temperature and the white precipitate that formed was collected by filtration. The precipitate was

thoroughly washed with dry THF (2 × 100 mL) and dried *in vacuo*. Yield: 0.59 g (76 %). ^{1}H NMR (DMSO) δ 3.1-3.7 (12H, m), 4.58 (2H, s), 5.80 (1H, s), 7.50 (3H, m), 7.68 (2H, m). ^{13}C NMR (DMSO, 1,4-dioxane(66.7 ppm)) δ 52.0, 56.1, 56.5, 60.39, 66.7, 123.3, 128.7, 129.6, 131.9.

N-benzyl-1,4,7-triazacyclononane. (btacn)

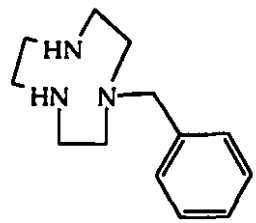

The compound btacnBr (0.30 g, 0.97 mmol) was added to 1 M NaOH (50 mL) and heated at 90 °C for 3 days. Upon cooling, N-benzyl-1,4,7-triazacyclononane was extracted into dichloromethane (3 × 100 mL) and concentrated *in vacuo*. The ligand was used without further purification. Yield: 0.13 g (63 %). ^{1}H NMR ($CDCl_3$,TMS) δ 2.6-2.8 (12H), 3.80 (2H, s), 7.2-7.4 (5H, m). ^{13}C NMR ($CDCl_3$, 1,4-dioxane(66.7 ppm)) δ 45.8, 45.9, 52.0, 61.2, 126.1, 127.3, 127.9.

Cu(1,4,7-triazacyclononane)Cl_2. (Cu(II)tacn)

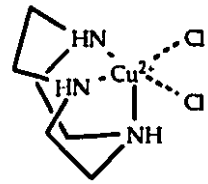

The complex Cu(II)tacn was prepared as previously described by Schwindinger *et al.*[125] Anal. Calcd. for $C_6H_{15}N_3Cl_2Cu$: C, 27.33; H, 5.73; N, 15.94. Found: C, 27.33; H, 5.98; N, 15.53.

$Cu_2$1,8-Bis(1,4,7-triazacyclononyl-N-methyl)naphthaleneCl_4. ($Cu(II)_2$tntn)

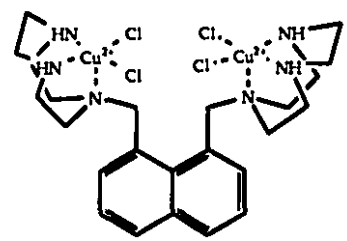

A solution of 1,8-Bis(1,4,7-triazacyclononyl-N-methyl)naphthalene (0.533 g, 1.29 x10^{-4} mol) in 100 % ethanol (3 mL) was added to a $CuCl_2$ (0.383 g, 2.86 x10^{-4} mol) solution in 100% ethanol (2 mL). The green precipitate that formed was filtered,

washed with 100% ethanol, and dried overnight *in vacuo*. Yield: 0.076 g (87%). Anal. Calcd. for $C_{24}H_{38}N_6Cu_2Cl_4.H_2O$: C, 41.33; H, 5.78; N, 12.05. Found: C, 41.51; H, 5.77; N, 11.77.

Cu(N-benzyl-1,4,7-triazacyclononane)Cl_2. (Cu(II)btacn)

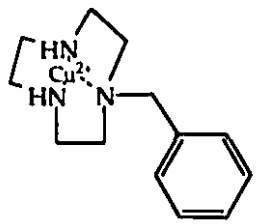

N-benzyl-1,4,7-triazacyclononane (0.013 g, 8.39×10^{-4} mol) in 100% ethanol (5 mL) was added to copper(II) chloride (0.113 g, 8.39×10^{-4} mol) in 100% ethanol (5 mL). The blue precipitate was filtered, washed with cold 100% ethanol (3×5 mL), and dried overnight *in vacuo*. Yield: 0.21 g (70 %). Anal. Calcd. for $C_{13}H_{21}N_3CuCl_2$: C, 44.14; H, 5.98; N, 11.88. Found: C, 43.87; H, 6.09; N, 11.58.

3.4.4. Potentiometric Titrations.

3 mL (1.5 mM) solutions of Cu(II)tacn, Cu(II)btacn, and $Cu(II)_2$tntn in 0.1 M $NaNO_3$ (25 °C) were titrated with a 0.01 M NaOH solution. The 0.01 M NaOH solution was prepared with 0.1 M NaOH and 0.1 M $NaNO_3$.

3.4.5. Kinetic Studies.

Aliquots of the reaction mixture for the cleavage of ApA and 2'3'-cAMP were analyzed by HPLC analysis under the following conditions: a flow rate of 0.5 mL/min of $NH_4H_2PO_4$ (0.2 M at pH 5.5) for five minutes followed by a linear gradient up to 50% of a 60/40 methanol/water solution over the next 10 min. Aliquots of the reaction mixture for $Cu(II)_2$tntn promoted cleavage of 2'3'-cAMP were quenched with 50 mM EDTA solutions prior to analysis by HPLC. The rate constants for Cu(II)tacn and Cu(II)btacn promoted cleavage of ApA and 2'3'cAMP were obtained by the initial rate method while

those for $Cu(II)_2$tntn promoted cleavage of the substrates were obtained by fitting the first three half-lives of the reaction according to the first-order kinetics equation.

3.4.6. X-ray Diffraction Studies.

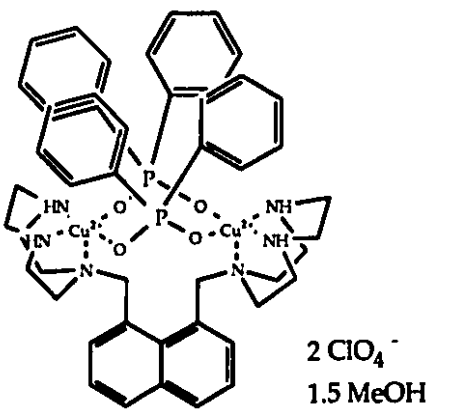

The perchlorate salt of $Cu(II)_2$tntn was isolated by adding a solution of tntn (0.0430 g, 1.04×10^{-4} mol) in 100 % ethanol (4 mL) to a solution of $Cu(ClO_4)_2.6H_2O$ (0.0854 g, 2.30×10^{-4} mol) in 100% ethanol (4 mL). The blue precipitate that immediately formed was filtered and washed with cold 100% ethanol (2×5 mL) (40% yield). Cu_2tntn$(ClO_4)_4$ was used without further purification.

Blue crystals appeared after 6 days of gradual evaporation of solvent from a solution containing $Cu(II)_2$tntn$(ClO_4)_4$ (23.8 mg, 2.54×10^{-5} mol) and diphenylphosphinic acid (11.1 mg, 5.09×10^{-5} mol) in 23 mL methanol and 1 mL acetonitrile.

Absorption correction and data reduction was done using the NRCVAX program.[126] Structure was solved by direct methods (SHELXS-86) and refined using SHELXL-93.[127,128] Compound is a dimer about a two-fold axis, atoms C12 and C13 in the naphthalene ring are situated on the axis. One perchlorate counter-ion was found by difference map. It is on the bar-4 site at 0 0 1/2. To balance charges, 12 more perchlorates were needed in the cell. A heavily disordered region remained near the origin but no chemically meaningful fragment could be identified. The contribution from this region was removed from the structure factors using the programs PLATON[129] and SQUEEZE.[130] PLATON was used to calculate a void of 2161 $Å^3$/cell at roughly

coordinates 0 0 0. Squeeze calculated that the electron count in the void was 809 electrons/cell. If we assume the presence of the 12 ClO_4^- anions (588e$^-$), 221 electrons remain for solvent. The compound was recrystallized from a mixture of methanol and acetonitrile. The remaining electrons correspond to 10 MeCN or 12 MeOH molecules (or any mixture of the 2). Using MeOH, we get a general formula of $[Cu_2(O_2PPh_2)_2(tntn)](ClO_4)_2 \cdot 1.5MeOH$ {tntn = 1,8-bis(1,4,7-triazacyclononyl-N-methyl)naphthalene}. The volume for the void is 2161 Å^3 which corresponds to 25 Å^3 per non-H atom, a rather lager value indicating that there is probably more solvent unaccounted for. The final model refined against the solvent-free F_o contains the dimer and one perchlorate anion. One on the phenyl rings on phosphorus is disordered over two sites at 0.72 and 0.28 occupancies. The two parts of the disorder were restrained to similar bond distances and thermal parameters, they were kept isotropic. All other non-H atoms were refined anisotropically.

APPENDIX 3A. Tables of Data from Chapter 3.

Table 3A.1. pH-rate profile data for $Cu(II)_2$tntn (2.0 mM) promoted cleavage of ApA (0.05 mM) at 50 °C (10 mM MES). The errors are given as ± one standard deviation based upon triplicate runs.

pH	kobs (s-1) ApA	error
5.0	1.01×10^{-4}	$\pm 1 \times 10^{-6}$
5.5	1.63×10^{-4}	$\pm 5 \times 10^{-6}$
6.0	2.23×10^{-4}	$\pm 4.2 \times 10^{-5}$
6.5	7.54×10^{-5}	$\pm 3.2 \times 10^{-5}$
7.0	2.89×10^{-5}	$\pm 1.8 \times 10^{-5}$

Table 3A.2. pH-rate profile data for $Cu(II)_2$tntn (2.0 mM) promoted cleavage of 2'3'-cAMP (0.05 mM) at 25 °C (10 mM MES). The errors are given as ± one standard deviation based upon triplicate runs.

pH	kobs (s-1) 2'3'-cAMP	error
5.0	6.93×10^{-4}	$\pm 3.6 \times 10^{-4}$
5.5	1.49×10^{-3}	$\pm 3.6 \times 10^{-4}$
6.0	2.52×10^{-3}	$\pm 2.8 \times 10^{-4}$
6.5	1.28×10^{-3}	$\pm 1.1 \times 10^{-4}$
7.0	6.57×10^{-4}	$\pm 2.0 \times 10^{-4}$

APPENDIX 3B. X-ray Diffraction Tables of $[Cu_2(O_2PPh_2)_2(tntn)](ClO_4)_2 \cdot 1.5MeOH$. ORTEP diagram showing at 30% probability.

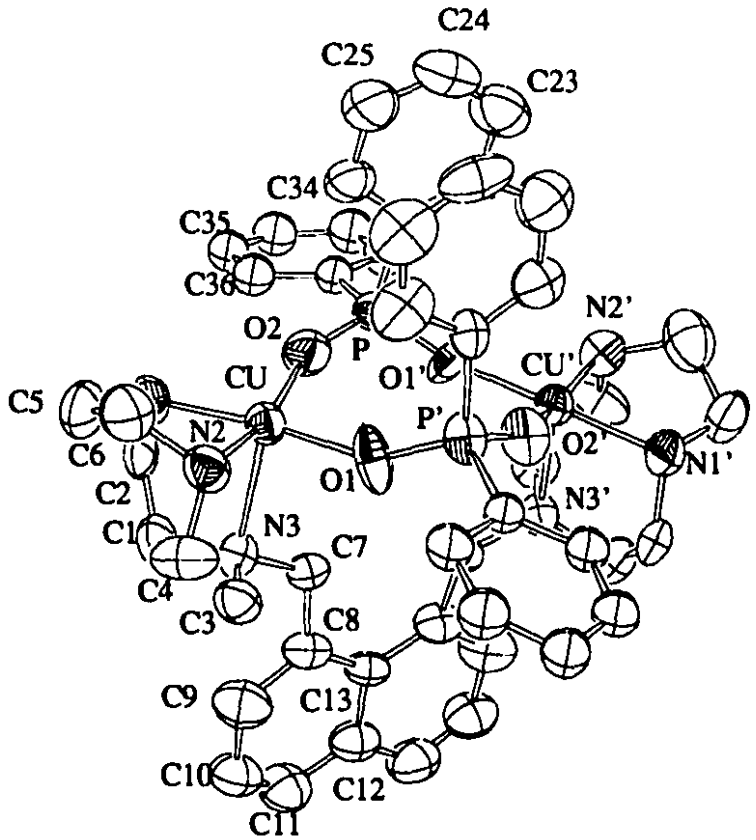

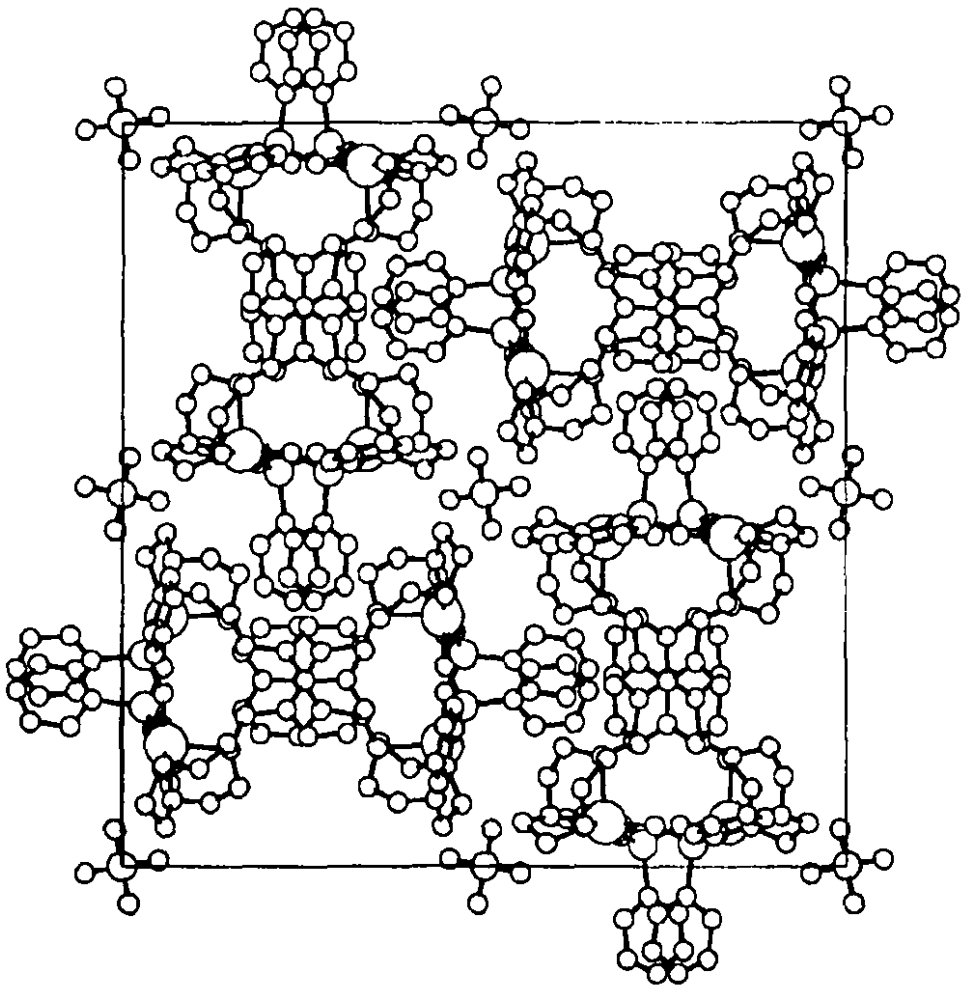

Packing diagram of $[Cu_2(O_2PPh_2)_2(tntn)](ClO_4)_2 \cdot 1.5MeOH$.

Table 3B.1. Crystal data and structure refinement for $[Cu_2(O_2PPh_2)_2(tntn)](ClO_4)_2 \cdot 1.5MeOH$.

Empirical formula	C49.5 H64 O13.5 N6 P2 Cl2 Cu2
Formula weight	1219.03
Temperature	293(2) K
Wavelength	1.54056 Å
Crystal system	Tetragonal
Space group	I-42d
Unit cell dimensions	a = 26.085(4) Å alpha = 90 deg.
	b = 26.085(4) Å beta = 90 deg.
	c = 16.260(5) Å gamma = 90deg.
Volume	11064(4) $Å^3$
Z	8
Density (calculated)	1.464 Mg/m^3
Absorption coefficient	2.962 mm^{-1}
F(000)	5064
Crystal size	0.30 × 0.25 × 0.25 mm
Theta range for data collection	3.0 to 60.0 deg.
Index ranges	-29<=h<=29, -10<=k<=20, -18<=l<=18
Reflections collected	10169
Independent reflections	3730 [R(int) = 0.0720]
Absorption correction	Psi scan
Refinement method	Full-matrix least-squares on F^2
Data / restraints / parameters	3730 / 32 / 286
Goodness-of-fit on F^2	1.098
Final R indices [I>2sigma(I)]	R1 = 0.0733, wR2 = 0.1843
R indices (all data)	R1 = 0.1066, wR2 = 0.2052
Absolute structure parameter	0.07(6)
Largest diff. peak and hole	0.252 and -0.306 $e^-/Å^3$

Table 3B.2. Atomic coordinates ($\times 10^4$) and equivalent isotropic displacement parameters ($A^2 \times 10^3$) for $[Cu_2(O_2PPh_2)_2(tntn)](ClO_4)_2 \cdot 1.5MeOH$. U(eq) is defined as one third of the trace of the orthogonalized Uij tensor.

	x	y	z	U(eq)
Cu	4406(1)	1639(1)	539(1)	57(1)
P	4702(1)	2848(1)	151(1)	67(1)
O(1)	4443(3)	2326(2)	135(4)	88(2)
O(2)	4547(3)	1795(3)	1673(4)	83(2)
N(1)	4314(3)	898(3)	830(5)	72(2)
N(2)	4444(3)	1364(3)	-611(4)	73(2)
N(3)	3518(3)	1596(3)	329(4)	64(2)
C(1)	3395(4)	1071(4)	629(7)	84(3)
C(2)	3792(4)	866(3)	1188(6)	72(3)
C(3)	3547(4)	1666(4)	-584(5)	74(3)
C(4)	3955(4)	1320(5)	-1018(6)	97(4)
C(5)	4410(5)	533(4)	127(7)	92(3)
C(6)	4683(5)	839(5)	-517(8)	116(4)
C(7)	3311(3)	2033(3)	807(5)	55(2)
C(8)	2738(4)	2106(4)	770(5)	69(3)
C(9)	2433(5)	1763(5)	312(6)	96(4)
C(10)	1896(4)	1791(5)	322(7)	90(4)
C(11)	1655(5)	2105(5)	799(7)	93(4)
C(12)	1913(5)	2500	1250	73(4)
C(13)	2486(5)	2500	1250	55(3)
C(21)	5400(4)	2763(3)	169(5)	61(2)
C(22)	5620(4)	2355(4)	-244(5)	102(4)
C(23)	6113(4)	2286(4)	-220(5)	114(5)
C(24)	6416(5)	2643(6)	175(7)	101(4)
C(25)	6227(5)	3059(5)	573(9)	108(4)
C(26)	5694(4)	3109(4)	560(7)	80(3)
C(31)	4586(5)	3145(4)	-797(7)	49(2)
C(32)	4564(5)	2860(5)	-1523(7)	68(3)
C(33)	4444(6)	3117(5)	-2263(7)	78(4)

Table 3B.2 continued.

	x	y	z	U(eq)
C(34)	4304(6)	3617(4)	-2315(8)	75(3)
C(35)	4351(5)	3883(5)	-1599(7)	65(3)
C(36)	4461(7)	3664(4)	-844(7)	63(3)
C(31A)	4467(14)	3181(8)	-858(15)	49(2)
C(32A)	4259(12)	2831(8)	-1411(16)	68(3)
C(33A)	4063(12)	3036(9)	-2161(15)	78(4)
C(34A)	3813(11)	3508(9)	-2114(17)	75(3)
C(35A)	4193(12)	3839(8)	-1805(16)	65(3)
C(36A)	4423(15)	3697(9)	-1050(18)	63(3)
Cl(1)	5000	5000	0	87(2)
O(3)	5095(6)	4506(5)	387(8)	80(4)
O(3A)	5037(13)	4753(10)	686(15)	117(10)

Table 3B.3. Bond lengths [Å] for $[Cu_2(O_2PPh_2)_2(tntn)](ClO_4)_2 \cdot 1.5MeOH$.

Cu-O(1)	1.908(6)	Cu-O(2)	1.925(6)
Cu-N(1)	2.006(7)	Cu-N(2)	2.006(7)
Cu-N(3)	2.342(7)	P-O(2)#1	1.496(7)
P-O(1)	1.521(6)	P-C(31)	1.752(11)
P-C(21)	1.835(10)	P-C(31A)	1.96(2)
O(2)-P#1	1.496(7)	N(1)-C(2)	1.482(11)
N(1)-C(5)	1.510(12)	N(2)-C(6)	1.511(14)
N(2)-C(4)	1.440(13)	N(3)-C(3)	1.499(10)
N(3)-C(7)	1.482(10)	N(3)-C(1)	1.489(11)
C(1)-C(2)	1.477(13)	C(3)-C(4)	1.563(14)
C(5)-C(6)	1.50(2)	C(7)-C(8)	1.507(12)
C(8)-C(9)	1.411(14)	C(8)-C(13)	1.449(11)
C(9)-C(10)	1.40(2)	C(10)-C(11)	1.29(2)
C(11)-C(12)	1.432(13)	C(12)-C(11)#1	1.432(13)
C(12)-C(13)	1.49(2)	C(13)-C(8)#1	1.449(11)
C(21)-C(26)	1.344(13)	C(21)-C(22)	1.384(12)
C(22)-C(23)	1.30	C(23)-C(24)	1.38(2)
C(24)-C(25)	1.36(2)	C(25)-C(26)	1.40(2)
C(31)-C(36)	1.395(13)	C(31)-C(32)	1.397(13)
C(32)-C(33)	1.412(14)	C(33)-C(34)	1.36(2)
C(34)-C(35)	1.361(14)	C(35)-C(36)	1.383(14)
C(31A)-C(36A)	1.39(2)	C(31A)-C(32A)	1.39(2)
C(32A)-C(33A)	1.43(2)	C(33A)-C(34A)	1.39(2)
C(34A)-C(35A)	1.41(2)	C(35A)-C(36A)	1.41(2)
Cl(1)-O(3A)#2	1.29(3)		
Cl(1)-O(3A)#3	1.29(3)	Cl(1)-O(3A)	1.29(3)
Cl(1)-O(3A)#4	1.29(3)	Cl(1)-O(3)#3	1.456(12)
Cl(1)-O(3)#2	1.456(12)	Cl(1)-O(3)	1.456(12)
Cl(1)-O(3)#4	1.456(12)		

Table 3B.4. Bond angles [deg] for $[Cu_2(O_2PPh_2)_2(tntn)](ClO_4)_2 \cdot 1.5MeOH$.

O(1)-Cu-O(2)	97.0(3)	O(1)-Cu-N(1)	172.6(3)
O(2)-Cu-N(1)	89.9(3)	O(1)-Cu-N(2)	90.8(3)
O(2)-Cu-N(2)	163.6(3)	N(1)-Cu-N(2)	83.1(3)
O(1)-Cu-N(3)	92.7(3)	O(2)-Cu-N(3)	109.8(3)
N(1)-Cu-N(3)	82.5(3)	N(2)-Cu-N(3)	84.0(3)
O(2)#1-P-O(1)	116.8(4)	O(2)#1-P-C(31)	108.9(5)
O(1)-P-C(31)	107.8(5)	O(2)#1-P-C(21)	109.3(4)
O(1)-P-C(21)	109.5(4)	C(31)-P-C(21)	103.8(5)
O(2)#1-P-C(31A)	104.8(9)	O(1)-P-C(31A)	104.2(8)
C(21)-P-C(31A)	112.2(11)	P-O(1)-Cu	149.0(5)
P#1-O(2)-Cu	152.5(4)	C(2)-N(1)-C(5)	114.3(8)
C(2)-N(1)-Cu	104.9(5)	C(5)-N(1)-Cu	114.2(6)
C(4)-N(2)-C(6)	110.0(9)	C(4)-N(2)-Cu	114.3(6)
C(6)-N(2)-Cu	104.5(6)	C(7)-N(3)-C(1)	117.3(7)
C(7)-N(3)-C(3)	116.3(7)	C(1)-N(3)-C(3)	116.7(7)
C(7)-N(3)-Cu	104.3(5)	C(1)-N(3)-Cu	102.1(6)
C(3)-N(3)-Cu	95.0(5)	C(2)-C(1)-N(3)	112.5(8)
C(1)-C(2)-N(1)	112.5(8)	N(3)-C(3)-C(4)	114.2(8)
N(2)-C(4)-C(3)	110.5(8)	C(6)-C(5)-N(1)	105.7(8)
C(5)-C(6)-N(2)	110.9(10)	N(3)-C(7)-C(8)	115.9(7)
C(9)-C(8)-C(13)	118.6(9)	C(9)-C(8)-C(7)	120.0(9)
C(13)-C(8)-C(7)	121.3(9)	C(10)-C(9)-C(8)	121.6(11)
C(11)-C(10)-C(9)	121.7(12)	C(10)-C(11)-C(12)	122.3(11)
C(11)#1-C(12)-C(11)	124(2)	C(11)#1-C(12)-C(13)	118.1(7)
C(11)-C(12)-C(13)	118.1(7)	C(8)#1-C(13)-C(8)	125.9(12)
C(8)#1-C(13)-C(12)	117.1(6)	C(8)-C(13)-C(12)	117.1(6)
C(26)-C(21)-C(22)	120.7(10)	C(26)-C(21)-P	119.6(7)
C(22)-C(21)-P	119.7(8)	C(23)-C(22)-C(21)	120.2(6)
C(22)-C(23)-C(24)	119.2(7)	C(25)-C(24)-C(23)	123.5(12)
C(24)-C(25)-C(26)	115.6(13)	C(21)-C(26)-C(25)	120.7(12)
C(36)-C(31)-C(32)	117.4(10)	C(36)-C(31)-P	121.2(8)
C(32)-C(31)-P	121.0(8)	C(31)-C(32)-C(33)	118.4(10)

Table 3B.4 continued.

C(34)-C(33)-C(32)	124.8(12)	C(33)-C(34)-C(35)	114.3(12)
C(34)-C(35)-C(36)	124.6(11)	C(35)-C(36)-C(31)	119.8(10)
C(36A)-C(31A)-C(32A)	117(2)	C(36A)-C(31A)-P	130(2)
C(32A)-C(31A)-P	112(2)	C(31A)-C(32A)-C(33A)	117(2)
C(34A)-C(33A)-C(32A)	117(2)	C(33A)-C(34A)-C(35A)	103(2)
C(34A)-C(35A)-C(36A)	117(2)	C(31A)-C(36A)-C(35A)	119(2)
O(3A)#2-Cl(1)-O(3A)#3	138.3(13)	O(3A)#2-Cl(1)-O(3A)	61(2)
O(3A)#3-Cl(1)-O(3A)	138.3(13)	O(3A)#2-Cl(1)-O(3A)#4	138.3(13)
O(3A)#3-Cl(1)-O(3A)#4	61(2)	O(3A)-Cl(1)-O(3A)#4	138.3(13)
O(3)#3-Cl(1)-O(3)#2	100.7(4)	O(3)#3-Cl(1)-O(3)	100.7(4)
O(3)#2-Cl(1)-O(3)	128.8(11)	O(3)#3-Cl(1)-O(3)#4	128.8(11)
O(3)#2-Cl(1)-O(3)#4	100.7(4)	O(3)-Cl(1)-O(3)#4	100.7(4)
Cl(1)-O(3A)-O(3A)#2	59.8(10)		

Symmetry transformations used to generate equivalent atoms:

#1 x+1-1,-y+1/2,-z+1/4

#2 -x+1,-y+1,z

#3 y,-x+1,-z #4 -y+1,x,-z

Table 3B.5. Anisotropic displacement parameters ($A^2 \times 10^3$) for $[Cu_2(O_2PPh_2)_2(tntn)](ClO_4)_2 \cdot 1.5MeOH$. The anisotropic displacement factor exponent takes the form: $-2\ pi^2\ [\ h^2\ a^{*2}\ U11 + ... + 2\ h\ k\ a^*\ b^*\ U12\ ]$

	U11	U22	U33	U23	U13	U12
Cu	58(1)	54(1)	60(1)	-5(1)	1(1)	-2(1)
P	77(2)	61(2)	62(1)	-4(1)	20(1)	-9(2)
O(1)	122(6)	57(4)	86(4)	-6(3)	33(4)	-46(4)
O(2)	98(5)	78(5)	72(4)	-3(3)	-22(4)	10(4)
N(1)	72(5)	56(4)	88(5)	-8(4)	-1(5)	-8(5)
N(2)	78(5)	76(5)	66(4)	3(4)	-8(4)	-9(5)
N(3)	70(5)	55(4)	68(4)	-1(4)	7(4)	5(4)
C(1)	84(7)	60(6)	108(8)	2(6)	5(7)	-17(7)
C(2)	84(7)	40(5)	91(6)	9(5)	9(6)	-11(5)
C(3)	78(6)	83(6)	62(5)	-4(5)	-12(5)	-4(6)
C(4)	70(7)	152(12)	70(6)	-13(7)	-8(6)	26(8)
C(5)	103(8)	58(6)	116(8)	19(6)	4(7)	-8(7)
C(6)	111(10)	103(9)	134(10)	-29(9)	-22(9)	9(9)
C(7)	47(5)	63(5)	57(4)	4(4)	0(4)	6(5)
C(8)	53(5)	90(7)	63(5)	14(5)	-8(5)	-2(6)
C(9)	86(8)	127(10)	76(7)	-3(7)	-3(6)	-1(8)
C(10)	62(7)	111(9)	98(8)	10(7)	-13(6)	-8(7)
C(11)	66(7)	104(9)	110(9)	15(7)	3(7)	-10(8)
C(12)	62(9)	93(11)	65(7)	19(8)	0	0
C(13)	40(6)	77(9)	49(6)	7(7)	0	0
C(21)	70(6)	50(5)	63(5)	-9(4)	9(5)	-5(5)
C(22)	95(9)	108(10)	103(8)	21(7)	40(8)	11(8)
C(23)	115(11)	129(12)	99(9)	7(8)	30(9)	15(11)
C(24)	76(8)	154(13)	72(7)	54(8)	12(6)	33(9)
C(25)	98(10)	101(9)	126(10)	21(8)	16(9)	0(9)
C(26)	71(7)	84(7)	84(6)	26(6)	13(6)	-2(7)
Cl(1)	93(3)	93(3)	77(3)	0	0	C
O(3)	71(8)	81(9)	89(9)	38(8)	-25(8)	8(8)
O(3A)	121(19)	123(24)	107(16)	-24(14)	38(16)	-8(25)

Table 3B.6. Hydrogen coordinates ($\times 10^4$) and isotropic displacement parameters ($A^2 \times 10^3$) for $[Cu_2(O_2PPh_2)_2(tntn)](ClO_4)_2 \cdot 1.5MeOH$.

	x	y	z	U(eq)
H(1)	4542(3)	822(3)	1236(5)	86
H(2)	4655(3)	1566(3)	-917(4)	88
H(1A)	3069(4)	1078(4)	916(7)	101
H(1B)	3360(4)	843(4)	161(7)	101
H(2A)	3715(4)	510(3)	1311(6)	86
H(2B)	3784(4)	1056(3)	1700(6)	86
H(3A)	3627(4)	2022(4)	-700(5)	89
H(3B)	3213(4)	1594(4)	-819(5)	89
H(4A)	3842(4)	966(5)	-1007(6)	117
H(4B)	3990(4)	1424(5)	-1588(6)	117
H(5A)	4619(5)	247(4)	306(7)	111
H(5B)	4088(5)	401(4)	-86(7)	111
H(6A)	4668(5)	659(5)	-1038(8)	139
H(6B)	5041(5)	876(5)	-364(8)	139
H(7A)	3473(3)	2345(3)	611(5)	67
H(7B)	3409(3)	1989(3)	1378(5)	67
H(9)	2592(5)	1511(5)	-4(6)	116
H(10)	1708(4)	1578(5)	-24(7)	108
H(11)	1301(5)	2074(5)	852(7)	112
H(22)	5414(4)	2130(4)	-540(5)	123
H(23)	6260(4)	2000(4)	-467(5)	137
H(24)	6770(5)	2596(6)	168(7)	121
H(25)	6438(5)	3294(5)	838(9)	130
H(26)	5541(4)	3386(4)	825(7)	96
H(32)	4627(5)	2509(5)	-1520(7)	82
H(33)	4462(6)	2930(5)	-2749(7)	94
H(34)	4187(6)	3766(4)	-2800(8)	90
H(35)	4306(5)	4236(5)	-1618(7)	78
H(36)	4451(7)	3863(4)	-369(7)	76
H(32A)	4249(12)	2482(8)	-1298(16)	82

Table 3B.6 continued.

	x	y	z	U(eq)
H(33A)	4101(12)	2864(9)	-2658(15)	94
H(34A)	3476(11)	3585(9)	-2253(17)	90
H(35A)	4289(12)	4135(8)	-2083(16)	78
H(36A)	4542(15)	3946(9)	-688(18)	76

APPENDIX 3C. Derivation of Equations From Chapter 3.

Derivation of Equation 3.1.

Titration of $Cu(II)_2tntn$ in the presence of a strong acid ($HClO_4$) with the titrant sodium hydroxide (0.1 M).

$K_w = [H^+][OH^-]$ 3C.1

Acid dissociation constant of perchloric acid:

$K_a = [H^+][ClO_4^-]/[HClO_4] = 10^{10}$ 3C.2

Base dissociation constant of sodium hydroxide:

$K_b = [Na^+][OH^-]/[NaOH] = 10^{10}$ 3C.3

First acid dissociation constant of $Cu(II)_2tntn$ (M):

$K_1 = [H^+][HM^-]/[H_2M]$ 3C.4

Second acid dissociation constant of $Cu(II)_2tntn$ (M):

$K_2 = [H^+][M^{2-}]/[HM^-]$ 3C.5

Charge Balance:

$[Na^+] + [H^+] = [ClO4^-] + [OH^-] + [MH^-] + 2[A^{2-}]$ 3C.6

V_o = original volume of solution

V = volume of titrant added

F_a = original concentration of perchloric acid

F_b = concentration of titrant being added

M = original concentration of $Cu(II)_2tntn$

$[M]_T = VM/(V_o + V)$ 3C.6

Mass Balance Equations:

$[HClO_4] + [ClO_4^-] = V_oF_a/(V_o + V)$ 3C.8

$[NaOH] + [Na^+] = VF_b/(V_o + V)$ 3C.9

$[M]_T = [MH_2] + [MH^-] + [M^{2-}]$ 3C.10

Substitute 3C.3 into 3C.9;

$$[Na^+] = K_bF_b(V/(V + V_o))/(K_b + [OH^-]) \qquad 3C.11$$

Substitute 3C.2 into 3C.8;

$$[ClO_4^-] = K_aFa(V_o/(V + V_o))/([H^+] + K_a) \qquad 3C.12$$

Substitute 3C.4 and 3C.5 into 3C.10;

$$[MH_2] = [M]_T[H^+]^2/([H^+]^2 + K_1[H^+] + K_1K_2) \qquad 3C.13$$

Substitute 3C.8, 3C.9, and 3C.10 into 3C.6;

$$[ML_2] = \{ \frac{K_bFbV/(V + V_o) + [H+] - K_aFaV/([H+] + K_a) - K_w/[H+] - [M]_T}{(K_1K_2 - [H^+]^2)} \} [H+]^2$$

3C.14

Set 3C.13 = 3C.14

Volume of titrant being added (V) =

$$V_o\{\frac{K_w/[H+] + K_aFa/([H+] + Ka) - [H+] + M(2K_1K_2 + K_1[H+]/([H+]\text{^}2 + K_1[H+] + K_1K_2)}{(K_bF_b[H^+]/K_b[H^+] + K_w + [H^+] - K_W/[H^+]}$$

equation 3.1

Derivation of Equation 3.2.

Rate Equation for the hydrolysis of a substrate by a complex with two water bound acid dissociation constants and the active form of the complex being the mono-hydroxo form.

Cu_2 represents the dinuclear Cu(II) complex in the tetraaquo form.

$Cu_2(OH^-)$ represents the dinuclear Cu(II) complex in the mono hydroxo form.

$Cu_2(OH^-)_2$ represents the dinuclear Cu(II) complex in the dihydroxo form.

$[Cu_2]_T$ represents total concentration of dinuclear Cu(II) complex.

$$Cu_2 \overset{K_{a1}}{\rightleftharpoons} Cu_2(OH^-) + H^+ \overset{K_{a2}}{\rightleftharpoons} Cu_2(OH^-)_2 + H$$

$$+$$

Substrate

$$\downarrow k$$

Products

K_{a1} represents the first acid dissociation of the water bound to $Cu(II)_2$tntn.

K_{a2} represents the second acid dissociation of the water bound to $Cu(II)_2$tntn.

$K_{a1} = [Cu_2(OH^-)][H^+]/[Cu_2]$ 3C.15

$K_{a2} = [Cu_2(OH^-)_2][H^+]/[Cu_2(OH^-)]$ 3C.16

Rate equation;

$rate = k[Cu_2(OH\text{-})][Substrate]$ 3C.17

Under pseudo first order conditions in (3C.17);

$k_{obs} = k[Cu_2(OH^-)]$ 3C.18

Total complex concentration;

$[Cu_2]_T = [Cu_2] + [Cu_2(OH^-)] + [Cu_2(OH^-)_2]$ 3C.19

Substitute (3C.15) and (3C.16) into (3C.19);

$[Cu_2]_T = [Cu_2(OH^-)]([H^+]/K_{a1} + 1 + K_{a2}/[H^+])$ 3C.20

Substitute (3C.20) into (3C.18);

$k_{obs} = k[Cu_2]_T/[H^+]/K_{a1} + 1 + K_{a2}/[H^+]$ equation 3.2

Contributions to Knowledge

Metal Alkoxide Versus Metal Hydroxide Reactivity for Cleaving an Activated Phosphate Diester.

(1) A copper(II) complex with a pendant hydroxypropyl group (Cu(II)hpbpa) has been shown to be ~37 fold more reactive than a copper(II) complex without a pendant alcohol group (Cu(II)bpa) and ~80 fold more reactive than a copper(II) complex with a pendant hydroxyethyl group (Cu(II)hebpa) for cleaving an activated phosphate diester, bis(2,4-dinitrophenyl) phosphate (BDNPP). A separate series, using zinc(II) as the metal with the same ligands, demonstrated the same order of reactivity as the copper(II) complexes for the cleavage of BDNPP.

(2) HPLC product analyses of the reactions of BDNPP with Cu(II)bpa, Cu(II)hebpa, and Cu(II)hpbpa provided evidence that the three copper(II) complexes do not cleave the substrate by the same mechanism. Cu(II)bpa and Cu(II)hebpa cleaves BDNPP predominantly by hydrolysis whereas Cu(II)hpbpa cleaves BDNPP mostly by transesterification.

(3) The differences in the reactivities and mechanisms of phosphate diester cleavage by Cu(II)bpa, Cu(II)hebpa, and Cu(II)hpbpa are explained on the basis of structural differences of the three copper(II) complexes. This explanation is supported by X-ray studies of two complex analogs.

Dinuclear Copper(II) Cleavage of RNA

(4) A dinuclear copper(II) complex ($Cu(II)_2$tntn) has been developed that shows high cooperativity between the two metal centers for cleaving RNA. $Cu(II)_2$tntn is not the most reactive transition metal complex reported[47] for the hydrolysis of ApA, however it does represent the first transition metal complex that efficiently effects the hydrolysis of both ApA and 2'3'-cAMP.

(5) The dinuclear copper(II) complex is observed to be between 200-500 times more reactive, per metal center, than the mononuclear copper(II) complexes for cleaving ApA and 2'3'-cAMP.

(6) The reactivity of $Cu(II)_2$tntn for cleaving RNA is proposed to result from double Lewis acid activation. Support for this mechanism is provided by a crystal structure of $Cu(II)_2$tntn bridging a substrate analog, diphenyl phosphinate.

Publications Resulting From This Research:

(1) Mary Jane Young, Daphne Wahnon, Rosemary C. Hynes, and Jik Chin. "Reactivity of Copper(II) Hydroxide and Copper(II) Alkoxides for cleaving an Activated Phosphate Diester." *J. Am. Chem. Soc.* **1995,** 117 9441-9447.

(2) Mary Jane Young and Jik Chin. "Dinuclear Copper(II) Complex That Hydrolyzes RNA." *J. Am. Chem. Soc.* **1995,** 117, 10577-10578.

References

(1) Watson, J. D.; Crick, F. H. C. *Nature* **1953**, *171*, 737-738.

(2) Watson, J. D.; Crick, F. H. C. *Nature* **1953**, *171*, 964-967.

(3) Chin, J.; Banaszcyk, M.; Jubian, V.; Zou, X. *J. Am. Chem. Soc.* **1989**, *111*, 186-190.

(4) Davis, A. M.; Hall, A. D.; Williams, A. *J. Am. Chem. Soc.* **1988**, *110*, 5105-5108.

(5) Järvinen, P.; Oivanen, M.; Lönnberg, H. *J. Org. Chem.* **1991**, *56*, 5396-5401.

(6) Westheimer, F. H. *Acc. Chem. Res.* **1968**, *1*, 70-78.

(7) Gillespie, P.; Ramirez, F.; Ugi, I.; Marquarding, D. *Angew. Chem. Int. Ed. Engl.* **1973**, *12*, 91-119.

(8) Holmes, R. R.; Deiters, J. A. *J. Am. Chem. Soc.* **1977**, *99*, 3318-3326.

(9) Oivanen, M.; Lönnberg, H. *Trends in Organic Chemistry* **1991**, *2*, 183-198.

(10) Hengge, A. C.; Tobin, A. E.; Cleland, W. W. *J. Am. Chem. Soc.* **1995**, *117*, 5919-5926.

(11) Thatcher, G. R. J.; Kluger, R. *Adv. Phys. Org. Chem.* **1989**, *25*, 99-265.

(12) Suck, D.; Oefner, C. *Nature* **1986**, *321*, 620-625.

(13) Nogués, M. V.; Vilanova, M.; Cuchillo, C. M. *Biochim. Biophys. Acta* **1995**, *1253*, 16-24.

(14) Altman, S. *Angew. Chem. Int. Ed. Engl.* **1990**, *29*, 749-758.

(15) Brown, J. W. *Nucleic Acids Res.* **1996**, *24*, 236-237.

(16) Steitz, T. A.; Steitz, J. A. *Proc. Natl. Acad. Sci. USA* **1993**, *90*, 6498-6502.

(17) Richards, F. M.; Wyckoff, H. W. *The Enzymes* **1971**, *4*, 647-804.

(18) Messmore, J. M.; Fuchs, D. N.; Raines, R. T. *J. Am. Chem. Soc.* **1995**, *117*, 8057-8060.

(19) Breslow, R.; Huang, D.-L.; Ansyln, E. *Proc. Natl. Acad. Sci. USA* **1989**, *86*, 1746-1750.

(20) Anslyn, E.; Breslow, R. *J. Am. Chem. Soc.* **1989**, *111*, 4473-4482.

(21) Breslow, R.; Huang, D.-L. *J. Am. Chem. Soc.* **1990**, *112*, 9621-9623.

(22) Menger, F. M. *J. Org. Chem.* **1991**, *56*, 6251-6252.

(23) Haim, A. *J. Am. Chem. Soc.* **1992**, *114*, 8384-8388.

(24) Herschlag, D. *J. Am. Chem. Soc.* **1994**, *116*, 11631-11635.

(25) Kirby, A. J.; Marriott, R. E. *J. Am. Chem. Soc.* **1995**, *117*, 833-834.

(26) Beese, L. S.; Steitz, T. A. *EMBO J.* **1991**, *10*, 25-33.

(27) Kim, E. E.; Wyckoff, H. W. *J. Mol. Biol.* **1991**, *218*, 449-464.

(28) Davies, J., F., II; Hostomska, Z.; Hostomsky, Z.; Jordan, S. R.; Matthews, D. A. *Science* **1991**, *252*, 88-95.

(29) Volbeda, A.; Lahm, A.; Sakiyama, F.; Suck, D. *EMBO J.* **1991**, *10*, 1607-1618.

(30) Hough, E.; Hansen, L. K.; Birkness, B.; Jynge, K.; Hansen, S.; Hordvik, A.; Little, C.; Dodson, E.; Derewenda, Z. *Nature* **1989**, *338*, 357-360.

(31) Casareno, R. L. B.; Cowan, J. S. *J. Am. Chem. Soc.* **1995**, *117*, 11011-11012.

(32) Black, C. B.; Cowan, J. A. *J. Am. Chem. Soc.* **1994**, *116*, 1174-1178.

(33) Jou, R.; Cowan, J. A. *J. Am. Chem. Soc.* **1991**, *113*, 6685-6686.

(34) Pyle, A. M. *Science* **1993**, *261*, 709-714.

(35) Smith, H. O. *Science* **1979**, *205*, 455-462.

(36) Newman, M.; Strzelecka, T.; Dorner, L. F.; Schildkraut, I.; Aggarwal, A. K. *Science* **1995**, *269*, 656-663.

(37) Moser, H. E.; Dervan, P. B. *Science* **1987**, *238*, 645-650.

(38) De Mesmaeker, A.; Häner, R.; Martin, P.; Moser, H. E. *Acc. Chem. Res.* **1995**, *28*, 366-374.

(39) Thuong, N. T.; Hélène, C. *Angew. Chem. Int. Ed. Engl.* **1993**, *32*, 666-690.

(40) Strobel, S. A.; Dervan, P. B. *J. Am. Chem. Soc.* **1989**, *111*, 7286-7287.

(41) Povsic, T. J.; Devan, P. B. *J. Am. Chem. Soc.* **1989**, *111*, 3059-3061.

(42) Sigman, D. S.; Mazumder, A.; Perrin, D. M. *Chem. Rev.* **1993**, *93*, 2295-2316.

(43) Sigman, D. S. *Biochemistry* **1990**, *29*, 9097-9105.

(44) Thomas, M.; White, R. L.; Davis, R. W. *Proc. Natl. Acad. Sci. USA* **1976**, *73*, 2294-229.

(45) Woolford, J., John L.; Rosbash, M. *Nucleic Acids Res.* **1979**, *6*, 2483-2497.

(46) Rosbash, M.; Blank, D.; Fahrner, K.; Hereford, L.; Ricciardi, R.; Roberts, B.; Ruby, S.; Woolford, J. *Methods Enzymol.* **1979**, *68*, 454-469.

(47) Linkletter, B.; Chin, J. *Angew. Chem. Int. Ed. Engl.* **1995**, *34*, 472-474.

(48) Takasaki, B. K.; Chin, J. *J. Am. Chem. Soc.* **1994**, *116*, 1121-1122.

(49) Komiyama, M.; Takeda, N.; Takahashi, Y.; Uchida, H.; Shiiba, T.; Kodama, T.; Yashiro, M. *J. Chem. Soc. Perkin Trans. 2* **1995**, 269-274.

(50) Hall, J.; Husken, D.; Pieles, U.; Moser, H. E.; Haner, R. *Chem. Biol.* **1994**, *1*, 185-190.

(51) Lipscomb, W. N. *Acc. Chem. Res.* **1970**, *3*, 81-89.

(52) Mathews, B. W. *Acc. Chem. Res.* **1988**, *21*, 333-340.

(53) Benning, M. M.; Kuo, J. M.; Raushel, F. M.; Holden, H. M. *Biochemistry* **1995**, *34*, 7973-7978.

(54) Roderick, S. L.; Matthews, B. W. *Biochemistry* **1993**, *32*, 3907-3912.

(55) Sträter, N.; Klabunde, T.; Tucker, P.; Witzel, H.; Krebs, B. *Science* **1995**, *268*, 1489-1492.

(56) Buckingham, D. A.; Harrowfield, J. M.; Sargeson, A. M. *J. Am. Chem. Soc.* **1974**, *96*, 1726-1729.

(57) Zhu, L.; Kostic, N. M. *Inorg. Chim. Acta* **1994**, *217*, 21-28.

(58) Pan, T.; Uhlenbeck, O. C. *Biochemistry* **1992**, *31*, 3887-3895.

(59) Groves, J. T.; Baron, L. A. *J. Am. Chem. Soc.* **1989**, *1989*, 5442-5448.

(60) Sutton, P. A.; Buckingham, D. A. *Acc. Chem. Res.* **1987**, *20*, 357-364.

(61) Chin, J.; Banaszczyk, M.; Jubian, V. *J. Chem. Soc., Chem. Commun.* **1988**, 734.

(62) Hendry, P.; Sargeson, A. M. *Progress in Inorganic Chemistry: Bioinorganic Chemistry* **1990**, *38*, 201-258.

(63) Matsumoto, Y.; Komiyama, M. *J. Chem. Soc., Chem. Commun.* **1990**, 1050-1051.

(64) Kirby, A. J. *Adv. Phys. Org. Chem.* **1980**, *17*, 183-278.

(65) Tsubouchi, A.; Bruice, T. C. *J. Am. Chem. Soc.* **1995**, *117*, 7399-7411.

(66) Tsubouchi, A.; Bruice, T. C. *J. Am. Chem. Soc.* **1994**, *116*, 11614-11615.

(67) Dempcy, R. O.; Bruice, T. C. *J. Am. Chem. Soc.* **1994**, *116*, 4511-4512.

(68) Browne, K. A.; Bruice, T. C. *J. Am. Chem. Soc.* **1992**, *114*, 4951-4958.

(69) Wall, M.; Hynes, R. C.; Chin, J. *Angew. Chem. Int. Ed. Engl.* **1993**,

(70) Murthy, N. N.; Mahroof-Tahir, M.; Karlin, K. D. *J. Am. Chem. Soc.* **1993**, *115*, 10404-10405.

(71) Mahroof-Tahir, M.; Karlin, K. D.; Chen, Q.; Zubieta, J. *Inorg. Chim. Acta* **1993**, *207*, 135-138.

(72) Bashkin, J. K.; Frolova, E. I.; Sampath, U. *J. Am. Chem. Soc.* **1994**, *116*, 5981-5982.

(73) Magda, D.; Miller, R. A.; Sessler, J. L.; Iverson, B. L. *J. Am. Chem. Soc.* **1994**, *116*, 7439-7440.

(74) Matsumura, K.; Endo, M.; Komiyama, M. *J. Chem. Soc., Chem. Commun.* **1994**, 2019-2020.

(75) Stern, M. K.; Bashkin, J. K.; Sall, E. D. *J. Am. Chem. Soc.* **1990**, *112*, 5357-5359.

(76) Wahnon, D.; Lebuis, A.-M.; Chin, J. *Angew. Chem. Int. Ed. Engl.* **1995**, *34*, 2412-2414.

(77) Williams, N. H.; Chin, J. *J. Chem. Soc., Chem. Commun.* **1996**, 131-132.

(78) Basile, L. A.; Raphael, A. L.; Barton, J. K. *J. Am. Chem. Soc.* **1987**, *109*, 7550-7551.

(79) Wahnon, D.; Hynes, R. C.; Chin, J. *J. Chem. Soc., Chem. Commun.* **1994**, 1441-1442.

(80) Piccirilli, J. A.; Vyle, J. S.; Caruthers, M. H.; Cech, T. R. *Nature* **1993**, *361*, 85-88.

(81) Fothergill, M.; Goodman, M. F.; Petruska, J.; Warshel, A. *J. Am. Chem. Soc.* **1995**, *117*, 11619-11627.

(82) Kimura, E.; Kodama, Y.; Koike, T.; Shiro, M. *J. Am. Chem. Soc.* **1995**, *117*, 8304-8311.

(83) Morrow, J. R.; Aures, K.; Epstein, D. *J. Chem. Soc., Chem. Commun.* **1995**, 2431-2432.

(84) Young, M. J.; Wahnon, D.; Hynes, R. C.; Chin, J. *J. Am. Chem. Soc.* **1995**, *117*, 9441-9447.

(85) Menger, F. M.; Ladika, M. *J. Am. Chem. Soc.* **1987**, *109*, 3145-3146.

(86) Kim, J. H.; Chin, J. *J. Am. Chem. Soc.* **1992**, *114*, 9792-9795.

(87) Bashkin, J. K.; Jenkins, L. A. *J. Chem. Soc., Dalton Trans.* **1993**, 3631-3632.

(88) Sigel, H.; Hofstetter, F.; Marin, R. B.; Milburn, R. M.; Scheller-Krattiger, V.; Scheller, K. H. *J. Am. Chem. Soc.* **1984**, *106*, 7935-7946.

(89) Groves, J. T.; Kady, I. O. *Inorg. Chem.* **1993**, *32*, 3868-3872.

(90) Uma, R.; Viswanathan, R.; Paliandavar, M.; Lakshminarayanan, M. *J. Chem. Soc., Dalton Trans.* **1994**, 1219-1226.

(91) Karlin, K. D.; Hayes, J. C.; Juen, S.; Hutchinson, J. P.; Zubieta, J. *Inorg. Chem.* **1982**, *21*, 4106-4108.

(92) Oberhausen, K. J.; O'Brien, R. J.; Richardson, J. F.; Buchanan, R. M. *Inorg. Chim. Acta* **1990**, *173*, 145-154.

(93) Nishida, Y.; Takahashi, K. *J. Chem. Soc., Dalton Trans.* **1988**, 691-699.

(94) Morrow, J. R. *Inorg. Chem.* **1988**, *27*, 3387-3394.

(95) Langford, C. H. *Inorg. Chem.* **1965**, *4*, 265-266.

(96) Kady, I. O.; Tan, B.; Ho, Z.; Scarborough, T. *J. Chem. Soc., Chem. Commun.* **1995**, 1137-1138.

(97) Gellman, S. H.; Petter, R.; Breslow, R. *J. Am. Chem. Soc.* **1986**, *108*, 2388-2394.

(98) Norman, P. R.; Cornelius, R. D. *J. Am. Chem. Soc.* **1982**, *104*, 2356-2361.

(99) Jones, D. R.; Lindoy, L. F.; Sargeson, A. M. *J. Am. Chem. Soc.* **1983**, *105*, 7327-7336.

(100) Courtney, R. C.; Gustafson, R. L.; Chaberek, S., Jr.; Martell, A. E. *J. Am. Chem. Soc.* **1959**, *81*, 519-524.

(101) Gustafson, R. L.; Martell, A. E. *J. Am. Chem. Soc.* **1959**, *81*, 525-529.

(102) Burstyn, J. N.; Deal, K. A. *Inorg. Chem.* **1993**, *32*, 3585-3586.

(103) Connolly, J.; Kim, J. H.; Banaszczyk, M.; Drouin, M.; Chin, J. *Inorg. Chem.* **1995**, *34*, 1094-1099.

(104) Larsen, S.; Michelson, K.; Pedersen, E. *Acta Chem. Scand. A* **1986**, *40*, 63-76.

(105) Rawji, G.; Milburn, R. M. *J. Org. Chem.* **1981**, *46*, 1205-1206.

(106) Bunton, C. A.; Farber, S. J. *J. Org. Chem.* **1969**, *34*, 767-772.

(107) Barry Linkletter, Ph. D. Thesis.

(108) Romary, J. K.; Barger, J. D.; Bunds, J. E. *Inorg. Chem.* **1968**, *7*, 1142-1145.

(109) Christian, E. L.; Yarus, M. *Biochemistry* **1993**, *32*, 4475-4480.

(110) Vance, D. H.; Czarnik, A. W. *J. Am. Chem. Soc.* **1993**, *115*, 12165-12166.

(111) Chapman, J., William H.; Breslow, R. *J. Am. Chem. Soc.* **1995**, *117*, 5462-5469.

(112) Yashiro, M.; Ishikubo, A.; Komiyama, M. *J. Chem. Soc., Chem. Commun.* **1995**, 1793-1794.

(113) Chung, Y.; Akkaya, E. U.; Venkatachalam, T. K.; Czarnik, A. W. *Tetrahedron Lett.* **1990**, *31*, 5413-5416.

(114) Schwarzenbach, G.; Moser, P. *Helv. Chim. Acta* **1953**, *36*, 581-597.

(115) Sacconi, L.; Paoletti, P.; Ciampolini, M. *J. Chem. Soc.* **1964**, 5046-5051.

(116) Ng, C. Y.; Motekaitis, R. J.; Martell, A. E. *Inorg. Chem.* **1979**, *18*, 2982-2986.

(117) Haake, P. C.; Westheimer, F. H. *J. Am. Chem. Soc.* **1961**, *83*, 1102-1109.

(118) Abrash, H. I.; Cheung, C.-C. S.; Davis, J. C. *Biochemistry* **1967**, *6*, 1298-1303.

(119) Thompson, J. E.; Kutateladze, T. G.; Schuster, M. C.; Venegas, F. D.; Messmore, J. M.; Raines, R. T. *Bioorg. Chem.* **1995**, *23*, 471-481.

(120) Kamada, T.; Wasada, N.; Yamamoto, O. *Bull. Chem. Soc. Jpn.* **1976**, *49*, 275-282.

(121) Mitchell, R. H.; Sondheimer, S. *Tetrahedron* **1968**, *24*, 1397-1405.

(122) Atkins, T. J.; Richman, J. E.; Oettle, W. F. *Organic Syntheses* **1978**, *58*, 86-97.

(123) Richman, J. E.; Atkins, T. J. *J. Am. Chem. Soc.* **1974**, *96*, 2269-2270.

(124) Weslman, G. R.; Vachon, D. J.; Johnson, V. B.; Grenbeck, D. A. *J. Chem. Soc., Chem. Commun.* **1987**, 886-887.

(125) Schwindinger, W. F.; Fawcett, T. G.; Lalancette, R. A.; Potenza, J. A.; Schugar, H. J. *Inorg. Chem.* **1980**, *19*, 1379-1381.

(126) Gabe, E. J.; LePage, Y.; Charland, J. P.; Lee, F. L.; White, P. S. *J. Appl. Crystallogr.* **1989**, *22*, 384-387.

(127) Sheldrick, G. **1985**, SHELXS86: Program for the solution of crystal structures. University of Göttingen, Germany.

(128) Sheldrick, G. **1995**, SHELX93: Program for the refinement of crystal structures. University of Göttingen, Germany.

(129) Speck, A. L. **1994**, PLATON94: Molecular Geometry Program, Version July 1994. University of Utrecht, The Netherlands.

(130) SQUEEZE, implementation in PLATON94 of the BYPASS procedure. (van der Sluis, P.; Speck, A. L; Acta. Cryst. A46, 1990,194. BYPASS: an effective Method for the Refinement of Crystal Structures Containing Disordered Solvent Regions.).